

# Interferon-induced and Constitutive Expression of Immunity-related GTPases (IRG) in Mouse Tissues

INAUGURAL-DISSERTATION

zur

Erlangung des Doktorgrades

der Mathematisch-Naturwissenschaftlichen Fakultät

der Universität zu Köln



vorgelegt von

**Jia Zeng**

aus

Shandong, P. R. China

Köln, 2007

Referees/Berichterstatter: Prof. Dr. Jonathan C. Howard  
Prof. Dr. Maria Leptin

Date of oral examination: 21<sup>st</sup> Jan 2008

Tag der mündlichen Prüfung 21<sup>st</sup> Jan 2008

The present research work was carried out under the supervision of Prof. Dr. Jonathan C. Howard, in the Institute for Genetics, University of Cologne, Cologne, Germany from April 2004 to November 2007.

Diese Arbeit wurde von April 2004 bis November 2007 am Institut für Genetik der Universität zu Köln unter der Leitung von Prof. Dr. Jonathan C. Howard durchgeführt.

# TABLE OF CONTENTS

## 1. Introduction

1.1 Interferons	1
1.1.1 Three types of interferons	1
1.1.2 Signaling pathways activated by IFNs	3
1.2 Interferon inducible GTPases	5
1.2.1 Mx	5
1.2.2 The guanylate-binding proteins	6
1.2.3. The IRG GTPases	6
1.2.3.1 <i>Irg</i> genes	7
1.2.3.2 The expression of IRGs	8
1.2.3.3 Biochemical properties, structure and interaction of IRG proteins	9
1.2.3.4 Subcellular localization of IRG proteins	11
1.2.3.5 Resistance of IRG proteins to intracellular pathogens	12
1.2.3.6 Cell-autonomous resistance mediated by IRG Proteins	13
1.3 NKT cell	14
1.3.1 NKT cell distribution	15
1.3.2 NKT cell ligands	15
1.3.3 Lipid presentation in NKT cell	16
1.3.4 NKT cell development	17
1.3.5 NKT cell function	17
1.3.5.1 NKT cell activation by $\alpha$ GalCer	17
1.3.5.2 NKT cell activation by bacterial infection	18
1.3.5.3 NKT cell and parasitic and viral infection and noninfectious diseases	19
1.4 Aim of the work	19

## 2. Materials and Methods

2.1 Materials	21
2.1.1 Chemicals, Enzymes and Kits	21
2.1.2 Media	21
2.1.3 Serological reagents	22
2.1.4 Mice	23

2.2 Molecular biology	23
2.2.1 PCR, ligation and agarose gel electrophoresis	23
2.2.2 Competent cells and transformation	24
2.2.3 Plasmid DNA isolation from bacteria	24
2.2.4 DNA-Sequencing	25
2.2.5 Total RNA isolation and cDNA synthesis	25
2.2.6 Reverse-transcriptase PCR	25
2.2.7 Real-time PCR	26
2.2.8 T cell receptor repertoire screening	27
2.2.9 Northern blot analysis	28
2.2.10 Western blot analysis	28
2.3 Histology	29
2.3.1 Tissue preparation and section	29
2.3.2 Immunohistochemistry	29
2.3.3 Immunofluorescence	30
2.3.4 In situ hybridization	31
2.3.5 Laser Microdissection (LMD)	32
2.4 Cell biology	33
2.4.1 Mammalian cell line culture	33
2.4.2 Mouse hepatocytes isolation and culture	33
2.4.3 Immunofluorescence for cells	34
2.5 <i>T. gondii</i> passage and infection	34
2.6 Promoter analysis	35

### **3. Results**

3.1 Irga6 is constitutively expressed in mouse tissues	36
3.1.1 Irga6 has high and constant level of constitutive expression in mouse liver	36
3.1.2 Irga6 constitutive expression in liver has general and focal patterns	39
3.1.3 Irga6 has constitutive expression in many mouse tissues	41
3.2 Interferons show different influences on constitutive expression of Irga6 in different tissues	43
3.3 Irga6 has two transcriptional forms using 2 distinct promoters	45
3.4 IRG proteins are constitutively expressed in primary hepatocytes	47
3.4.1 IRG proteins are expressed constitutively in murine primary hepatocyte	48

3.4.2 Constitutively expressed Irga6 is localized mainly in ER but not in Golgi in murine primary hepatocytes	50
3.5 IRG proteins participate in IFN- $\gamma$ induced resistance against <i>Toxoplasma gondii</i> infection	51
3.5.1 IFN- $\gamma$ mediates growth inhibition of <i>Toxoplasma gondii</i> in murine primary hepatocytes	51
3.5.2 Both constitutively expressed and IFN- $\gamma$ stimulated Irga6 accumulated at <i>Toxoplasma gondii</i> vacuoles in murine primary hepatocytes	52
3.5.3 <i>Toxoplasma gondii</i> vacuoles coated by Irga6 mature in murine primary hepatocytes	55
3.6 Irga6 focal expression in liver and kidney exploits interferon pathway	56
3.6.1 The focal expression of Irga6 in liver and kidney is developmentally regulated	56
3.6.2 Irgm3 is coexpressed at Irga6 expression foci in liver and kidney	58
3.6.3 Irga6 cored patch in liver and patch in kidney is dependent on interferons	59
3.6.4 Irga6 focal expression is eliminated in STAT-1 <sup>-/-</sup> but not gp130 <sup>-/-</sup> liver and kidney	63
3.7 Two transcriptional forms of Irga6 are expressed differentially in liver	65
3.7.1 Irga6 1B form is more abundant in liver	66
3.7.2 Irga6 1A form is remarkably more abundant in Irga6 expression foci in liver	67
3.7.3 Irga6 1A form in cored patch is expressed at similar level as in patch in liver	69
3.7.4 IFN- $\gamma$ is expressed in Irga6 cored patch but not in patch in liver	70
3.8 T cells are essential for Irga6 cored focal expression in liver	71
3.8.1 T cells and macrophages are present in the center of Irga6 cored focal expression in liver and kidney	71
3.8.2 Irga6 cored patch expression in liver is eliminated in RAG-1 <sup>-/-</sup> mice	72
3.9 V $\beta$ 8 V $\alpha$ 14 NK T cell is the major T cell population in Irga6 cored expression patch in liver	74
3.9.1 T cell receptor V $\beta$ 8 subfamily is preferentially used by T cells in Irga6 cored expression patch in liver	74
3.9.2 T cells carrying V $\beta$ 8 TCR exist in Irga6 cored expression patch in liver	77
3.9.3 T cell receptor V $\alpha$ 14-J $\alpha$ 18 is preferentially used by T cells in Irga6 cored expression patch in liver	78
3.10 Irga6 focal expression is not caused by bacteria and endotoxin	81

3.10.1 Irga6 focal expression is intact in germ-free mice	81
3.10.2 Irga6 focal expression persists in TLR pathway deficient mice	84
3.11 Irga6 expression after <i>Listeria monocytogenes</i> infection	86
<b>4. Discussion</b>	
4.1 IRG proteins are constitutively expressed in mice liver	91
4.2 The expression of Irga6 in liver was under the control of alternative activation of distinct promoters	92
4.3 Constitutively expressed IRG proteins participate in cell-autonomous resistance to <i>Toxoplasma gondii</i> in primary hepatocytes	95
4.4 IRG proteins are constitutively expressed in many other tissues	96
4.5 Irga6 focal expression in liver and kidney exploits interferon pathway	98
4.6 NKT cell activation in Irga6 cored expression patch in liver	100
4.7 What are the causes of local NKT cell activation?	102
4.8 Where does Irga6 focal expression without cores originate?	104
<b>5. Summary/ Zusammenfassung</b>	106
<b>6. References</b>	109
<b>Aknowlegement</b>	133
<b>Erklärung</b>	134
<b>Curriculum Vitae/Lebenslauf</b>	135

## 1. Introduction

Mammalian cells respond to interferons (IFNs) by the transcriptional upregulation of more than a thousand genes. Surprisingly, among those genes many of the most abundantly induced proteins are GTPases. For instance, immunity-related GTPases (IRG) were discovered because of their massive induced-expression in response to IFN- $\gamma$ . Later on it turned out that many members of IRG proteins play indispensable roles in IFN-orchestrated intracellular anti-pathogen programs. Therefore it is totally logical that the expression of IRGs should be under the tight control of IFNs, as has also been proved by many reports. Unexpectedly, however, we found that IRG proteins do have constitutive expression in many mouse tissues. Despite of this tissue specific expression, our attention was then attracted by well-defined intense focal expression of IRG proteins in liver and kidney. Interestingly, this focal expression, which was exclusively IFN dependent, turned out to be related to local activation of NKT cells. In the following introduction, I will first describe the IFN system before give the depiction of IRG proteins, and finally a description of NKT cells will be presented.

### 1.1. Interferons

Interferons (IFNs) are a family of structurally related cytokines discovered because of their hallmark function of antiviral activity, and are found only in vertebrates (Isaacs and Lindenmann, 1957; Wheelock, 1965). Despite their distinct antiviral activities, IFNs exhibit a diversity of biological functions, such as cell proliferation or immunomodulatory effects.

#### 1.1.1 Three types of interferons

IFNs consist of several types namely type I, II and III IFNs. The type I IFNs (MacMicking *et al.*, 2003; Martens and Howard, 2006; Roberts *et al.*, 1998) consist of IFN- $\alpha$ , - $\beta$ , - $\omega$ , - $\epsilon$  (Langer *et al.*, 2004; Pestka *et al.*, 2004) and - $\kappa$  (LaFleur *et al.*,

2001). All these members are massively induced in virus-infected cells. Type I IFNs, IFN- $\alpha/\beta$  play a vital role in innate resistance to a wide variety of viruses through the induction of antiviral effects, both directly and indirectly, e.g. up-regulation of iNOS, Mx, PKR, 2'-5' oligoadenylate synthetase, MHC molecules etc. (Taylor *et al.*, 2000; Theofilopoulos *et al.*, 2005). IFN- $\alpha/\beta$  also has an immunomodulatory effect of activating natural killer (NK) cells, macrophages both of which are essential effector cells in the innate immune system (Biron *et al.*, 1999; Taylor *et al.*, 2004; Theofilopoulos *et al.*, 2005). In addition, by virtue of their potentiating effect on DC maturation, type I IFNs are currently recognized as pivotal cytokines bridging two aspects of host defence, innate and adaptive immune systems (Banchereau and Steinman, 1998).

Type II IFN comprises solely IFN- $\gamma$  (Ikeda *et al.*, 2002). Even though IFN- $\gamma$  has similar antiviral activity and thereby is defined as an interferon, this cytokine is strongly produced not by virus infected cells, rather by activated NK cells (Perussia, 1991), activated T helper cells of the Th1 subset (Mosmann and Coffman, 1989), and activated CD8 cytotoxic cells (Sad *et al.*, 1995). In T cells the main inducer of IFN- $\gamma$  is cross-linking of the T cell receptor (Ullman *et al.*, 1990), whereas in NK cells, IFN- $\gamma$  production is stimulated by macrophage-derived cytokines, especially TNF- $\alpha$  and IL-12 (Trinchieri, 1995) and is stimulate by IFN- $\gamma$  itself (Hardy and Sawada, 1989). IFN- $\gamma$  has direct antiviral effects partially overlapping that of type I IFNs by up-regulation of antiviral effectors like PKR, 2'-5' oligoadenylate synthetase, dsRAD (Beretta *et al.*, 1996; Patterson *et al.*, 1995). Nevertheless, the antiviral responses of IFN- $\gamma$  are not completely the same as type I IFNs, for instance, anti-viral GTPase, Mx is solely induced by type I IFNs. IFN- $\gamma$ , in addition to its antiviral function, is essential for the elimination of intracellular microorganisms through the activation of macrophages accompanied by the release of reduced oxygen intermediates. This is achieved by up-regulation of genes like gp91-phox, iNOS, and NRAMP (Baek *et al.*, 1993; Cassatella *et al.*, 1989; Govoni *et al.*, 1995). Despite its complex responses in innate immunity, IFN- $\gamma$  is involved in immunoregulatory action such as synergism and antagonism with pivot cytokines like IL-12 or IL-4, the Th phenotype

determination, and antigen presentation pathway (Lehn *et al.*, 1989; Ma *et al.*, 1996; Rousset *et al.*, 1988; Seder and Paul, 1994; Trinchieri, 1995).

Newly identified IFN members, IFN- $\lambda$ s or IL-28/29 are similar to type I IFNs, and they are induced upon viral infection and exert similar antiviral functions (Kotenko *et al.*, 2003; Sheppard *et al.*, 2003; Vilcek, 2003). However, the major differences are that they are structurally distinct from type I IFNs and that they utilize their specific receptor subunit, IFN- $\lambda$ R1 or IL-28R $\alpha$  and IL-10R2, nevertheless the signaling pathways appear to be shared with type I interferons. And interestingly Mx1 was shown to be able to be induced by IFN- $\lambda$ s.

### **1.1.2 Signaling pathways activated by IFNs**

All IFN- $\alpha/\beta$  subtypes interact with the same receptor complex, termed the IFN- $\alpha/\beta$  receptor (IFNAR), which consists of at least two subunits, IFNAR-1 and IFNAR-2 (Darnell *et al.*, 1994; Novick *et al.*, 1994; Stark *et al.*, 1998; Uze *et al.*, 1990) (Fig. 1). The intracellular domains of these two subunits, IFNAR-1 and IFNAR-2, are associated with Janus protein tyrosine kinases (Jak PTKs), Tyk2 and Jak1 respectively. As for type II IFN signaling, IFN- $\gamma$  binds to the IFN- $\gamma$  receptor complex (IFNGR), comprising IFNGR-1 and IFNGR-2; the IFNGR1 subunit is constitutively associated with Jak1, whereas IFNGR2 with Jak2 (Bach *et al.*, 1997; Chen *et al.*, 2004; Stark *et al.*, 1998). The binding of both types of IFNs to IFNAR or IFNGR results in the cross-activation of these Jak protein kinases, which then phosphorylate their downstream substrates, Stat1 and Stat2 (signal transducers and activators of transcription) (Darnell *et al.*, 1994; Ihle and Kerr, 1995; Schindler and Darnell, 1995; Stark *et al.*, 1998), causing the formation of STAT1-STAT2 heterodimers for type I IFNs, and STAT1 homodimers for IFN- $\gamma$ . Thereafter, STAT1-STAT2 heterodimers associate with a third protein, IRF9, and bind one class of type I IFN response elements, the ISRE, whereas STAT1 homodimers activate gene expression by binding to another class of IFN response elements, the GAS (Bluyssen *et al.*, 1996; Darnell *et al.*, 1994; Decker *et al.*, 1991; Haque and Williams, 1994; Lew *et al.*, 1991).

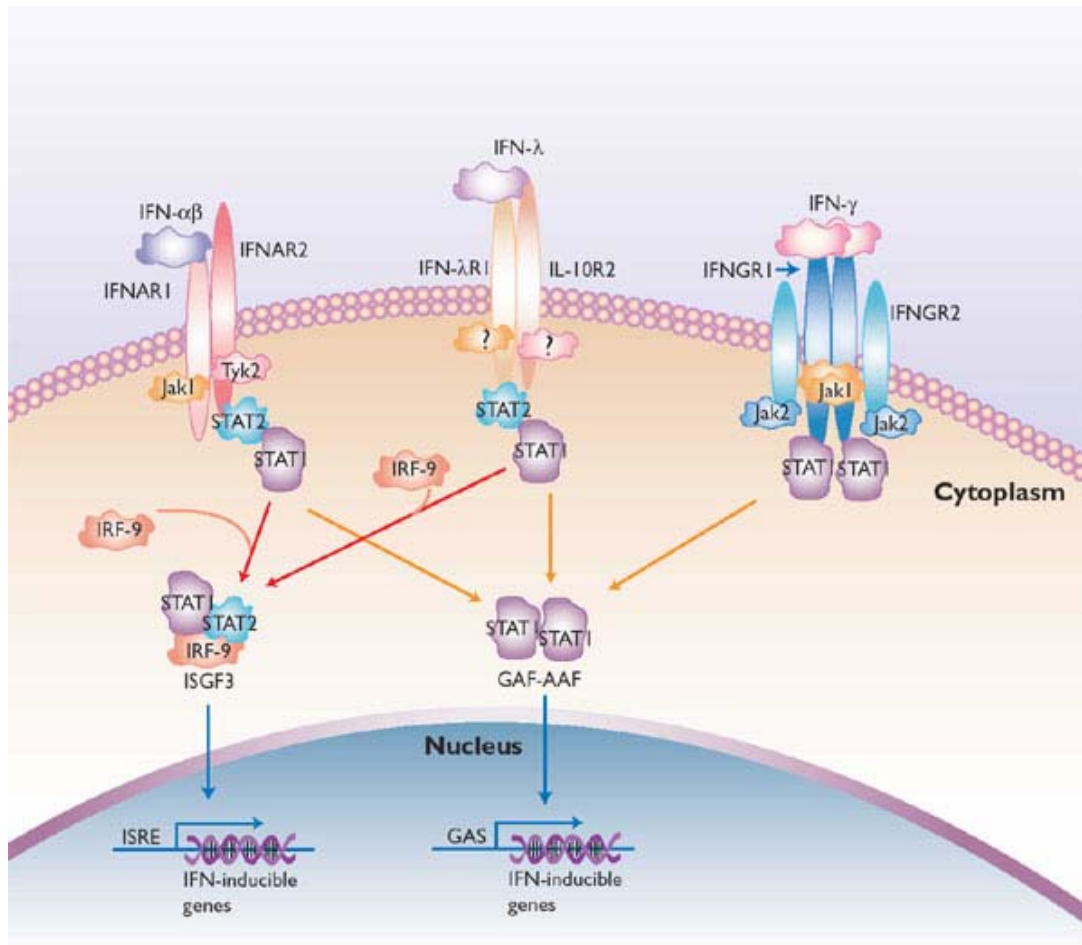


**Figure 1. IFNs signaling pathways.** IFN- $\alpha\beta$  (type I IFNs) and IFN- $\gamma$  (type II IFN) bind to specific and distinct heterodimeric receptors. Binding of IFN- $\alpha$  or IFN- $\beta$  to their receptor leads to the activation of two receptor-associated tyrosine kinases, Jak1 and Tyk2; this is followed by tyrosine phosphorylation of the STAT1 and STAT2 proteins. Phosphorylated STAT1 and STAT2 combine with IRF-9 (IFN-regulatory factor 9) to form the trimeric ISGF-3 complex, which, upon translocation to the nucleus, binds to the cis element ISRE (IFN-stimulated response element), which is present in most IFN- $\alpha$  and IFN- $\beta$ -responsive genes. In contrast, binding of IFN- $\gamma$  to its receptor leads to tyrosine phosphorylation of the Jak1 and Jak2 tyrosine kinases, resulting in the phosphorylation of STAT1 but not STAT2. Phosphorylated STAT1 homodimerizes to form the GAF-AAF complex, which translocates to the nucleus and binds to the IFN- activation site (GAS) element present in most IFN- $\gamma$ -inducible genes. Like IFN- $\gamma$ , IFN- $\alpha$  and IFN- $\beta$  signaling can also lead to the formation of the GAF-AAF complex and its binding to the GAS regulatory element. The three newly identified IFN- $\lambda$  proteins (also termed IL-28A, IL-28B and IL-29) bind to a heterodimeric receptor composed of a previously unknown IFN-R1 subunit and IL-10R2, which also serves as the second chain of the IL-10R. Although the tyrosine kinases activated by IFN- $\lambda$  have not yet been identified, available evidence indicates that both STAT1 and STAT2 are activated and the downstream signaling pathways activated by IFN- $\lambda$  appear to be indistinguishable from those activated by IFN- $\alpha$  and IFN- $\beta$ . (Vilcek, 2003).

IFN- $\lambda$  bind their receptors IFN- $\lambda$ R1 and IL-10R2 on the cell surface and signal also

through unidentified Jak kinases. Similar to type I IFN signaling, IFN- $\lambda$  receptor clustering leads to the activation of both STAT1 and STAT2 (Kotenko *et al.*, 2003; Sheppard *et al.*, 2003; Vilcek, 2003).

## **1.2. Interferon inducible GTPases**

During infection, mammalian cells respond to interferons (IFNs) by the transcriptional upregulation of more than a thousand genes, among which many of the most abundantly induced proteins are GTPases e.g. Mx, GBP, IRG proteins. All known IFN-inducible GTPase families share biochemical and probably also mechanistical characteristics with the dynamins.

### **1.2.1 Mx**

Rodent Mx1 and 2 homologs in human are MxA and B, the homologs of which are present in all vertebrates (Staheli and Haller, 1985). Mx is exclusively induced by type I IFNs (Goetschy *et al.*, 1989; Simon *et al.*, 1991). Mx proteins share unambiguous homology to dynamin and share many biochemical properties with dynamins as well, including  $\mu$ M guanine nucleotides binding affinity, capacity of oligomerization and independency of extra GAP for GTP hydrolysis (Kochs *et al.*, 2002; Melen and Julkunen, 1997; Melen *et al.*, 1992; Nakayama *et al.*, 1993; Schwemmle *et al.*, 1995). In IFN-stimulated cells human MxA and mouse Mx2 localize in the cytoplasm, whereas mouse Mx1 localizes to the nucleus due to a nuclear localization signal at the C-terminus (Meier *et al.*, 1988; Melen *et al.*, 1992; Staheli and Haller, 1985). Mx1 and human MxA have strong antiviral effects (Arnheiter and Meier, 1990; Hefti *et al.*, 1999; Miura *et al.*, 2001). MxA probably binds directly to viral nucleoproteins or capsid proteins, interfering with viral trafficking and assembly (Kochs *et al.*, 2002; Kochs and Haller, 1999). The mode of action for the nuclear Mx1 is less known, probably involving the inhibition of primary transcription of virus RNA (Pavlovic *et al.*, 1992). However, several Mx isoforms, such as human MxB, appear devoid of antiviral activity (Meier *et al.*, 1990; Pavlovic *et al.*, 1990). Nevertheless, a recent report suggested that MxB might have a function

in regulating nucleocytoplasmic transport and/or cell-cycle progression (King *et al.*, 2004).

### **1.2.2 The guanylate-binding proteins**

The guanylate-binding proteins (GBPs) were among the first IFN-inducible proteins identified because of their spectacular induction by IFNs esp. IFN- $\gamma$  (Boehm *et al.*, 1998; Cheng *et al.*, 1985; Cheng *et al.*, 1983). Seven GBP genes have been described, namely, *hGBP1-7* in human (Cheng *et al.*, 1991; Olszewski *et al.*, 2006) and *mGBP1-7* in mouse (Boehm *et al.*, 1998; Olszewski *et al.*, 2006; Wynn *et al.*, 1991), respectively. Recently, the number of *mGBP* genes seem to expand to 11 (Klaus Pfeffer, personal communication). Similar to dynamin proteins, GBPs bind nucleotides with low affinity, hydrolyze GTP cooperately and form multimers (Praefcke *et al.*, 2004; Praefcke and McMahon, 2004; Prakash *et al.*, 2000; Prakash *et al.*, 2000). The structures of hGBP1 in different nucleotide binding forms were solved, which suggested plausible G-domain dimers (Ghosh *et al.*, 2006; Prakash *et al.*, 2000; Prakash *et al.*, 2000).

Despite detailed knowledge of their structure and biochemistry, the function of the GBPs is still not clear. The antiviral effects of GBPs are weak (Anderson *et al.*, 1999; Carter *et al.*, 2005). Recently, however, GBPs have been proposed to exert complete different functions such as regulation of vasculogenesis (Gorbacheva *et al.*, 2002; Guenzi *et al.*, 2001; Guenzi *et al.*, 2003).

### **1.2.3. The IRG GTPases**

IFNs mediate antiviral effects to a broad spectrum of pathogens including viruses and various intracellular microbes. So far IFN-inducible GTPases mentioned above are mostly implicated in viral resistance. The last IFN-inducible GTPases described below however participate in cell-autonomous resistance against intracellular microbes.

### 1.2.3.1 *Irg* genes

There are 25 *Irg* coding units in the C57BL/6 mouse, with 2 pseudo-genes and 21 intact genes, locating on chromosome 7 (*Irgc*), 11 (*Irga* family), 18 (the rest of *Irg* genes) (Bekpen *et al.*, 2005) (Fig.2). Only two *Irg* genes, IRGC and IRGM, are present in humans. *Irg* gene homologs are also found in other vertebrates such as dogs, zebrafish (Bekpen *et al.*, 2005). In mouse, the open reading frame of *Irg* genes is typically encoded on a single long 3' exon behind one or more 5'-untranslated exons. Perfect interferon-inducible motifs, ISRE and GAS, but no other recurrent promoter motifs such as NF $\kappa$ B-binding sites can be found for most of the chromosome 11 and 18 *Irg* genes. *Irgc* on chromosome 7 is an exception (Bekpen *et al.*, 2005).

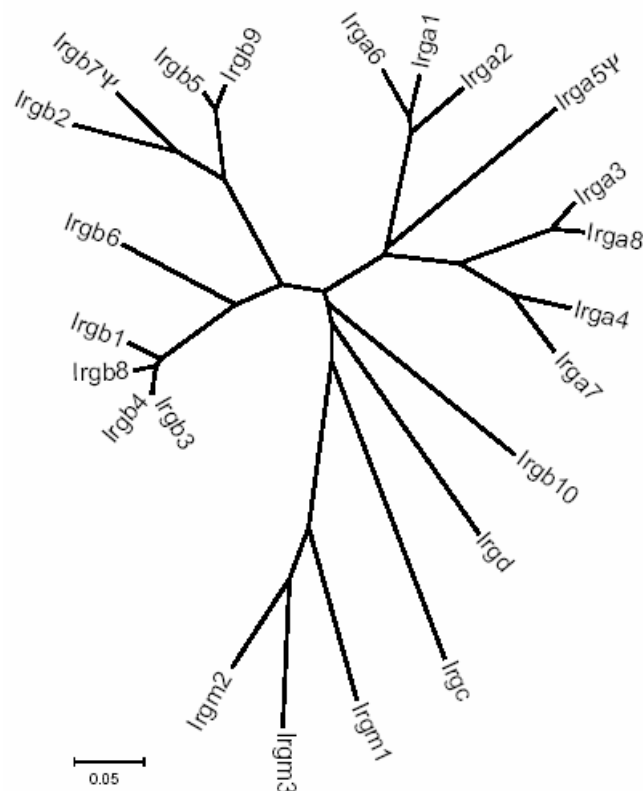


**Figure 2. Phylogenetic relationship of mouse *Irg* GTPases.** Unrooted tree (p-distance based on neighbour-joining method) of nucleotide sequences of the G-domains of the 23 mouse *Irg* GTPases, including the two presumed pseudo-genes *Irga5* and *Irgb7*. The sources of all *Irg* sequences are given in Additional data file 1, and the nucleotide and amino acid sequences themselves are collected in the p47 (IRG) GTPase database from our laboratory website [<http://db.aghoward.uni-koeln.de/public/database2/global/>]. (Bekpen *et al.*, 2005; Samadani *et al.*, 1996)

### 1.2.3.2 The expression of IRGs

The cDNA of IRG-47 (Irgd), the first *Irg* gene discovered, was found in murine IFN- $\gamma$ -induced pre-B cell lines (Gilly and Wall, 1992). Another 5 members of IRG family, TGTP (Irgb6), LRG-47 (Irgm1), IGTP (Irgm3), GTPI (Irgm2) and IIGP-1 (Irga6) were subsequently discovered (Carlow *et al.*, 1995; Carlow *et al.*, 1998; Sorace *et al.*, 1995; Taylor *et al.*, 1996; Zerrahn *et al.*, 2002). Based on phylogenetic principles, a naming scheme has been introduced using the core name IRG (immunity-related GTPases) (Bekpen *et al.*, 2005). All IRGs including Irgd were found to be induced in different cultured cell types such as peritoneal, Raw 264.7 or bone marrow macrophages, fibroblast or endothelial cell lines, B or T cell lines under stimulated conditions. The inducers include IFN- $\gamma$ , IFN- $\alpha/\beta$ , LPS or T cell receptor cross linking in the case of T cells, but not other cytokines such as IL-1, IL2, IL4, IL6, TNF- $\alpha$  (Carlow *et al.*, 1998; Taylor *et al.*, 1996; Zerrahn *et al.*, 2002). Notably, IFN- $\gamma$  was proved to be around 1,000 fold more efficient than IFN- $\alpha/\beta$  in the induction of tested members of IRG proteins (Carlow *et al.*, 1998; Taylor *et al.*, 1996). The importance of IFN pathway for the induction is evident. Mouse embryonic fibroblast from IFN- $\gamma$ R<sup>-/-</sup> but not IRF-1<sup>-/-</sup> mice was incapable of induction of IRG proteins with IFN- $\gamma$  (Boehm *et al.*, 1998). The induction by T cell receptor cross linking was obviously IFN- $\gamma$ R dependent (Zerrahn *et al.*, 2002). LPS employed type I IFN pathway to induce IRG proteins, since in IFN- $\alpha$ R<sup>-/-</sup> cells the induction was blocked (Lapaque *et al.*, 2006; Zerrahn *et al.*, 2002). In STAT-1<sup>-/-</sup> murine bone marrow derived macrophages (BBM) the expression of IRG proteins after IFN- $\gamma$  stimulation was completely abolished (MacMicking *et al.*, 2003). Interestingly, direct infection of BMM or dendritic cells by *Trypanosoma cruzi* or *Listeria monocytogenes* stimulated expression of IRG proteins, which turned out to be triggered by type I IFN signaling in an autocrine manner (Koga *et al.*, 2006). Two micro-array reports indicated that IRG proteins are expressed in hematopoietic stem cells, which is presumably due to bursts of developmentally regulated IFN synthesis (Terskikh *et al.*, 2001; Venezia *et al.*, 2004).

IRG proteins are expressed at very high levels in most tissue following infection with

pathogens. All 6 well known IRG proteins were strongly induced in liver infected by *Listeria monocytogenes* in an IFN- $\gamma$ R<sup>-/-</sup> dependent manner (Boehm *et al.*, 1998). The infection with *Listeria monocytogenes*, *Toxoplasma gondii* and murine cytomegalovirus massively induced the expression of IRG proteins in spleen and liver (Collazo *et al.*, 2001; Gavrilescu *et al.*, 2004; Taylor *et al.*, 2000), and a similar induction was observed in lung infected by *Mycobacterium tuberculosis* (MacMicking *et al.*, 2003). The induction in spleen infected by *Toxoplasma gondii* was clearly abrogated in STAT-1<sup>-/-</sup> mice.

Constitutive expression of *Irgd* and *Irgm3* in thymus and spleen in the absence of infection was reported (Collazo *et al.*, 2001; Taylor *et al.*, 1996), which like the expression of *Irg* genes in hematopoietic stem cell could be responses to bursts of IFN expression at early developmental stages of myeloid differentiation.

### 1.2.3.3 Biochemical properties, structure and interaction of IRG proteins

IRG proteins are typically 47-kDa molecular weight, with a canonical G domain. Three of the mouse IRG proteins have the noncanonical sequence GX<sub>4</sub>GMS in place of the otherwise conserved form, GX<sub>4</sub>GKS, in the G1 nucleotide-binding motif. These two subfamilies have been designated GMS and GKS, respectively (Boehm *et al.*, 1998). The systematic biochemical and structural data are only available for one IRG protein, *Irga6*, a member from GKS group. (Ghosh *et al.*, 2004; Uthaiyah *et al.*, 2003). *Irga6* has low nucleotide binding affinity ( $\mu$ M range), hydrolyzes GTP to GDP cooperatively and oligomerizes in the presence of GTP, which recall the biochemical properties of dynamins (Ghosh *et al.*, 2004; Uthaiyah *et al.*, 2003). Under physiological conditions, *Irga6* should be predominantly GDP bound.

A crystal structure of *Irga6* was obtained recently, which is not similar to that of hGBP1. The apoprotein and GDP-bound forms both crystallized as symmetrical dimers, having a Ras-like G domain (Fig. 3A). Several lines of evidence suggest that the crystal dimer interface is not a definitive interface of the GTP-bound oligomer, and most probably a drastically different dimer interface is adapted by dramatic conformational change when the protein oligomers start to form (Ghosh *et al.*, 2004);

Pawlowski unpublished results). A second interface, involving a G domain: G domain dimer, has been suggested by site-directed mutagenesis, though no crystal structure of this hypothetical dimer is yet available (Pawlowski and Wolf unpublished results). The putative second interface together with the dimer interface may allow for the construction of an oligomer with alternating use of these two interfaces (Fig. 3B).

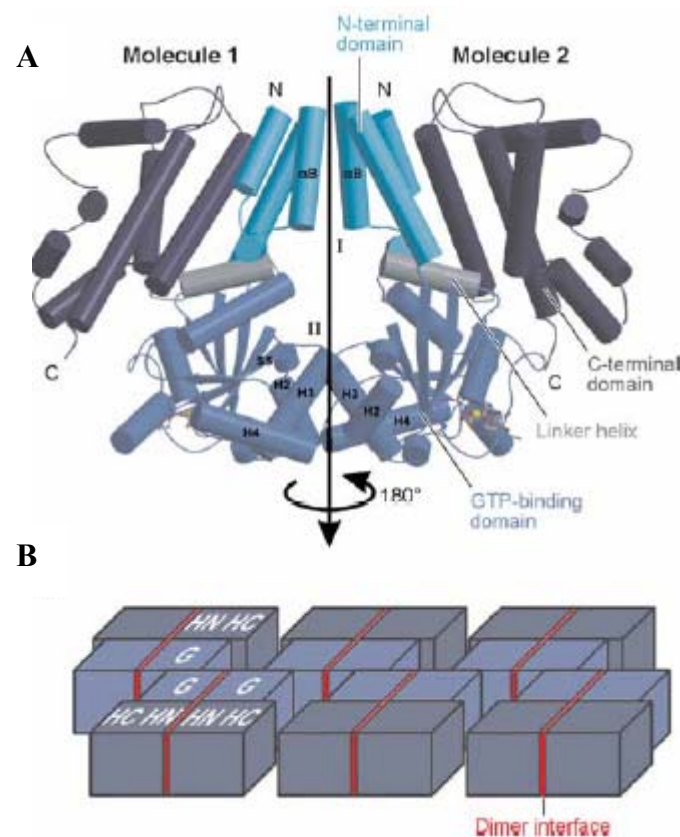


**Figure 3. Structure and model of oligomerization for Irga6.** (A) Crystal structure of Irga6 in the GDP-bound form (reprinted Ghosh et al. 2004, with permission from Elsevier, copyright 2004). The unit cell of the Irga6 crystal contained a rotationally symmetrical dimer with interactions between monomers in both the N-terminal domain and nucleotide-binding domain. A linker helix connects the helical C-terminal domain to the nucleotide-binding domain. A myristoylation motif at the extreme N terminus is not resolved in the structure. (B) Model for the oligomeric structure of Irga6 based on the dimer shown in A and an unpublished second interface in the G domain. The dimer interface in A is shown as a red line. HN, helical N-terminal domain; HC, helical C-terminal domain; G, nucleotide-binding domain. (Martens and Howard, 2006)

Irga6 like dynamins and GBPs can form oligomers which accelerate their hydrolysis of GTP. *In vitro* experiments demonstrated that one subunit of Irga6 protein can provide *in trans* a catalytic function to its interacting neighbour-subunit (Pawlowski unpublished results). *In vitro* Irga6 self-self interaction was detected, which was

totally dependent on GTP binding (Papic and Hunn unpublished results). Furthermore, hetero-oligomeric interaction between IRG proteins esp. between GMS and GKS proteins in a nucleotide binding dependent manner were discovered (Hunn unpublished results). Since *Irgm3* is mainly GTP bound under physiological conditions (Taylor *et al.*, 1996; Taylor *et al.*, 1997), in the IFN- $\gamma$  induced cells GTP-bound GMS proteins could have a plausible role in maintenance of the inactive GDP-bound GMS proteins until the arrival of an infectious stimulus that requires their activation. The only published interaction partner for *Irga6* is Hook-3 which is a microtubule motor-binding protein (Kaiser *et al.*, 2004) and the significance of this interaction deserves more research.

#### 1.2.3.4 Subcellular localization of IRG proteins

After stimulation with IFN, induced IRG proteins are distributed between different specific membrane compartments and the cytosol (Martens *et al.*, 2004). All IRG proteins except for *Irgd* are membrane associated in their resting location. *Irga6* is probably continuously exchanged between the cytosol and the ER membrane and the binding to the latter is due to an N-terminal myristoylation site. IRGM proteins are predominantly targeted to the Golgi membrane by a short sequence corresponding to helix K ( $\alpha$ K) in the *Irga6* crystal structure (Fig. 3A) (Ghosh *et al.*, 2004).

In inducible stable-transfected cell clones, where no IFN stimulation was present, *Irga6* and *Irgb6* fail to localize to their correct compartments e.g. the ER, which is not the case for GTP-binding deficient mutants (Martens *et al.*, 2004). This mislocalization can be rescued by additional induction with IFN- $\gamma$  or cotransfection with IRGM proteins, and in the latter case, IRGM GTP-binding deficient mutants are inactive (Hunn unpublished results).

All IRG proteins tested so far are rapidly relocalized from their resting compartment to vacuolar compartment during infection. In *Toxoplasma gondii* infection, IRG proteins reposition to *T. gondii* parasitophorous vacuole (Martens *et al.*, 2005), except for *Irgm1*, which however relocate to the mycobacterial phagosome (MacMicking *et al.*, 2003) or latex bead containing phagosomes (Martens *et al.*, 2004). *Irgm3* has also

been detected on latex bead phagosomes but not on phagosomes containing heat-killed *T. gondii* (Butcher *et al.*, 2005).

### 1.2.3.5 Resistance of IRG proteins to intracellular pathogens

Similar to Mx, IRG proteins are strongly implicated in IFN induced resistance however in distinct aspects. Mice deficient in IRG proteins have dramatic susceptibility phenotypes to many infectious intracellular bacteria and protozoa correlating well with loss of IFN- $\gamma$  dependent resistance in mice (Collazo *et al.*, 2001; MacMicking, 2004; MacMicking, 2005; Taylor *et al.*, 2000) (Table 1). A few reports of viral infection in IRG-deficient mice revealed no susceptible phenotype (Taylor *et al.*, 2000), and in transfected system *Irgb6* and *Irgm3* showed only weak, possibly insignificant effects to VSV and Coxsackie virus (Carlow *et al.*, 1998; Zhang *et al.*, 2003).

	Wild type	IFN- $\gamma$ <sup>-/-</sup>	<i>Irgm1</i> <sup>-/-</sup>	<i>Irgm3</i> <sup>-/-</sup>	<i>Irgd</i> <sup>-/-</sup>	<i>Irga6</i> <sup>-/-</sup>	<i>Irgb10</i>
<i>Toxoplasma gondii</i>	R <sup>b</sup>	S <sup>b</sup>	S	S	Sm <sup>b</sup> , Rc <sup>b</sup>	Rm <sup>b</sup> , Sc <sup>b</sup>	ND
<i>Leishmania major</i>	R	S	S	S	ND <sup>b</sup>	R	ND
<i>Trypanosoma cruzi</i>	R	S	S	R	ND	ND	ND
<i>Mycobacterium tuberculosis</i>	R	S	S	R	R	ND	ND
<i>Mycobacterium avium</i>	R	S	S	R	ND	ND	ND
<i>Listeria monocytogenes</i>	R	S	S	R	R	R	ND
<i>Salmonella typhimurium</i>	R	S	S	R	R	ND	ND
<i>Chlamydia trachomatis</i>	R	S	ND	Sc	ND	Rm, Sc*	Sc*

**Table 1. Susceptibilities of IRG-deficient mice and cells to intracellular pathogens.** This table summarizes various studies on *IRGm1* (Collazo *et al.*, 2001; Feng *et al.*, 2004; MacMicking *et al.*, 2003; Santiago *et al.*, 2005; Taylor *et al.*, 2004), *IRGm3* [(de Souza *et al.*, 2003) (Feng *et al.*, 2004; MacMicking *et al.*, 2003; Taylor *et al.*, 2000; Taylor *et al.*, 2004) Z. Bernstein-Hanley, J. Coers, W. Dietrich, personal communication (*Chlamydia*, in vitro)], and *IRGd* (Collazo *et al.*, 2001; MacMicking *et al.*, 2003). Data for *Irga6* (*Toxoplasma gondii*) are from Martens *et al.* (2005) and Parvanova and Reichmann (unpublished results); data for *Irga6* (*Leishmania* and *Listeria*) are from Parvanova, E. von Stebut, O. Utermöhlen (unpublished results); data for *Irga6* (*Chlamydia*) are from (Nelson *et al.*, 2005) (in vitro, RNAi) and Z. Bernstein-Hanley & I. Parvanova (unpublished results) (in vivo). Data for *Irgb10* (*Chlamydia*) are from Z. Bernstein-Hanley, J. Coers, W. Dietrich (personal communication) (in vitro, RNAi). bR, resistant; S, sensitive; Sm, knockout mouse sensitive; Rm, knockout mouse resistant; Sc, knockout cells sensitive; Sc., RNAi wild-type cells sensitive; Rc, knockout cells resistant. Where not speci.ed, the results are from knockout mice. ND, not determined. (Banchereau and Steinman, 1998; Martens and Howard, 2006)

The reasons why IRG-deficient mice died in these fatal diseases are not completely clear, possibly due to cytokine over-expression induced by an over-burden of pathogens arising from the failure of cell-autonomous resistance mediated by IRG GTPases (Feng *et al.*, 2004; Santiago *et al.*, 2005; Taylor *et al.*, 2000). Another argument for the susceptibility is based on a pathological defect in the *Irgm1* knock out mice which developed lymphopenia and bone marrow failure after infection with *Mycobacteria* and *Trypanosoma* (Feng *et al.*, 2004; Santiago *et al.*, 2005). The regulatory role of IRG proteins affecting lymphomyeloid differentiation needs to be further clarified, whereas the role of IRG proteins in cell-autonomous resistance against intracellular pathogens is increasingly supported.

#### **1.2.3.6 Cell-autonomous resistance mediated by IRG Proteins**

There is growing evidence favoring that the role of IRG proteins in resistance to intracellular pathogens is a cell-autonomous manner. Macrophages lacking *Irgm1* and *Irgm3* displayed greatly attenuated IFN- $\gamma$ -induced inhibition of *T.gondii* growth (Butcher *et al.*, 2005; Halonen *et al.*, 2001). IFN- $\gamma$  controls *T. gondii* infection significantly less efficiently in *Irga6*-deficient astrocytes (Martens *et al.*, 2005). Under IFN- $\gamma$  stimulation conditions five of known IRG proteins were concentrated very fast at the parasitophorous vacuoles in a GTP-binding dependent manner in *T.gondii* infected primary astrocytes (Martens *et al.*, 2005) or various of other cell types (Hunn and Könen-Waisman unpublished results). Remarkable vesiculation of parasitophorous vacuolar membranes that were positive for IRG proteins were observed and parasitophorous vacuolar membrane lost its integrity and subsequently *T. gondii* inside the disrupted vacuole undergoes deterioration (Martens *et al.*, 2005). Over-expression of wild-type *Irga6* accelerated the vacuolar disruption and the nucleotide binding mutant *Irga6* (K82A) acting as dominant negative form prevented relocalization and the cells do not control the infection normally (Martens *et al.*, 2005). Although no concentration of *Irgm1* was found at parasitophorous vacuoles (Butcher *et al.*, 2005; Martens *et al.*, 2005), it may exert its function distantly. As mentioned above, GMS interact with GKS proteins and in IFN- $\gamma$  induced cells

GTP-bound GMS is essential for correct subcellular localization of GDP-bound form of GKS. Since GDP-bound form of GTPases normally represents an inactive state of the protein, it is plausible to argue that GMS proteins interact with GKS proteins and act as negative regulators at cellular membrane. When *T. gondii* enter the cell, parasitophorous vacuole (PV) membrane is derived from plasma membrane which is free of GMS proteins. Hence on the PV membrane that is devoid of GKS inhibitors, GKS proteins may become activated and start to oligomerize. The situation however becomes complicated in view of the observation that, soon after *T.gondii* invasion (5 min), one member of GMS protein, Irgm2, starts to accumulate at the PV membrane (Yang Zhao personal communications).

It seems that the above model is not the only modality which IRGM proteins adopt in pathogen resistance. As mentioned Irgm1 is associated with the mycobacterial phagosome in IFN-treated macrophages, which correlates with delayed and limited phagosome acidification (MacMicking *et al.*, 2003).

Even though mechanisms of the resistance mediated by Irgm1 against *Listeria monocytogenes* (Collazo *et al.*, 2001) and *T.cruzi* (Santiago *et al.*, 2005) is not well understood, it cannot be explained by the same effector model as that for *T.gondii*, because these two pathogens escape rapidly from the vacuole to the cytosol after their entry into the cell. Several recent reports implicate Irgm1 in IFN- $\gamma$  induction of autophagy, which in turn has been suggested as a resistance mechanism against several intracellular pathogens including *Listeria monocytogenes* (Rich *et al.*, 2003) and *M. tuberculosis* (Gutierrez *et al.*, 2004).

The cell-autonomous resistance conferred by IRG proteins against several other intracellular pathogens such as *Legionella* and *Chlamydia trachomatis* was also reported with unexplained mechanisms (Martens and Howard, 2006; Nelson *et al.*, 2005).

### **1.3. NKT cell**

NKT cells are narrowly defined as a T cell lineage expressing NK lineage receptors, in addition to semi-invariant CD1d-restricted  $\alpha\beta$  TCRs. More than 80% of these TCRs

are V $\alpha$ 14-J $\alpha$ 18/V $\beta$ 8, V $\beta$ 7, and V $\beta$ 2 in mouse (or V $\alpha$ 24-J $\alpha$ 18/V $\beta$ 11 in human), and the remaining are V $\alpha$ 3.2-J $\alpha$ 9/V $\beta$ 8, V $\alpha$ 8/V $\beta$ 8, and other TCRs (Cardell *et al.*, 1995; Park *et al.*, 2001). Both the V $\alpha$ 14 and the non-V $\alpha$ 14 NKT cells exhibit autoreactivity to CD1d-expressing cells *in vitro* (Bendelac *et al.*, 2007).

### 1.3.1 NKT cell distribution

V $\alpha$ 14 NKT cells represent 0.5% of the T cell population in the blood and peripheral lymph nodes, 2.5% of T cells in the spleen, mesenteric, and pancreatic lymph nodes, and up to 30% of T cells in the liver (Matsuda *et al.*, 2000). V $\alpha$ 14 NKT cells reside within the liver sinusoids and their expression of CXCR6 matches the expression of CXCL16 on the endothelial cells lining the sinusoids and appears to be important for survival rather than for migration (Geissmann *et al.*, 2005). In humans, V $\alpha$ 24 NKT cells appear to be 10 times less frequent in all these locations. NKT cell frequency appears to be a stable phenotype under the genetic control of at least two recessive loci in mouse (Esteban *et al.*, 2003; Rocha-Campos *et al.*, 2006). Low V $\alpha$ 14 NKT cell expressors in mice include NOD and SJL (Baxter *et al.*, 1997; Gombert *et al.*, 1996; Yoshimoto *et al.*, 1995). V $\alpha$ 14 NKT cells are present in rats (Matsuura *et al.*, 2000; Pyz *et al.*, 2006), and, based on genomic and functional studies of CD1d, they may be absent in cows (Van Rhijn *et al.*, 2006).

### 1.3.2 NKT cell ligands

mV $\alpha$ 14 and hV $\alpha$ 24 NKT cells, irrespective of their V $\beta$ -D $\beta$ -J $\beta$  chain usage, recognize  $\alpha$ -galactosylceramide ( $\alpha$ GalCer) extracted from a marine sponge that prolonged survival of mice bearing B16 melanoma (Brossay *et al.*, 1998; Kawano *et al.*, 1997; Kobayashi *et al.*, 1995). Closely related structures were found as NKT cell ligands that act as substitutes for LPS in the cell wall of *Sphingomonas*, a Gram-negative, LPS-negative member of the class of  $\alpha$ -proteobacteria (Kawahara *et al.*, 2000; Kawasaki *et al.*, 1994). These glycosphingolipids have only one sugar, galacturonyl or glucuronyl,  $\alpha$ -anomerically branched to the ceramide backbone. Recently the self antigen of NKT cells in mouse and human, isoglobotrihexosylceramide (iGb3).

(Bendelac *et al.*, 1995; Exley *et al.*, 1997; Park *et al.*, 1998). This autoreactivity of endogenous ligand with CD1d is important for NKT cell activation in certain bacteria in infection and NKT cell thymic development (Bendelac, 1995; Brigl *et al.*, 2003; Mattner *et al.*, 2005; Park *et al.*, 2000; Zhou *et al.*, 2004). In contrast, the self and foreign antigens recognized by non-V $\alpha$ 14 NKT cells remain to be identified.

### 1.3.3 Lipid presentation in NKT cell

CD1d is prominently and constitutively expressed by APCs such as DCs, macrophages, and B cells (Brossay *et al.*, 1997; Roark *et al.*, 1998), with relatively modest changes stimulated by TLR activation and inflammatory cytokines (Skold *et al.*, 2005). CD1d is also expressed on cortical thymocytes, to which the autoreactivity is essential for NKT cell development (Bendelac, 1995), and on Kupffer cells and endothelial cells lining liver sinusoids (Geissmann *et al.*, 2005). Hepatocytes express CD1d constitutively in mouse and upon disease induction in human, for example, in the context of hepatitis C (de Lalla *et al.*, 2004).

Newly biosynthesized CD1d molecules, likely containing lipid chains, reach the plasma membrane and are internalized through an AP-2/AP-3 clathrin-dependent pathway to late endosomal/lysosomal compartments (Jayawardena-Wolf *et al.*, 2001; Kang and Cresswell, 2002; Kang and Cresswell, 2002; Roberts *et al.*, 2002), where lipid exchange is performed by saposins (Kang and Cresswell, 2004; Zhou *et al.*, 2004). CD1d extensively recycles between lysosome and plasma membrane, allowing further lipid exchange. Endosomal/lysosomal trafficking of CD1d is essential for lipid presentation to mV $\alpha$ 14 NKT cell, since mice deficient in biogenesis of lipid exchange proteins like saposins, microsomal triglyceride transfer protein (MTP) or NPC1, lack NKT cells and exhibited greatly impaired ability to present various endogenous and exogenous NKT ligands (Brozovic *et al.*, 2004; Honey *et al.*, 2002; Kang and Cresswell, 2004; Sagiv *et al.*, 2006; Zhou *et al.*, 2004). Notably, however, the non-V $\alpha$ 14 NKT cell ligands, which are still not identified, are normally presented by a tail-truncated CD1d, which is defective in endosomal trafficking and likely presents antigens loaded in the secretory pathway or at the cell surface (Chiu *et al.*, 1999).

### 1.3.4 NKT cell development

NKT cell precursors diverge from mainstream thymocyte development at the CD4<sup>+</sup>CD8<sup>+</sup> double-positive (DP) stage (Bendelac *et al.*, 1996; Gapin *et al.*, 2001). Upon expression of their canonical TCR $\alpha$  chain, NKT cell precursors are positively selected by interacting with endogenous ligands, presented by CD1d expressed on other DP thymocytes in the cortex (Benlagha *et al.*, 2005; Gapin *et al.*, 2001). Down-regulation of CD8 leads to appearance of CD4<sup>+</sup> and then further Down-regulation of CD4 in a subgroup of NKT cell precursors produce double-negative (DN) cells (Borowski and Bendelac, 2005; Cannons *et al.*, 2004; Pellicci *et al.*, 2002; Sivakumar *et al.*, 2003). NKT cell precursors then undergo several rounds of cell division characterized by production of IL4 and IFN- $\gamma$  and acquire a memory/effector phenotype prior to thymic emigration (Pellicci *et al.*, 2002; Stetson *et al.*, 2003). Acquisition of NK lineage receptors, including NK1.1, occurs after emigration to peripheral tissues, except for a minor subset of thymic NKT cell residents (Benlagha *et al.*, 2002; McNab *et al.*, 2005; Pellicci *et al.*, 2002).

### 1.3.5. NKT cell function

NKT cells have been implicated in a broad array of disease conditions ranging from infections, various forms of autoimmunity, atherosclerosis, allergy, and tumor.

#### 1.3.5.1 NKT cell activation by $\alpha$ GalCer

A cascade of activation events following the exogenous administration of NKT ligands such as  $\alpha$ GalCer has been characterized (Fig. 4). The central feature is a reciprocal activation of NKT cells and DCs. Resting DCs presents  $\alpha$ GalCer to NKT cells, inducing NKT cells to upregulate CD40L and Th1 and Th2 cytokines and chemokines; CD40 cross-linking induces DCs to upregulate CD40, B7.1 and B7.2, and IL-12, which in turn enhances NKT cell activation and cytokine production (Kitamura *et al.*, 1999; Tomura *et al.*, 1999). Propagation of this reaction involves the activation of NK cell cytotoxicity and IFN- $\gamma$  production (Carnaud *et al.*, 1999; Eberl and MacDonald, 2000) and, most importantly, the upregulation of DC costimulatory

properties and MHC class I– and MHC class II–mediated antigen presentation to prime robust adaptive immune responses (Fujii *et al.*, 2004; Fujii *et al.*, 2003; Gonzalez-Aseguinolaza *et al.*, 2002). Importantly, TLR signalling is not involved in these responses.

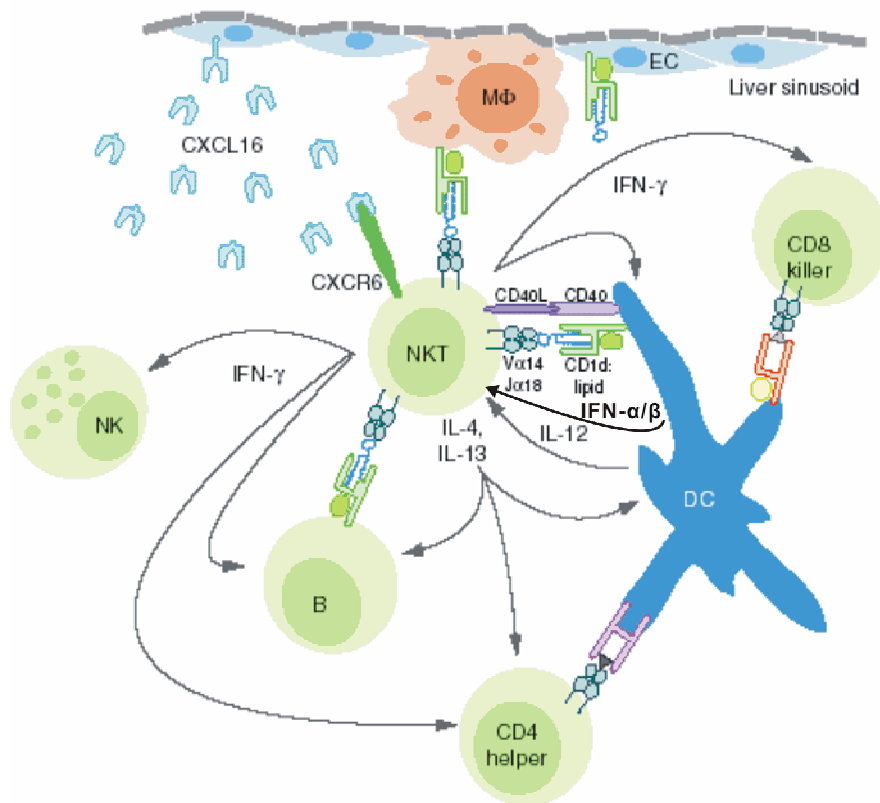


**Figure 4. Cellular and molecular network activated by the NKT ligand  $\alpha$ GalCer.** DCs and perhaps also Kupffer cells (macrophages) lining the liver sinusoids (where NKT cells accumulate) are at the center of a cellular network of cross-activation, starting with NKT cell upregulation of CD40L, secretion of Th1 and Th2 cytokines and chemokines, and DC superactivation to prime adaptive CD4 and CD8 T cell responses. NKT cells can provide help directly to B cells for antibody production and can also rapidly activate NK cells. CXCR6/CXCL16 interactions provide essential survival signals for NKT cells. EC, endothelial cell. (modified from Bendelac *et al.*, 2007; Costa *et al.*, 1988)

### 1.3.5.2 NKT cell activation by bacterial infection

Glycosphingolipids closely related to  $\alpha$ GalCer were reported in the cell wall of *Sphingomonas* (Kawahara *et al.*, 2000; Kawasaki *et al.*, 1994), a prominent Gram-negative, LPS-negative member of  $\alpha$ -proteobacteria. During infection, *Sphingomonas* is phagocytosed by macrophages and DCs and elicits an activation cascade similar to exogenous  $\alpha$ GalCer. NKT cell activation enhances microbial

clearance by 15- to 1000-fold within the first 2–3 days of infection (Kinjo *et al.*, 2005; Mattner *et al.*, 2005). TLR-mediated signaling exerts a much weaker direct effect relative to that of NKT cells.

Interestingly, many other bacteria, particularly the Gram-negative, LPS-positive ones, which though not having NKT cell ligands, can activate NKT cells, however, by triggering autoreactive NKT cell responses (Brigl *et al.*, 2003; Mattner *et al.*, 2005). In the case of *Salmonella*, blocking of biogenesis of iGb3 or blocking iGb3 itself in DC abrogated the activation of NKT cells (Mattner *et al.*, 2005). NKT cell activation by Gram-negative, LPS-positive *Salmonella* is also absolutely dependent upon TLR signaling, suggesting a possible relationship between TLR and endogenous NKT cell ligand presentation.

### **1.3.5.3 NKT cell and parasitic and viral infection and noninfectious diseases**

Only preliminary experimental data are available for NKT cell activation in parasitic and viral infection. Malaria circumsporozoite and *Schistosoma mansoni* eggs were reported to activate NKT cells (Mallevaey *et al.*, 2006; Molano *et al.*, 2000; Romero *et al.*, 2001). Modest defects in the clearance of some viruses have been reported in CD1d-deficient mice (Ilyinskii *et al.*, 2006) or coxsackie B3 (Huber *et al.*, 2003).

There are many reports suggesting a role of NKT cells in a wide variety of noninfectious disease conditions. A detailed mechanistic understanding however is still lacking. The relative deficiency of NKT cells in NOD mice (Baxter *et al.*, 1997; Gombert *et al.*, 1996), suggested a causal relationship with diabetes. Hyperreactive NKT cells accumulated in aging NZB/W mice (Forestier *et al.*, 2005) implying a role of NKT cells in lupus. CD1d- and Ja18- deficient mice exhibited decreased hyperreactivity in asthma (Lisbonne *et al.*, 2003). CD1d deficiency also decreased the level of stherosclerosis in LDL receptor deficient mice (Thomas *et al.*, 2006).

## **1.4 Aim of work**

It had long been accepted in the field that IRG proteins were expressed only upon stimulation of IFNs *in vitro*, and *in vivo* the expression was also exclusively induced

by IFNs secreted accompanying pathogen infection or inflammation events, with only a few exceptions like constitutive expression in lymphoid organ, which was presumably also due to developmental bursts of regulatory IFN- $\gamma$  expression. However all the observations above esp. those for *in vivo* expression were based on only a few reports that were neither systematic nor quantitative. Several basic questions were still open such as whether there was really constitutive expression for IRG proteins? If yes, how were the expression patterns and what were the causes of the expression *in vivo*? Finally what was the biological relevance of constitutively expressing IRG proteins? These were the questions we tried to answer in the current thesis. A combination of biochemical, cell biological, molecular biological and genetic approaches was applied to gain a detailed understanding of the expression of IRG proteins *in vivo*. Firstly, we would examine whether IRG proteins were constitutively expressed in uninfected laboratory mice tissues, with biochemical methods. Secondly, if basal expression is found, we would investigate the relationship of this expression with the IFN pathway. Thirdly, we would explore in which cell *in vivo* IRG proteins are constitutively expressed and what the relevance of this expression might be to the resistance of intracellular pathogens, using cell biological methods. Fourthly, we would try to understand the causes of particular focal expression patterns of Irga6 in liver and kidney, which maybe due to IFN production, using biochemical, and molecular biological and genetic methods. Fifthly if IFNs indeed induced the focal expression of Irga6, we would like to know if a certain subset of T cells like NKT cells should be responsible for the local production of IFN- $\gamma$  using molecular biological methods. Finally we would like to understand what might be the reasons of local NKT cell activation by biochemical methods.

## **2. Materials and Methods**

### **2.1 Materials**

#### **2.1.1 Chemicals, Enzymes and Kits**

All chemicals used were graded p.A. and purchased from Aldrich (Steinheim), Applichem (Darmstadt), Baker (Deventer, Netherlands), Boehringer Mannheim (Mannheim), GE Healthcare (München), GERBU (Gaiberg), Gibco BRL (Eggenstein), Merck (Darmstadt), Riedel de Haen (Seelze), Roth (Karlsruhe), Serva (Heidelberg), Sigma-Aldrich (Deisenhofen), ICN biochemicals, Oxoid (Hampshire, UK). Buffers and solutions were prepared with deionised and sterile water or Ultra pure water derived from Milli-Q-Synthesis (Millipore, Schwalbach). All solutions used for techniques designed to isolate, process or detect RNA were treated with DEPC.

All restriction enzymes were purchased from New England Biolabs (Frankfurt/Main); T4 DNA ligase (New England Biolabs); RNase A (Sigma); shrimp alkaline phosphatase (SAP) (USB, Staufeu; Amersham, Freiburg); Proteinase K (Merck); *Thermus aquaticus* (Taq) polymerase was prepared by Rita Lange; SP6 RNA polymerase and T7 RNA polymerase (Roche, Mannheim)

Plasmid Midi kit, RNeasy Mini kit, RNeasy Micro kit (QIAGEN, Hilden), Terminator-cycle Sequencing kit version 3.1 (ABI, Foster City, CA, USA), Rapid PCR product purification kit (Roche), SuperScript First-Strand Synthesis System for RT-PCR (Invitrogen, Karlsruhe), pGEM-T easy Vector System I (Promega, Madison, USA), Rediprime DNA labeling system (Amersham Life Sciences), HistoGreen (Linaris, Wertheim-Bettingen), alkaline phosphatase kit III (Vector laboratory, Linaris), LightCycler SYBR Green I PCR kit (Roche, Germany).

#### **2.1.2 Media**

Luria Bertani (LB) medium

10g bacto tryptone, 5g yeast extract, 10g NaCl, 1 l dH<sub>2</sub>O, for plates additionally 15g agar was added

IMDM (Iscove's Modified Dulbecco's Medium)

Supplemented with 10 % FCS, 2 mM Glutamine, 1 mM sodium pyruvate, 100 U/ml Penicillin, 100 µg/ml Streptomycin, 1x non-essential amino acids

DMEM (Dulbecco's Modified Eagle Medium)

Supplemented with 10% FCS, 100 U/ml Penicillin, 100 µg/ml Streptomycin, 1x non-essential amino acids

DMEM/Ham's F12 1:1 Medium

Supplemented with 10% FCS, 1% ITS+, 0.1 µM dexamethasone and 100 U/ml Penicillin/100 µg/ml streptomycin buffered by 15mM HEPES

### **2.1.3 Serological reagents**

Serological reagents used were: Anti-Irga6 165 rabbit antiserum (home made in Prof. Howard's lab, Institute for Genetics, Köln), anti-Irga6 mouse monoclonal antibody (mAb) 10D7 (Dr. Zerrahn, Berlin), anti-Irgm3 I68120 mAb (BD Transduction Laboratories, Lexington, Kentucky, United States), anti-Irgb6 A20 goat antiserum (Santa Cruz Biotechnology, Santa Cruz, California, United States), anti-Irgm1 A19 goat antiserum (Santa Cruz) for immunofluorescence and L115 B0 rabbit antiserum raised against the peptides QTGSSRLPEVSRSTE & NESLKNSLGV-RDDD, anti-Irgd 2078 rabbit antiserum raised against the peptides CKTPYQHPKYPKVIF & CDAKHLRKIETVNVA, anti-GRA7 5–241–178 mouse mAb (gift from R. Ziemann, Abbott Laboratories, Abbot Park, Illinois, United States), anti-Gm130 mAb (BD Transduction Laboratory), anti-calnexin rabbit antiserum (Biomol, Hamburg), rat anti-CD3-12 mAb (Vector Laboratories, Linaris), rat anti-F4/80 mAb (Serotech), anti-TCR Vβ8 mAb (BD Pharmingen), goat anti-mouse Alexa 546/488, goat anti-rabbit Alexa 546/488, donkey anti-goat Alexa 546/488, donkey anti-mouse Alexa 488, donkey anti-rabbit Alexa 488, (Molecular Probes, Eugene, Oregon, United States), donkey anti-rabbit HRP (Amersham), Goat anti-rat AP (SIGMA).

### 2.1.4 Mice

C57BL/6 and CB20 mice were obtained from the mouse facility in Institute for Genetics Uni. Köln, where all mice were maintained in specific pathogen-free conditions. Irga6<sup>-/-</sup> mice were kindly provided by Dr. Iana Parvanova (Uni. Köln, Köln). IFN receptor deficient mice (IFNAR, IFNGR, IFNAGR), TLR-2/4<sup>-/-</sup>, TLR-9<sup>-/-</sup> and MyD88<sup>-/-</sup> were kindly provide by Prof. Dr. Marina Freudenberg (Max-Planck-Institut für Immunbiologie, Freiberg). IFN- $\gamma$ <sup>-/-</sup> mice were kindly provided by Dr. Oberdan LEO (Université Libre de Bruxelles, BELGIUM). STAT-1<sup>-/-</sup> mice were kindly provided by Dr. Thomas Kolbe (University of Veterinary Medicine, Vienna). RAG-1<sup>-/-</sup> mice were kindly provided by Dr. Heike Weighardt (Technische Universitaet Muenchen, Munich). JHT mice were kindly provided by Prof. Dr. Ari Waisman (Johannes Gutenberg-Universität Mainz, Mainz). Gp130<sup>-/-</sup> mice were kindly provided by Prof. Dr. Jens Brüning (Uni. Köln, Köln). Germ-free mice were obtained from three sources namely, kindly provided by Mr. Rudolf Jörg (University of Zürich, Zürich) and Dr. Jocelyne Demengeot( Instituto Gulbenkian de Ciência, Portugal), or purchased from the Karolin's Institute in Stockholm.

Mice were infected i.p. with *L.monocytogenes* strain EGD at LD<sub>1/2</sub>.

## 2.2 Molecular biology

### 2.2.1 PCR, ligation and agarose gel electrophoresis

PCR (polymerase chain reaction) was used for the amplification of the templates for northern blot probes, the in situ hybridization probes and detection of gene-specific transcripts from cDNA. The standard reaction mix included template DNA that varies, 10 pmol of each primer, 2.5 U Taq DNA polymerase, 200 pmol dNTP-mix, 2.5  $\mu$ l 50mM MgCl<sub>2</sub>, 5  $\mu$ l 10x PCR buffer (200mM HEPES pH8.4, 500mM KCl), added up to total a volume of 50  $\mu$ l with H<sub>2</sub>O. Primers were bought from Invitrogen and Operon (Köln).

PCR products were purified using the Rapid PCR purification kit (Roche). Yield of DNA was estimated by agarose gel electrophoresis. Vector and insert were mixed at a ratio of 1:3 and ligated in a total volume of 10  $\mu$ l with T4 DNA ligase overnight at

16°C.

DNA was separated by agarose gel electrophoresis in 1x TAE buffer (0.04 M Tris, 0.5 mM EDTA, pH adjusted to 7.5 with acetic acid). Migration of the samples was visualized by using bromphenol blue and xylene-cyanol. The DNA was stained with ethidium bromide (0.3µg/ml), exposed to UV-light and documented with the BioDocAnalyze 2.1 equipment (Biometra, Göttingen).

### **2.2.2 Competent cells and transformation**

2 ml LB medium supplemented with 20 mM MgSO<sub>4</sub>, 10 mM KCl were inoculated with one E. coli colony and cultured overnight at 37°C. The culture was then diluted 1:100 and incubated at 37°C for approximately 2 h until a OD<sub>600</sub> density of 0.45 was reached. The Culture was incubated 10 min on ice and the cells were then collected by centrifugation for 5 min at 6.000 rpm at 4°C. The cells were resuspended in TFB 1 (30 mM KOAc, 50 mM MnCl<sub>2</sub>, 100 mM RbCl, 10 mM CaCl<sub>2</sub>, 15% (w/v) glycerine, pH 5.8; 30 ml for 100 ml culture) and incubated for 10 min on ice. After pelleted by centrifugation for 5 min at 6.000 rpm at 4°C, the cells were resuspended in TFB 2 (10 mM MOPS, pH 7.5, 75 mM CaCl<sub>2</sub>, 100 mM RbCl<sub>2</sub>, 15 % w/v glycerine; 4 ml for 100 ml culture). Aliquots of 100 µl of competent bacteria were frozen at -80°C.

A 100 µl aliquot of competent bacteria was thawed on ice. 2µl of the ligation reaction or 5 ng of plasmid was added and mixed well before incubating for 20 min on ice. The cells were then heat-shocked for 45 sec at 42°C, followed by 5 min incubation on ice. 1 ml of LB medium was added and cells were incubated for 30-45 min on roller at 37°C. 100-500 µl of this culture were plated on LB agar plates containing the appropriate antibiotics for selection.

### **2.2.3 Plasmid DNA isolation from bacteria**

1.5 ml from 3 ml overnight LB cultures supplemented with the appropriate antibiotics was harvested by centrifugation for 5 min at 13,000 rpm. Cells were resuspended in 100 µl P1 (50 mM Tris-Cl, pH 8.0, 10 mM EDTA, 100 µg/ml RNase A) and lysed by the addition of 100 µl P2 (200 mM NaOH, 1 % SDS) for 5 min at RT.

Alkaline lysis was stopped by adding 130  $\mu$ l P3 (3 M KAc, pH 5.5). Cellular debris and genomic DNA were pelleted by centrifugation for 20 min at 13,000 rpm. The supernatant was mixed with 700  $\mu$ l 100% ethanol and plasmid DNA was pelleted by centrifugation for 15 min at 13,000 rpm. The pellet was then washed with 1 ml 70% ethanol and spun again for 5 min at 13,000 rpm. The supernatant was removed and the pellet was air dried before resuspending in 50  $\mu$ l Tris pH 8.0. For larger yield the Plasmid Midi kit (QIAGEN) was used.

#### **2.2.4 DNA-Sequencing**

DNA was sequenced using the dideoxy-chain termination method (Sanger 1977). The ABI 3730 sequencer in the Cologne Centre for Genomics (CCG) was used with the ABIR Prism™ BigDye V3.1 Terminator Cycle Sequencing Reaction kit (PE Applied Biosystems).

#### **2.2.5 Total RNA isolation and cDNA synthesis**

Mice were sacrificed and organs were taken and stored in the RNA stabilizing solution RNeasy Lysis Buffer (QIAGEN). Total RNA was extracted from tissues using the RNeasy Mini Kit (QIAGEN) as described in user's manual. The integrity of total RNA was tested on agarose gels.

The SuperScript First-Strand Synthesis System for RT-PCR (Invitrogen, Karlsruhe) using oligo(dT) primers and random hexamers (1:1) was employed for generating cDNA from total RNA.

#### **2.2.6 Reverse-transcriptase PCR**

1  $\mu$ l cDNA from liver and T cells or 2-4  $\mu$ l of cDNA from laser dissected materials (2.3.5) were used in each of the following RT-PCR reaction as templates. Primers located in different exons were used to generate a specific product only from cDNA but not from genomic DNA (Table 2). For nested-PCR, 1  $\mu$ l PCR product of first round of PCR was used as template for the second PCR, which made use a second internal 5' or 3' primer and the common 3' or 5' primer, and the cycle number was

always 45 for each round of PCR. All final PCR-products were verified by sequencing.

**Table 2. Primers used in reverse-transcriptase PCR.**

primer name	primer sequence 5' to 3'	product size
IFN $\gamma$	CTGAGACAATGAACGCTACACA	507bp
	TTATTGGGACAATCTCTTCCC	
IFN $\gamma$ nest	ACTGGCAAAAGGATGGTGAC	332bp
	TTATTGGGACAATCTCTTCCC	
TCR $\beta$ chain	GGT (G/T) T (A/C/T) (C/T) TGGTA (C/T) (A/C/T) (A/G) (A/C/G/T) CA	450bp
	TCAGGCAGTAGCTATAA	
TCR $\beta$ chain nest	GGT (G/T) T (A/C/T) (C/T) TGGTA (C/T) (A/C/T) (A/G) (A/C/G/T) CA	280bp
	GGTGGAGTCACATTTCT	
TCR V $\alpha$ 14 chain	CTAAGCACAGCACGCTGCACA	350bp
	GAAGCTTGTCTGGTTGCTCCAG	
TCR V $\alpha$ 14 chain nest	CTAAGCACAGCACGCTGCACA	220bp
	TCGGTGAACAGGCAGAGGGTG	
TCR V $\alpha$ 2 chain	TGCAGTTATGAGGACAGCACTT	480bp
	GAAGCTTGTCTGGTTGCTCCAG	
TCR V $\alpha$ 2 chain nest	TGCAGTTATGAGGACAGCACTT	350bp
	TCGGTGAACAGGCAGAGGGTG	
TCR V $\alpha$ 8 chain	ACGCCACTCTCCATAAGAGCA	360bp
	GAAGCTTGTCTGGTTGCTCCAG	
TCR V $\alpha$ 8 chain nest	ACGCCACTCTCCATAAGAGCA	230bp
	TCGGTGAACAGGCAGAGGGTG	
TCR V $\alpha$ 17 chain	TTCCATCGGACTCATCATCAC	340bp
	GAAGCTTGTCTGGTTGCTCCAG	
TCR V $\alpha$ 17 chain nest	TTCCATCGGACTCATCATCAC	210bp
	TCGGTGAACAGGCAGAGGGTG	
mouse GAPDH	GTCTACATGTTCCAGTATGACTCCACTCACGG	837 bp
	GTTGCTGTAGCCGTATTCATTGTCATACCAGG	

### 2.2.7 Real-time PCR

Real-time quantitative polymerase chain reaction analysis was performed using the cDNA generated as described in 2.2.5 or 2.3.5. PCR was carried out in a Light Cycler I System (Roche, Germany) using a LightCycler SYBR Green I PCR kit (Roche, Germany) following the manufacturer's instructions. The 5' primers specific for Irga6 1A (5'-TGCTTCCTGAAGCTGAACTA-3') and 1B (5'-ACCGAGGGCTATTCCCTC

TCA-3') together with a 3' primer on the coding exon (5'-CAGAGAAGGGATGAT ATTCAC-3') were used to detect expression level of Irga6 1A and 1B transcript forms as target genes. 5' primer (5'-GTCTACATGTTCCAGTATGACTCCACTCACGG-3') and 3' primer (5'-GTTGCTGTAGCCGTATTCATTGTCATACCAGG-3') specific for mouse GAPDH were used to detect mGAPDH as reference gene as input control. cDNA was synthesized from total RNA extract of liver or collected sections of Irga6 focal and non-focal expression in liver with LMD technique as described in 2.3.5. 2-4  $\mu$ l of cDNA solution from materials collected by LMD was used as templates. PCR was programmed as recommended by the user's manual. Primer efficiency for Irga6 1A, 1B or mGAPDH was determined using liver cDNA dilution serial (1, 1/10, 1/100...) as templates and the method was described previously (Pfaffl, 2001). The ratio of "patch" to "non-patch" for Irga6 1A or 1B expression was then determined by PFAFFL METHOD (Pfaffl, 2001). Melting curve analyses were performed to verify the amplification specificity. Each sample was tested in duplicate or triplicate. To determine the ratio of Irga6 1A specific products in the final PCR products, final products of PCR for 1A were cloned in to pGEM-T-easy (Promega) vector and many clones were sequenced. The percentage of 1A clones was then calculated.

### 2.2.8 T cell receptor repertoire screening

In order to determine the T cell receptor V $\beta$  usage and V $\alpha$ 14 junctional diversity, nested-RT-PCR was first performed. cDNA from more than 50 Irga6 cored patches collected by LMD or cDNA of 1,000 lymphocytes from mesenteric and cervical lymph nodes were synthesized as described in 2.3.5. 1 $\mu$ l or 2-4 $\mu$ l cDNA from T cells or Irga6 patches were taken as template for the first round of PCR, the product of which was used as template for the next round of PCR. 45 cycles were used for both PCR reactions. The V $\beta$ 8 and C $\beta$  primers (Kawagishi *et al.*, 2003), V $\alpha$ 14 and C $\alpha$  primers (Lantz and Bendelac, 1994), V $\alpha$ 2, V $\alpha$ 8, V $\alpha$ 17 primers (Yoshida *et al.*, 2000b) were described before (Table 2). The final products of nested-PCR were cloned into pGEM-T-easy (Promega) and clones were sequenced. The sequences were then compared to classical TCR V $\alpha$  sequences in the database online using

IMGT/V-QUEST (<http://imgt.cines.fr/>), and the clones with a sequence identity of more than 95% to known V $\alpha$  sequences were identified as correct V $\alpha$  clones. Clones were classified into groups with same junctions and representatives from each group were selected aligned and analyzed with free software GeneDoc (Version 2.6.002) (<http://www.nrbsc.org>) and Vector NTI (Version 9, Invitrogen).

### **2.2.9 Northern blot analysis**

5  $\mu$ g of total RNA was separated on 1% agarose/formaldehyde gels and transferred onto Hybond-N+ membrane (Amersham Biosciences, Uppsala, Sweden) by standard procedures. The blots were probed with randomly primed [ $\alpha$ -<sup>32</sup>P]dCTP-labeled Irga6 or murine -GAPDH ORF using the Rediprime DNA labeling system (Amersham Life Sciences). Hybridizations were performed overnight at 42°C in a buffer containing 50% formamide, 5x Denhardt's solution, 5x standard saline-phosphate-EDTA (SSPE), 1% SDS, and 10% dextran sulfate. Membranes were washed under stringent conditions. The hybridization signal was detected by autoradiography, using Kodak X-OMAT AR films. Labeled ORF of mouse glyceraldehyde-3-phosphate dehydrogenase (GAPDH) was used as a control probe to reveal the amount of loaded total RNA, and the RNA Millenium Marker (Ambion) was used as the RNA size standard.

### **2.2.10 Western blot analysis**

Mice were sacrificed and organs were taken, snap frozen in liquid nitrogen and grinded. 10  $\mu$ l RIPA buffer (150 mM NaCl, 50 mM Tris, 1% NP-40, 0.1% SDS, 0.5% deoxycholate, 5 mM EDTA, 1% Triton X-100, pH 8.0, one Complete Mini Protease Inhibitor tablet per 10 ml buffer (Roche) was added for each mg of tissues. The tissues were then homogenized with 20 gauge syringe. The homogenized lysate was incubated for 20 min on ice and then centrifuged for 30 min at 23,000 g. The supernatant was taken and analyzed by Western blot.

Protein samples for instance tissue or cell lysates were separated by 10% SDS-PAGE and then transferred to a nitrocellulose membrane by electroblotting. After transfer the

membrane was stained with Ponceau S (0.1 % (w/v) Ponceau-S in 5 % (v/v) acetic acid) (SIGMA) to locate protein size standard Page Ruler™ on the membrane. Then unspecific protein binding sites on the membranes were blocked by incubation for 1 h at RT in 5 % milk powder, 0.1 % Tween20 in PBS. Antisera/antibodies were diluted in 10 % FCS, 0.1 % Tween20 in PBS. Protein bands were visualized using the enhanced chemiluminescence (ECL) substrate.

### **2.3. Histology**

#### **2.3.1 Tissue preparation and section**

Mice tissues were taken and fixed overnight in 4% paraformaldehyde in TBS at 4°C. Tissues were washed in PBS and 0.89% NaCl 1 hour each before dehydrated with an ethanol serial at 4°C (50%, 70%, 90%, 96% each step 4h) and then in isopropanol 8 h at RT. A paraffin:isopropanol (1:1) solution was applied to the tissues overnight before the evaporation of the isopropanol 8h at 60°C. Fresh paraffin was then exchanged several times (2h each) at 60°C before the tissues were incubated in fresh paraffin and moved to RT. The embedded tissues were cut with a microtome RM 2065 (Leica Microsystems, Wetzlar) into 6 µm thick serial sections, put on SuperFrost slides (Menzel, Braunschweig) and dried at 40°C overnight. Before staining, sections were dewaxed with Xylene (2x 10 min), then rehydrated by an ethanol series (100%, 95%, 90%, 70%, 30%, PBS each step 3-5 min) and postfixated for 1 h in 4% paraformaldehyde in PBS. For frozen section, tissues were snap-frozen in liquid nitrogen and cryosections were prepared on a cryotome CM 3050S (Leica Microsystems, Wetzlar) and dried at 40°C overnight. Before staining, cryosections were fixed in acetone at 4°C for 10min.

#### **2.3.2 Immunohistochemistry**

Dewaxed and postfixated paraffin sections were incubated 10 min in boiling 10 mM citrate buffer pH 6.0 to damask antigen epitopes and then washed 5 min with PBS. For the epitope-demasking in F4/80 staining or CD3 staining, paraffin sections were incubated in 0.1% Trypsin (SIGMA Type II) solution (with 0.1% CaCl<sub>2</sub>, pH7.8)

30mins at 37°C or in 1mM EDTA pH8.0 for 10mins at 100°C respectively. For frozen section no epitope-demasking was required. Unspecific protein binding and endogenous peroxidases were saturated by a 20 min incubation in Quenching buffer (1 % BSA, 0.3 % H<sub>2</sub>O<sub>2</sub> in PBS). After 3 times PBS washing (1 min each) at RT, the sections were incubated with the primary antibody diluted in DAKO diluent (DAKO, Hamburg) in a humid chamber for 1hour at RT or overnight at 4°C. After 3 times PBS washing (2 min each) the sections were incubated with the HRP-coupled or AP-coupled secondary antibody in a humid chamber for 1 hour at RT followed by another 3 times PBS washing. Colour-reaction was performed with peroxidase substrate kit HistoGreen (Linaris, Wertheim-Bettingen) or alkaline phosphatase kit III (Vector laboratory, Linaris) to produce green or blue color. The nuclei were counterstained with Nuclear Fast Red. For HistoGreen staining which produces water-soluble colour, the sections had to be dehydrated (3 times 30 sec 100% ethanol, 2 times 30 sec xylene at RT) before mounting with Entellan (Merck). For Irga6 and F4/80 or CD3 double staining, Irga6 was stained first with 165/3 and HRP-coupled secondary antibody using 1ml 0.5% AEC (SIGMA) N,N'-dimethylformamide mixed with 19ml 50mM Acetate pH5.2 and 3µl 30%H<sub>2</sub>O<sub>2</sub> as peroxidase substrate, and the sections were then incubated in PBS for 1h to quench the residue H<sub>2</sub>O<sub>2</sub> before F4/80 or CD3 was stained with AP-coupled secondary antibody using alkaline phosphatase kit III mentioned above. Samples were analysed using Zeiss Axioplan II microscope (Zeiss, Jena) equipped with SPOT RT slider digital camera (Diagnostic instruments).

### **2.3.3 Immunofluorescence**

Fixed cryosections were washed with PBS and fixed in 3% paraformaldehyde for 20 min at room temperature. Cells were permeabilized with 0.1% saponin and blocked with 3% BSA (Roth) for 1h at RT. The cells were then incubated with the primary antibody diluted in blocking buffer for 1 h in a humid chamber, washed, incubated with the secondary antibodies with DAPI, washed again and mounted with with Prolong Gold antifade reagent (Invitrogen) and sealed with nail polish. The cells were analyzed using a Zeiss (Oberkochen, Germany) Axioplan II fluorescence microscope

equipped with a cooled charge-coupled device camera (Quantix; Photometrix, Tucson, AZ).

#### **2.3.4 In situ hybridization**

The templates for the probe were amplified from the vector pGW1H-IIGP1 using Irga6 antisense primer (5'-CGGGGAAGTCATAGTGACAA-3') and sense primer (5'-GGATCAGGGAAGTCCAGCTT-3') cloned into the vector pGEM-T-easy (Promega). The templates for the sense and antisense probes were then amplified including either the promoter of the Sp6- or T7-RNA-polymerase. The RNA-probes were synthesized using the proper RNA-polymerase and labelled with DIG using the DIG labelling reaction mix (Roche) and then purified by ethanol precipitation.

After dewaxing and postfixation, paraffin embedded sections of mice liver were digested with Proteinase K (10 µg/ml in 0.1 M Tris pH 7.5) for 10 min at 37°C, which was stopped by incubation in 0.2% glycine in PBS for 10 min at RT. Sections were then washed (2 times PBS, once 0.2 N HCl then once PBS) and positively charged amino acids were blocked by incubation in 0.1 M triethanolamine pH 8.0, 0.25% acetic acid anhydrate. After washing with PBS and H<sub>2</sub>O the samples were incubated for 2 hours at 70°C with prehybridization buffer (50% formamide, 5x SSC pH 7.0, 1x Denhardt's solution, 0.1% Tween20). 1-5 µl of the proper probe was preheated to 70°C mixed with 50 µl prehybridization buffer and 2 µl yeast tRNA (final concentration 0.1 mg/ml) and put on ice immediately. 55 µl of the hybridization solution was added on the slide, covered with a coverslip and incubated in humid chamber overnight at 70°C. After hybridization the slides were first washed 3 times for 30 min at 70°C with Solution I (50% formamide, 5x SSC pH 7.0, 1% SDS) and then 3 times for 30 min at 65°C with Solution II (50 % formamide, 2x SSC pH 7.0, 0.2% SDS), which was followed by 3 times washes (5 min each) at RT with MAB (100 mM maleic acid, 150 mM NaCl, 0.1% Tween20, 2 mM Levamisole, adjust to pH 7.5 with NaOH). The slides were then blocked for 2-3 hours at RT with 1% blocking reagent (Roche) in MAB before application of Anti-Digoxigenin-AP Fab fragments (Roche) (1:4000 in MAB/block) in a humid chamber at 4°C overnight. The sections

were then washed with MAB (3 times 10 min and 3 times 30 min at RT) and 3 times 10 min with NTMT (100 mM Tris pH 9.5, 50 mM MgCl<sub>2</sub>, 100 mM NaCl, 2 mM Levamisole, 0.1% Tween20). BM purple substrate (Roche) with 2 mM Levamisole was used for the colour reaction which took 2 to 5 days. When the staining was finished the slides were washed with H<sub>2</sub>O and mounted with Kaiser's glycerine (Merck). Note that all the solutions were made with DEPC H<sub>2</sub>O and glassware were baked to avoid RNase contamination.

### **2.3.5 Laser Microdissection (LMD)**

Mice liver were taken and snap-frozen in liquid nitrogen. 6 µm thick cryosections were cut using a cryotome CM 3050S (Leica Microsystems, Wetzlar) and sections were put on PALM MembraneSlides (P.A.L.M. Microlaser Technologies, Bernried), which was covered with a PEN membrane. Consecutive sections were cut and all odd numbered sections were on one slide (named 'A') and the adjacent even numbered sections were on another slide (named 'B'). Slides were then fixed for 20 min at -20°C in 70 % ethanol and then washed with H<sub>2</sub>O for 5 min. 'B' slide was stored at -80°C and 'A' slide was then stained for Irga6 with 165/3 using histogreen substrates. Pictures of Irga6 focal expression were taken. 'B' slide was then taken out and only counter-stained with Nuclear Fast Red, dehydrated by an ethanol series (70%, 96%, 100% each step 2 min) and dried for 10 min at 50°C. Irga6 focal expression was found by comparison to the photos of adjacent sections on 'B' slide, and expression foci were cut with laser beam of lower power but high focus using the Laser Microdissection (LMD) equipment of the Institute for Pathology (University Clinic, Köln) consisting of an Interface Microbeam Mini laser (P.A.L.M Microlaser Technologies) and an Axiovert 135 microscope (Zeiss, Jena). The cut samples were collected in a small drop (less than 1µl) of mineral oil in the cap of LPC Microfuge tubes (P.A.L.M. Microlaser Technologies).

Total RNA from the dissected samples was extracted using the RNeasy Micro kit (QIAGEN), using the 10fold amount of carrier RNA and the RNA was eluted in the smallest possible volume (12 µl). cDNA was made with 8µl of total RNA using the

Superscript First-Strand Synthesis System for RT-PCR kit (Invitrogen, Karlsruhe).

## **2.4. Cell biology**

### **2.4.1 Mammalian cell line culture**

L929 mouse fibroblasts, and TIB-75 hepatocytes (Martens *et al.*, 2004) were cultured in IMDM supplemented with 10% FCS (Sigma-Aldrich, Deisenhofen, Germany), 2 mM L-glutamine (Invitrogen Life Technologies, Eggenstein, Germany), 1 mM sodium pyruvate (ICN, Eschwege, Germany), 100 U/ml penicillin (Invitrogen Life Technologies), and 100 µg/ml streptomycin (Invitrogen Life Technologies). Cells were induced with mouse IFN-γ (Cell Concepts, Umkirch, Germany) at a concentration of 200 U/ml for 24 hours.

### **2.4.2 Mouse hepatocytes isolation and culture**

Hepatocytes were isolated from liver using a two-step liver perfusion method (Modified from Klaunig *et al.*, 1981). Mice were anaesthetized with 2-5 ml Avertin (kindly provided by Prof. Jens Brüning, Köln) and injected with 100µl Heparin-Na (5000IU/ml). Mice were then dissected and liver portal vein was cannulated and perfused with prewarmed (37°C) Krebs-Ringer-Buffer (KRB) (115 mM NaCl, 5.9 mM KCl, 1.2 mM MgCl<sub>2</sub>, 1.2 mM NaH<sub>2</sub>PO<sub>4</sub>, 1.2 mM Na<sub>2</sub>SO<sub>4</sub>, 2.5 mM CaCl<sub>2</sub>, 25 mM NaHCO<sub>3</sub>, 10 mM glucose) at a flow rate of 3ml/min for 30 mins. Subsequently prewarmed 50ml KRB with 1mM EDTA was used for perfusion followed by 100ml KRB with 0.5mM CaCl<sub>2</sub> and 0.05% collagenase (SIGMA) at the same flow rate. Hepatocytes were then liberated from liver capsule, filtered through 100µm gauze and cell suspension was washed 2 times at 4°C first with washing buffer (1xHanks buffer, 0.5% BSA, 10mM HEPES pH7.65) at low speed (50g) and then 2 times with DMEM/Ham's F12 1:1 Medium. Cells were then preseeded for 15min on collagen coated plates and transferred to other collagen coated plates for culture for several days. Note: All buffers and gauze were sterilized and great care should be taken when handling the cells to avoid high mortality.

### 2.4.3 Immunofluorescence for cells

Cells were washed with PBS and fixed in 3% paraformaldehyde for 20 min at room temperature. Cells were permeabilized with 0.1% saponin and blocked with 3% BSA (Roth) for 1 h at RT. The cells were then incubated with the primary antibody diluted in blocking buffer for 1 h in a humid chamber, washed, incubated with the secondary antibodies with DAPI, washed again and mounted with with Prolong Gold antifade reagent (Invitrogen) and sealed with nail polish. The cells were analyzed using a Zeiss (Oberkochen, Germany) Axioplan II fluorescence microscope equipped with a cooled charge-coupled device camera (Quantix; Photometrix, Tucson, AZ).

### 2.5. *T. gondii*. passage and infection

Tachyzoites from *T. gondii* strain ME49 were maintained by serial passage in confluent monolayers of human foreskin fibroblasts (HS27, ATCC). Following infection of fibroblasts, 3 days later parasites were harvested from the culture supernatant and purified from host cell debris by differential centrifugation (5min at 50 g, 15 min at 500g). Parasites were resuspended in medium and immediately used for inoculation of host cells.

Murine primary hepatocytes were either left untreated or stimulated with IFN- $\gamma$  (R&D Systems, Minneapolis, Minnesota, United States) at 200 U/ml for 24 h prior to infection. For determination of *T. gondii* growth via uptake of [3H]-uracil, hepatocytes were inoculated with *T. gondii* at different multiplicity of infection (MOI). After 48 h of incubation, cultures were labeled with 11Ci/well [3H]-uracil (Hartmann Analytical) for an additional 24 h. The amount of incorporated uracil, directly proportional to the parasite growth, was determined by liquid scintillation counting. For immunostaining, hepatocytes were inoculated with *T. gondii* at a MOI of 10 for 2 h. Extracellular parasites were then removed by extensive washing with PBS and cells were fixed. Vacuoles containing intracellular parasites were identified by immunostaining for the *T. gondii* dense granule protein GRA7 that is associates with the intravacuolar network and the PV membrane. The immunostaining protocol is as described in 2.4.3.

## 2.6. Promoter analysis

All available public databases were screened with the Basic local alignment search tool BLAST (Altschul *et al.*, 1990) for ESTs of Irga6 sequences. These included the databases of NCBI (<http://www.ncbi.nlm.nih.gov>), ENSEMBL (<http://www.ensembl.org>). Sequence alignments were performed with Vector NTI and edited manually. Shading of alignments and the amino acid identity and similarity matrix were conducted with GeneDoc (Version 2.6.002) (<http://www.nrbsc.org>). The region 500bp upstream of the transcription start point were designated as the putative promoter regions and screened for transcription factor binding sites. Putative conserved transcription factor binding sites in the promoters of Irga6 were identified using ConSite (<http://www.phylofoot.org>) (Sandelin *et al.*, 2004) and confirmed manually.

### 3. Results

#### 3.1. Irga6 is constitutively expressed in mouse tissues

The well established view in the field that IRG proteins are expressed under the tight regulation of IFNs has been fully accepted. There are however, a few reports of constitutive expression of IRG proteins in mouse tissues (Collazo *et al.*, 2001; Taylor *et al.*, 1996). Nevertheless a systematic and quantitative search for constitutive expression of IRG *in vivo* is still missing. In order to examine whether there are constitutive expression of IRG proteins *in vivo*, several quantitative experiments were performed here to determine the expression of Irga6 as well as Irgm3 in a variety of mouse tissues.

##### 3.1.1 Irga6 has high and constant level of constitutive expression in mouse liver

It has been described by Boehm and colleague that in uninfected mouse liver, *IIGP1* (*Irga6*) gene had insignificant, if any, basal expression, whereas upon *Listeria monocytogenes* infection the *IIGP1* (*Irga6*) expression was induced to an extremely

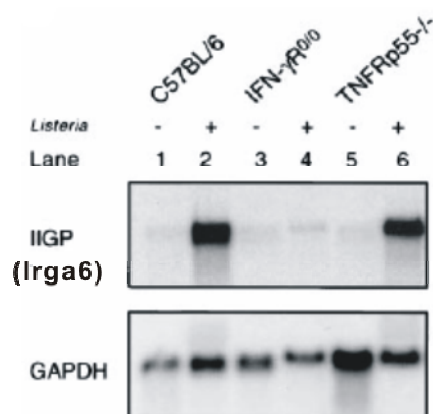


**Figure 5. Inducibility of IIGP1 (Irga6) in different mouse strains upon infection with *L. monocytogenes*.** As shown by Northern blot analysis of liver RNA, mice were infected with one-tenth of the LD50. Livers were isolated 24 h postinfection. Ten micrograms of total RNA was loaded per lane. *lanes 1 and 2* C57BL/6 mice; *lanes 3 and 4*, IFN- $\gamma$ <sup>0/0</sup> mice; *lanes 5 and 6*, TNFRp55<sup>-/-</sup> mice; *lanes 1, 3, and 5*, uninfected control mice. GAPDH hybridization is shown as a loading control. (modified from Boehm *et al.*, 1998)

high level and the induction was totally IFN- $\gamma$  dependent (Fig. 5) (Boehm *et al.*, 1998). Later on however, it was observed that in uninfected mouse liver Irga6 protein had relatively high level of expression which was comparable to that in IFN- $\gamma$ -induced L929 cells. In order to examine whether there was constitutive expression of Irga6 in liver, northern blot analysis using almost the same setup as that of Boehm *et al.* was performed with IFN- $\gamma$ -induced or uninduced L929 cells as control (Fig. 6).

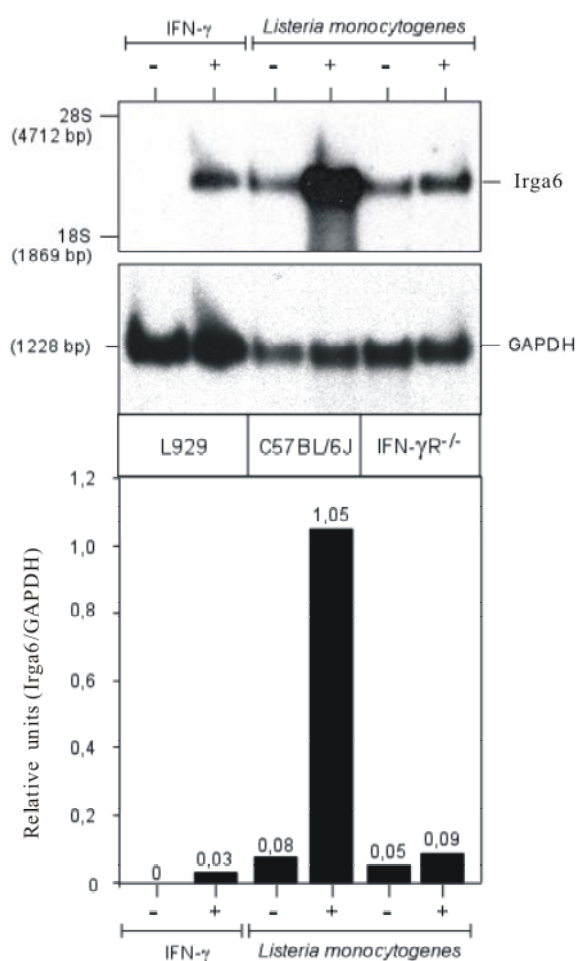


**Figure 6. Irga6 has strong constitutive expression in mouse liver on RNA level.** Northern blot analysis of Irga6 expression in mouse liver was carried out. WT (C57BL/6J) or IFN- $\gamma$  receptor knock out (IFN- $\gamma$ R<sup>-/-</sup>) mice were infected with *Listeria monocytogenes* at LD<sub>50</sub> for 24 hours. Total RNA was extracted from infected (+) and uninfected (-) tissues. L929 cells unstimulated (-) or stimulated (+) with IFN- $\gamma$  (200U/ml) for 24 hours were used as control. The total RNA was subjected to northern blot. The Irga6 ORF was labeled by [ $\alpha$ -<sup>32</sup>P]-dCTP as probe. GAPDH was also detected as loading control. The signal intensity was quantified by phosphorimager and Autoradiography was performed. The histogram presents relative units of Irga6 signal after normalization to GAPDH signal. (modified from Jia Zeng Master Thesis, 2003)

Total RNA extracts from liver tissues of WT or IFN- $\gamma$  receptor knock out mice infected with *Listeria monocytogenes*. Murine fibroblast cell line L929 stimulated or unstimulated by IFN- $\gamma$  was used as control. The Irga6 ORF was chosen as probe for detecting Irga6 mRNA. After normalization to GAPDH signals, which served as a loading control, a significant level of Irga6 expression in uninfected liver was detected while there was no expression in unstimulated L929 cells. The Irga6 expression in uninfected liver was almost three times higher than that in IFN- $\gamma$  stimulated L929 cells. In the infected liver, however, this resting expression rose more than 13 fold, which is well known due to in vivo massive production of IFN- $\gamma$ . For uninfected IFN- $\gamma$  receptor knock out mice, there was still a significant level of Irga6 expression and this expression was only slightly increased when the mice were infected (Fig. 6). The quantitative northern blot clearly demonstrated that Irga6 had a strong constitutive RNA expression in liver and this expression was not very much influenced by IFN- $\gamma$ .

Secondly, western blot was carried out to determine if this RNA expression is translated into protein. Liver tissues of baby (3, 4 days) and adult (4, 6 weeks) mice from different litters were ground in liquid nitrogen and lysed in RIPA buffer. Protein lysates were analyzed using Irga6 monoclonal antibody 10D7 in western blot. Indeed Irga6 showed a very strong protein expression, which judging by the Irga6 signal intensity normalized to the loading control calnexin, was even higher than that in IFN- $\gamma$  stimulated L929 cells (Fig. 7). The Irga6 expression in liver was also very stable, as seen from the constant level of expression in livers from all the mice individuals of different ages and litters. Irgm3 was also tested here, which exhibited a similar expression profile in liver as Irga6 but at a much lower expression level. Irgm3 western blot exhibited 3 bands and the intensity of each band varies between constitutive expression in liver and induced expression in L929 cells, for which we do not have an explanation yet (Fig. 7).

In conclusion, in liver Irga6 (also Irgm3) does have high constitutive expression both on RNA and protein level and this expression is almost independent on IFN- $\gamma$ .

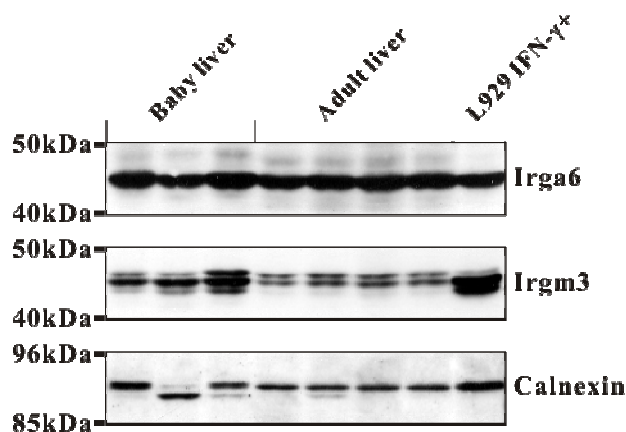


**Figure 7. Irga6 has strong constitutive expression in mouse liver on protein level.** Western blot analysis of Irga6 expression in mouse liver was made. Livers from CB20 baby mice (3 or 4 days) and adult mice (4 or 6 weeks) were first ground in liquid nitrogen, weighed and lysed in RIPA buffer. L929 cells stimulated (+) with IFN- $\gamma$  (200U/ml) for 24 hours were used as positive control. Loading for liver lysates is 100 $\mu$ g/lane and for L929 is 5,000cells/lane. Irga6 mAb 10D7 and anti-Irgm3 mAb 168120 were used for detecting respective proteins. Calnexin was also probed as a loading control. (modified from Jia Zeng Master thesis, 2003)

### 3.1.2 Irga6 constitutive expression in liver has general and focal patterns

To analyze the distribution of Irga6 constitutive expression, in situ hybridization was carried out. Fixed C57BL/6 mouse liver were embedded in paraffin and cut into 6 $\mu$ m

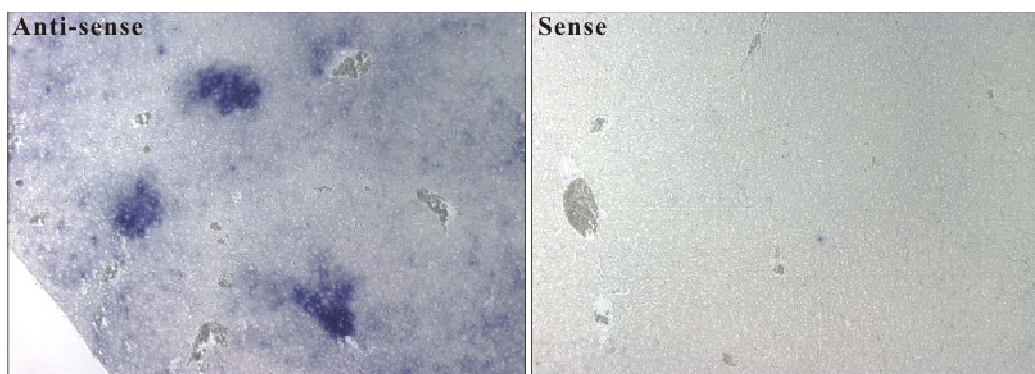


**Figure 8. Irga6 has general and focal expression pattern in mouse liver.** In situ hybridization analysis of Irga6 expression in mouse liver was performed. Fixed C57BL/6 adult mice liver were embedded in paraffin and cut into 6 $\mu$ m sections. DIG-labeled single stranded RNA sense and anti-sense probe was made by in vitro transcription using the 5' part of Irga6 ORF (1-490bp) as template. The hybridized RNA probe was detected by anti-DIG antibody, and visualized by color reaction catalyzed by alkaline phosphatase (AP) coupled to the antibody using BM purple (Roche) as substrate. Pictures were taken using light microscopy (10x10, ZEISS Axiophot).

sections. DIG labeled RNA probe was made by in vitro transcription using the 5' part of Irga6 ORF as template. The positive hybridization signal was visualized by color reaction catalyzed by alkaline phosphatase (AP) coupled to anti-DIG antibody using BM purple (Roche) as substrate. The anti-sense probe revealed an overall expression of Irga6 mRNA expression in the liver and in addition there was very intense focal expression, which was normally sparsely dispersed (Fig. 8).

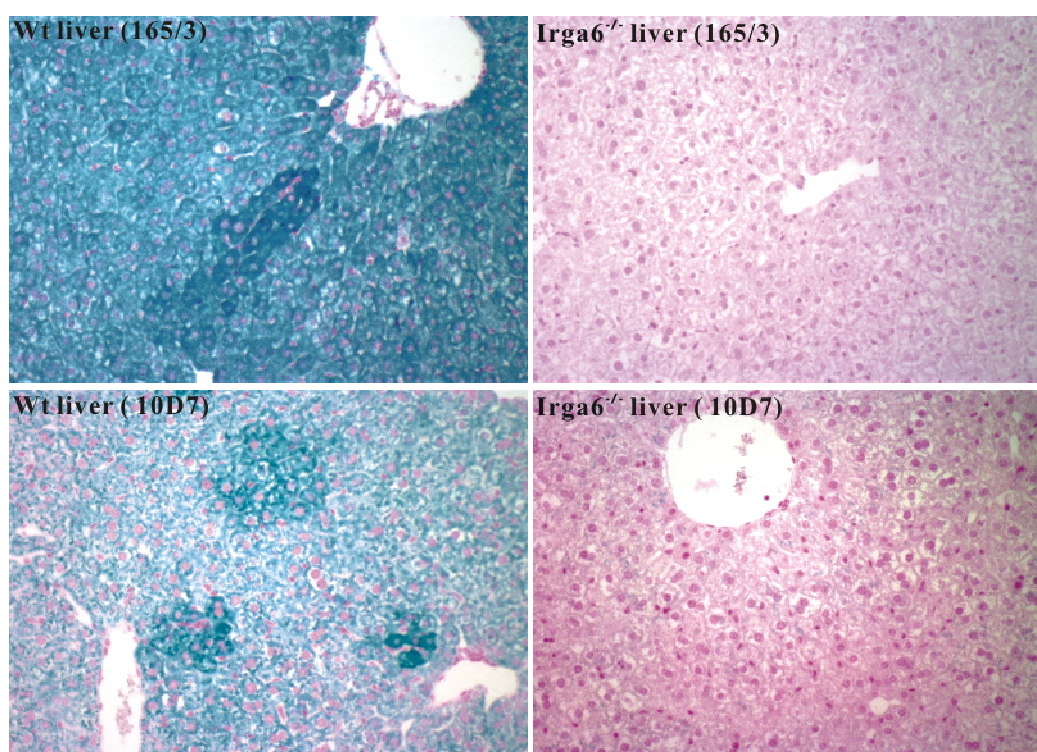


**Figure 9. Irga6 has general and focal expression pattern in mouse liver.** Immunohistological analysis of Irga6 expression in mouse liver was made. C57BL/6 WT and Irga6<sup>-/-</sup> adult mice liver were embedded in paraffin and cut into 6µm sections. Irga6 antiserum 165/3 and mAb 10D7-FITC was used for immunostaining. The secondary antibody for 10D7-FITC was against FITC to avoid unspecific binding by anti-mouse secondary antibody. The antibody specific binding was visualized by a green color reaction catalyzed using a Horseradish peroxidase (HRP) substrate Histogreen. Counter staining of nucleus (red) was done by nuclear fast red (NFR). Pictures were taken using light microscopy (10x10, ZEISS Axiophot).

Immunohistochemistry method was also applied to detect the expression pattern of Irga6 protein. Paraffin sections of mouse liver were stained with both Irga6 antiserum 165/3 and mAb 10D7 (green). In contrast to liver from Irga6<sup>-/-</sup> mouse, WT liver presented a very strong overall protein expression of Irga6 in both antibodies' staining.

Also extremely intensive Irga6 focal staining could be observed, which normally had very clear-cut boundaries and took the shape of patches (Fig. 9).

Both in situ hybridization and immunohistochemistry demonstrated that in liver Irga6 is constitutively expressed in two distinct patterns, overall general expression and intensive focal expression.

### 3.1.3 Irga6 has constitutive expression in many mouse tissues

Western blot analysis of different mouse tissues was carried out. Various mouse tissues including liver, heart, skin, spleen, intestine, thymus, lung, testis, kidney and brain were lysed in RIPA buffer and protein lysates were then subjected to western blot analysis. Irga6 was also expressed in many other tissues.

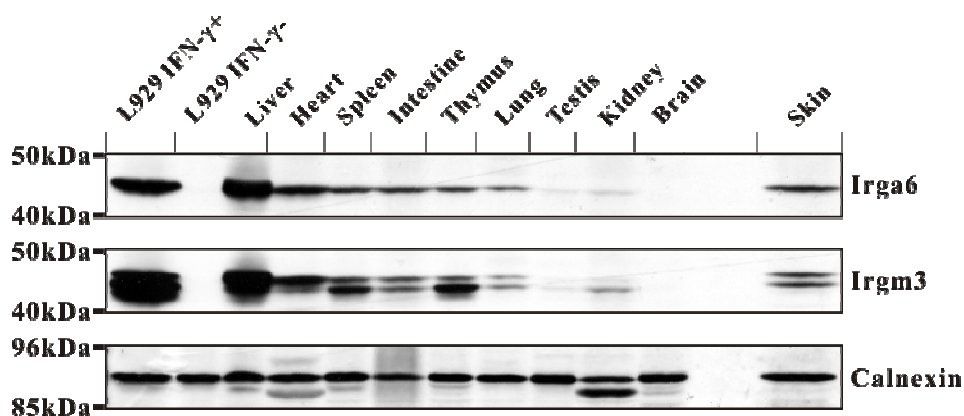


**Figure 10. Irga6 is constitutively expressed in many mouse tissues in western blot.** Western blot analysis of Irga6 expression in several mouse tissues was made. Liver, heart, skin, spleen, intestine, thymus, lung, testis, kidney, brain were first ground in liquid nitrogen, weighed and then lysed in RIPA buffer. L929 cells stimulated (+) by IFN- $\gamma$  (200U/ml) for 24 hours were used as positive control. Loading for all tissue lysates is 50 $\mu$ g/lane except for skin, for which it was 150 $\mu$ g/lane. For L929 the loading is 5,000cells/lane. Irga6 mAb 10D7 and anti-Irgm3 mAb 168120 were used for detecting respective proteins. Calnexin was also probed as loading control. (modified from Jia Zeng Master Thesis, 2003)

Judging by the Irga6 signal normalized to loading control calnexin, the tissue that expressed highest level of the Irga6 was the liver and the heart was the tissue that had the second highest expression level. Spleen, skin, intestine and thymus expressed relative fewer Irga6. Lung, kidney and testis had only very low Irga6 expression. Finally the brain did not have any Irga6 expression. Irgm3 was also examined using

the same set-up and the expression level was found to be very low. With an over-exposure of the film, Irgm3 expression in tissues other than liver could be visualized and exhibited the expression profile is very similar to that of Irga6 (Fig. 10).

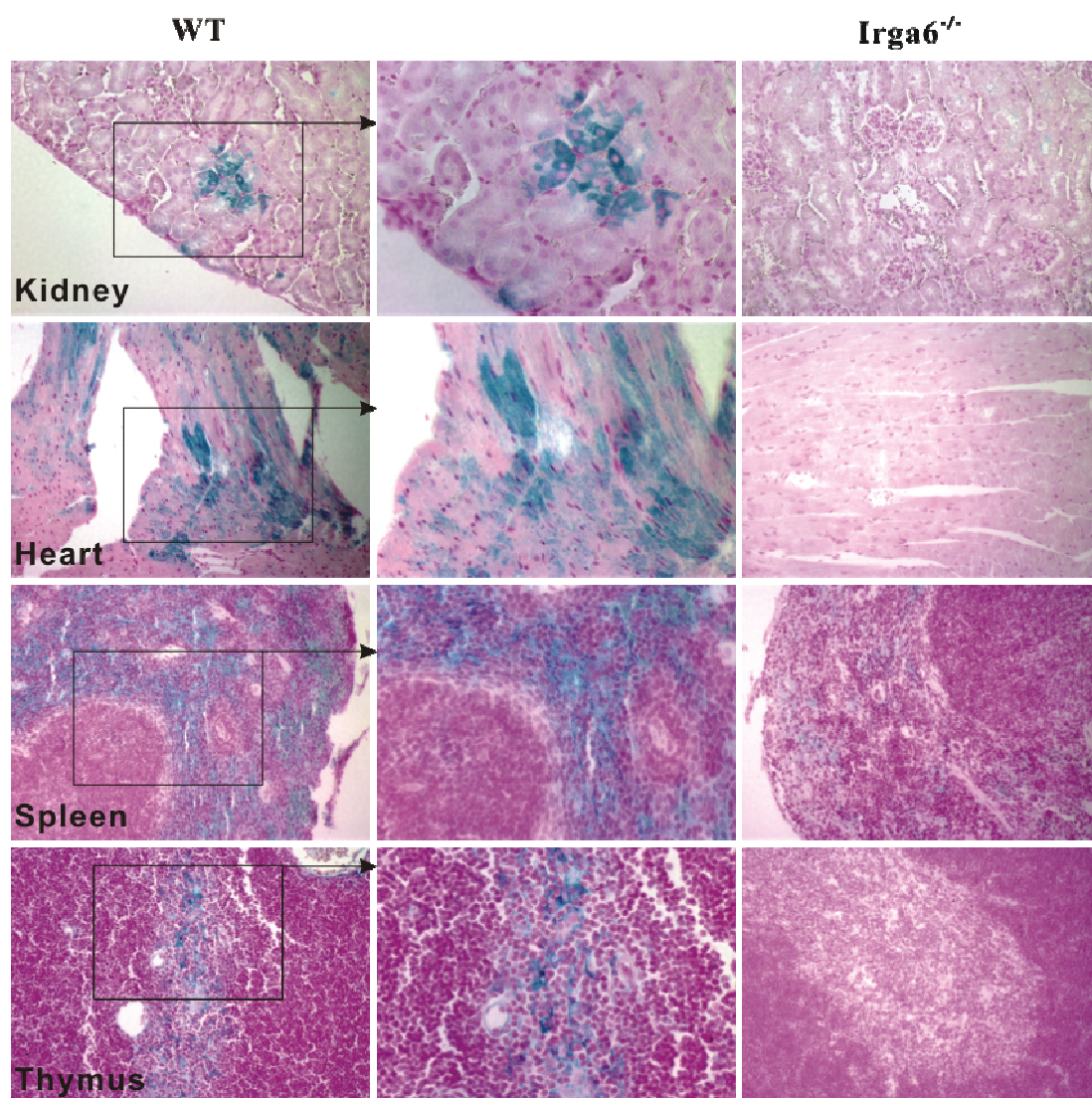


**Figure 11. Irga6 is constitutively expressed in many mouse tissues.** Immunohistochemical analysis of Irga6 expression in several mouse tissues was made. C57BL/6 WT and Irga6<sup>-/-</sup> adult mouse kidney, heart, spleen and thymus were embedded in paraffin and cut into 6µm sections. Irga6 was stained by mAb 10D7 (green). Counter staining (red) was done with nuclear fast red (NFR). Frames and arrows showed enlarged images (10x20). Pictures were taken using light microscopy (10x10, ZEISS Axiophot).

The distribution of Irga6 expression was also investigated by immunohistochemical methods for several mouse tissues. Paraffin sections of mouse kidney, heart, spleen and thymus were stained for Irga6 by 165/3 (green). In contrast to Irga6<sup>-/-</sup> mouse

tissues, WT tissues all had strong Irga6 protein expression in specific patterns. In kidney, Irga6 expression was detected as small round patches and each such patch covered kidney tubule wall cells from several different tubules; in heart Irga6 expression took the shape of elongated patches, which obviously consisted mainly of heart muscle cell; in spleen most Irga6 were expressed in the red pulp; in thymus the expression was mainly detected in the thymus medulla (Fig. 11).

Therefore, Irga6 is expressed not only in liver but also in many other tissues. Liver is the tissue with most abundant Irga6 expression. In kidney, even though the Irga6 total expression level is not among the highest, the expression is very concentrated in well defined pattern, which can be easily quantified. Hence, the following expression study was mostly focused on liver and kidney.

### **3.2 Interferons show different influences on constitutive expression of Irga6 in different tissues**

IRG proteins were discovered because they are massively induced by interferons. To determine whether the constitutive expression of IRG proteins is dependent on interferons, interferon receptor deficient mice were analyzed.

Ten mouse tissues, including liver, heart, skin, spleen, intestine, thymus, lung, testis, kidney and brain, from type I, type II interferon single receptor knock out and the double knock out mice were obtained. Tissue lysates containing equal amount of protein were subsequently subjected to western blot analysis. Judging by the Irga6 signal intensity normalized to the loading control calnexin, it was observe that in different tissues the Irga6 expression displayed different dependency on interferons. Interferons had almost no influence on the Irga6 expression in liver and heart, since neither tissues from single interferon receptor knock out mice showed any decrease in expression, and the double knock out displayed only a little bit, if any, expression reduction (Fig. 12).

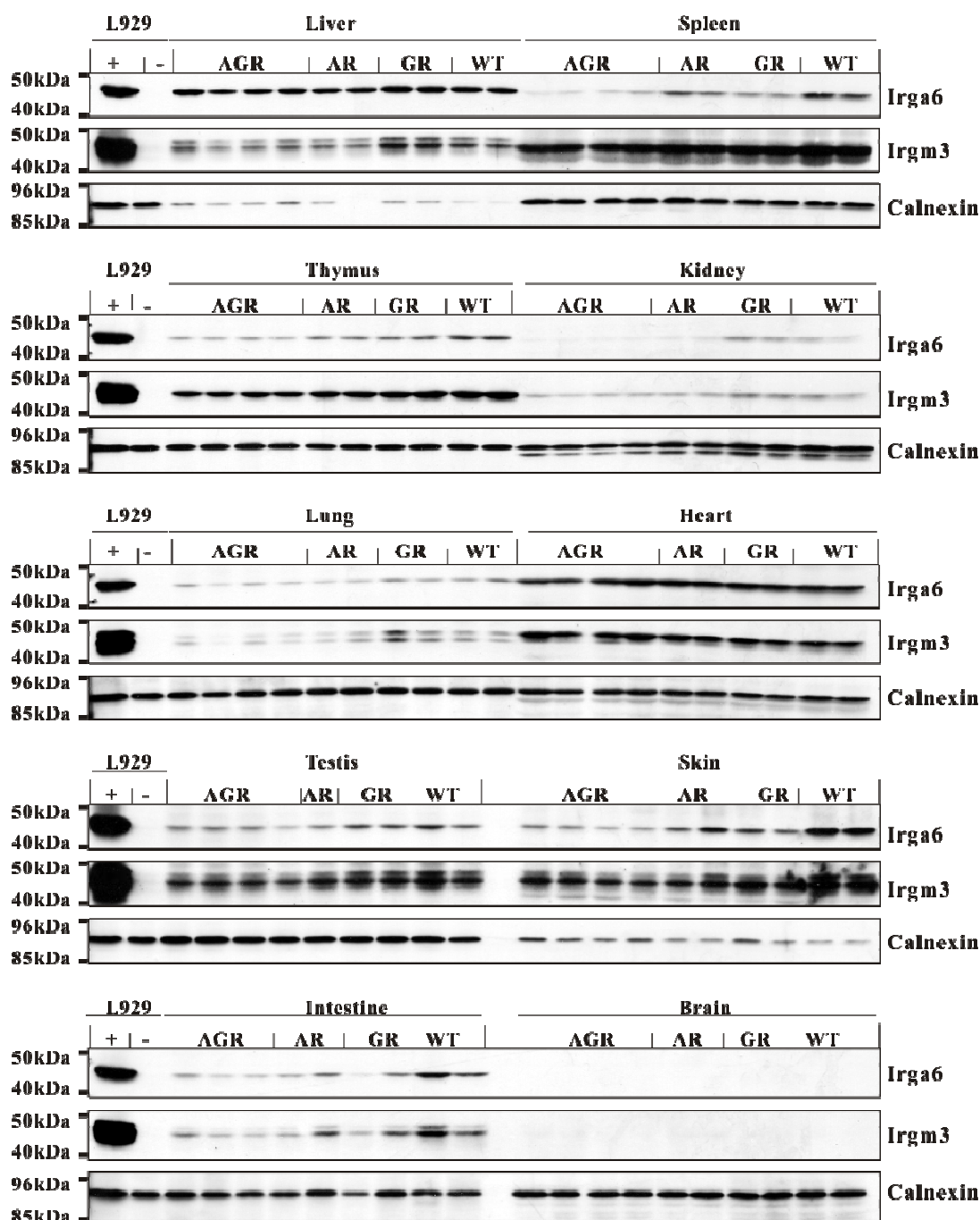


**Figure 12. Irga6 constitutive expression in different mouse tissues was influenced differentially by interferons.** Western blot analysis of Irga6 expression in IFNR knock out mouse tissues was carried out. Type I interferon receptor knock out (AR), type II interferon receptor knock out (GR), the double knock out (AGR) mice and WT 129sv mice were obtained. Organs indicated were taken from 4 mice of the double knock out and 2 mice of each single knock out. Organs were first ground in liquid nitrogen, weighed and then lysed in RIPA buffer. L929 cells unstimulated (-) or stimulated (+) by IFN- $\gamma$  (200U/ml) for 24 hours were used as control. The loading for all tissue lysates is 150 $\mu$ g/lane except for liver, which had 80 $\mu$ g/lane. The loading of L929 cells is 5,000cells/lane. Irga6 mAb 10D7 and anti-Irgm3 mAb 168120 were used for detecting respective proteins. Calnexin was also probed as loading control. (modified from Jia Zeng Master Thesis, 2003)

In spleen, kidney and skin however, the *Irga6* expression was much down-regulated in either single interferon receptor knock out tissues and to an even greater extent in the double knock out (Fig. 12). In the case of thymus, lung, intestine and testis, the expression of *Irga6* in the WT tissues was quite low and the decrease in the interferon receptor knock out was also rather mild.

In brief, *Irga6* expression in liver and heart seems not to be a response to interferons, whereas, kidney, skin and spleen have a more interferon-sensitive *Irga6* expression.

### **3.3 *Irga6* has two transcriptional forms using 2 distinct promoters**

In liver the high level of universal expression of *Irga6* that is not IFN-inducible, strongly suggested that this expression might be tissue-specific, for instance under the control of a liver-specific promoter. The *Irga6* gene is known to consist of a long coding exon and two short 5' exons called exon1A and exon1B, which are alternatively used together with the 3' exon to produce two forms of *Irga6* transcripts (Fig. 13A). The putative promoter regions of both these two 5' short exons contain type I and II interferon regulatory elements.

To define the promoter regions for *Irga6* 1A and 1B more accurately, a screen for *Irga6* ESTs with the furthest 5' end through the database was conducted. Two such ESTs were found, namely BY157974 for 1A and BI657093 for 1B. The putative transcriptional starting point defined according to these ESTs for 1A and 1B is exactly the same as formerly reported (Beckpen *et al.*, 2005).

Genomic sequences of 500bp upstream of the putative transcriptional starting points were taken as putative proximal promoters for *Irga6* 1A and 1B, which were then extensively analyzed using an online software, CONSITE, which can search transcription factor binding sites for a given sequence utilizing known consensus sequences, (<http://mordor.cgb.ki.se/cgi-bin/CONSITE/>), as well as manually seeking by comparison to published consensus binding sequences. As previously published, in *Irga6* 1A promoter there are two ISRE and three GAS sites, whereas in 1B promoter only one ISRE and one GAS sites (Fig. 13B). ISRE and GAS are classical type I and type II interferon responding elements and the existence of which explains the

inducibility of *Irga6* by interferons (Beckpen *et al.*, 2005). An elaborated search for

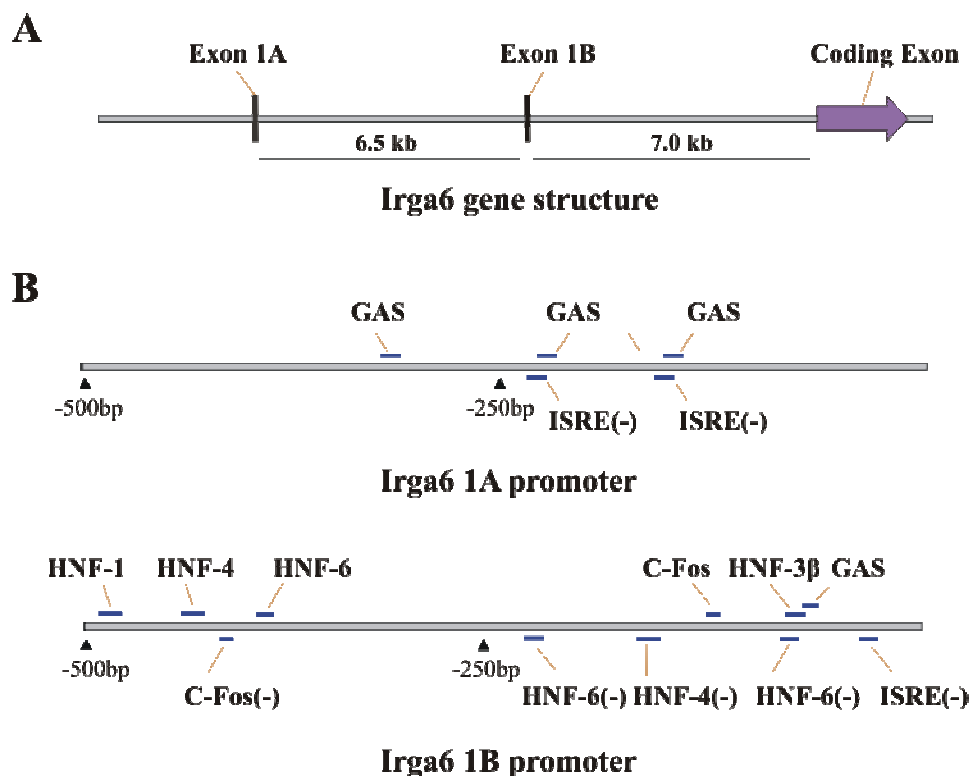


**Figure 13. *Irga6* gene has two transcriptional forms using distinct promoters.** A scheme of *Irga6* gene structure (A) was shown. The length of 1A, 1B and the coding exon is 103 bp, 184 bp and 2233 bp. The 5' starting point of each exon was defined by ESTs with the furthest 5' end, namely BY157974 for 1A and BI657093 for 1B. The distance between 1A and 1B is around 6.5 kb; between 1B and coding exon is around 7.0 kb. The scheme is to scale. A scheme for *Irga6* 1A and 1B promoter (500bp) and putative transcription factor binding sites was also shown (B). The scheme is not to scale. The binding sites on the negative strand were marked by '(-)'.

liver specific transcription factor binding sites, however, revealed that *Irga6* 1B but not 1A promoter possesses multiple hepatocyte nuclear factor (HNF) binding sites, specifically HNF4, HNF1, HNF3 and HNF6 (Table 3). HNF1 and HNF3 binding sites were detected by CONSITE, and HNF4 and HNF6 binding sites were attained by manual comparison to published consensus binding sequences (Jiang and Sladek, 1997; Sladek *et al.* 1990; Lemaigre *et al.*, 1996; Sladek *et al.*, 1990; Samadani & Costa 1996). These HNF binding sites seem to be segregated into two clusters, one close to the transcriptional starting point and the other one 200bp further upstream, both of which have HNF4 sites. Clustering of various hepatocyte nuclear factors was

reported to be a characteristic feature of many hepatocyte specific promoters (Schrem *et al.* 2002; Jiang & Sladek 1997; Lemaigre *et al.* 1996; Samadani & Costa 1996). Furthermore, HNF4 has been established to be of vital importance in being the first to bind the promoter and subsequently initiating recruitment of other hepatocyte nuclear factors and the transcriptional initiation machinery. Therefore, Irga6 1B promoter is strongly indicated to be a hepatocyte specific promoter.

<b>HNF-4</b>	
-159 to -171	AGGTCAG A AG ATC
-445 to -432	AGGTCAT G AGGCTC (-)
consensus	AGGTCAN (N) AGG TC
<b>HNF-1</b>	
-499 to -485	TGT TAATCATTCAA
consensus	DGT TAATNATTAAH
<b>HNF-3<math>\beta</math></b>	
-88 to -77	CAA TTTCTACTT
consensus	CAATATTACTT
<b>HNF-6</b>	
-83 to -92	AAATTGTGTT (-)
-215 to -224	AGATTGTTT (-)
-400 to -391	TTATGGACTC
consensus	WWATKGAYTT

**Table 3. Putative HNF sites used by Irga6 1B promoter.** In putative Irga6 1B promoter HNF-1 and HNF-3 $\beta$  sites were found electronically using an online promoter analysis tool, CONSITE, (<http://mordor.cgb.ki.se/cgi-bin/CONSITE/>). HNF-4 and HNF-6 sites were found manually by comparison with published consensus binding sequences. The sequences of putative binding sites were compared to the consensus sequences and the position of the sequences upstream the putative transcriptional starting point was marked. Identical bases are shaded in black. Binding sites on the negative strand were marked by '(-)'. D=A/G/T, H=A/C/T, N=A/C/G/T, W=A/T, K=G/T, Y=C/T.

### 3.4. IRG proteins are constitutively expressed in primary hepatocytes

Irga6 expression in liver was examined more closely by immunofluorescence technique. Liver cryosections was stained for Irga6 by its antiserum 165/3. Irga6 displayed clear cytoplasmic localization in liver parenchymal cells (Fig. 14).

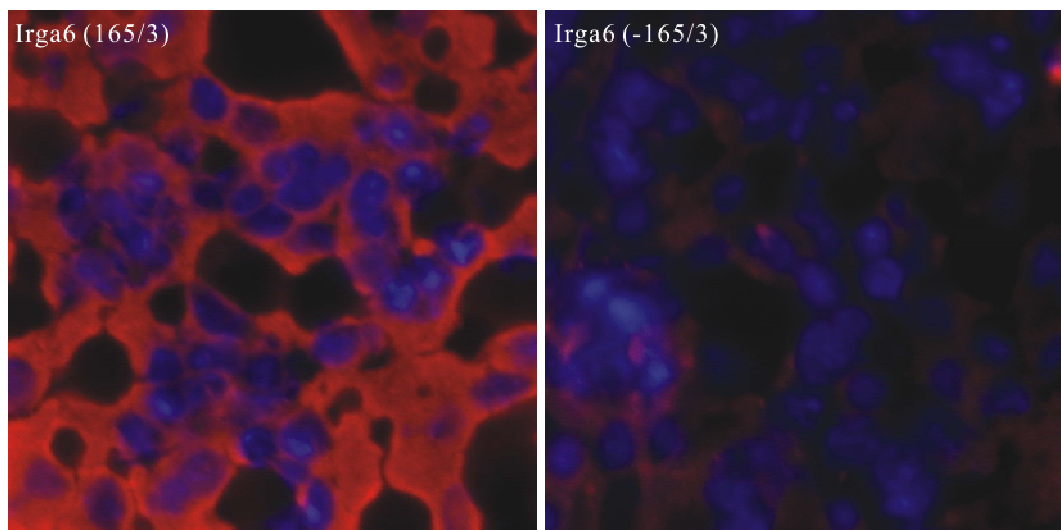


**Figure 14. Irga6 is likely to be expressed in liver parenchymal cells.** Immunofluorescence analysis of Irga6 expression in liver was carried out. C57BL/6 adult mouse liver was cut into 6 $\mu$ m cryo-sections and stained for Irga6 by its antiserum 165/3 (red). Staining without primary antibody (-165/3) was made as negative control. Alexa-546 coupled to secondary antibody was visualized by fluorescence microscopy. DAPI (blue) stained the nuclei. Pictures were taken using fluorescence microscopy (10x63, ZEISS Axiophot).

#### **3.4.1 IRG proteins are expressed constitutively in murine primary hepatocyte**

To establish that Irga6 is truly expressed in liver parenchymal cells, murine primary hepatocytes were isolated by a two-step in situ liver collagenase perfusion technique (modified from Klaunig *et al.*, 1981). The liver of an anaesthetized mouse was perfused in situ through the hepatic portal vein by collagenase buffer and the primary hepatocytes were then isolated and cultured on collagen coated plates. The cells were then lysed at different time points and analyzed by western blot with IRG antibodies. Primary hepatocytes immediately after isolation had almost the same level of Irga6 expression as liver (Fig. 15). The expression in the primary cells kept constant after 6 hours of culture. 12 hours post isolation, however, the amount of Irga6 showed a slight decrease, and then dropped very drastically at 24 hours and finally got further reduced to an extremely low level from 2 days on. The rapid drop of gene expression in isolated primary cells is known to be the typical behavior for many hepatocyte specific genes (Clayton and Darnell, 1983; Clayton *et al.*, 1985). Not surprisingly, IFN- $\gamma$  could induce Irga6 expression in primary hepatocytes to a much higher level.

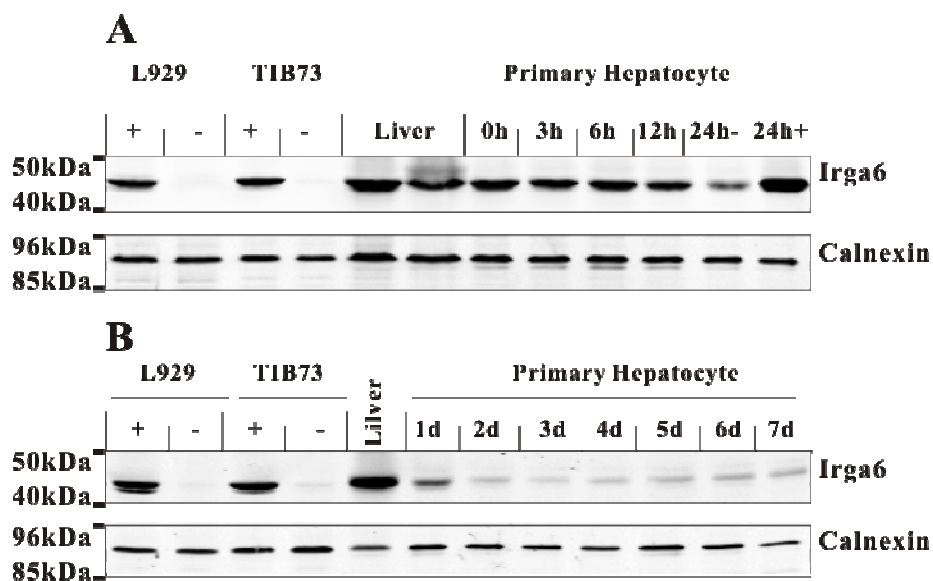


**Figure 15. Irga6 are constitutively expressed in murine primary hepatocytes.** Western blot analysis of Irga6 expression in murine primary hepatocyte was made. C57BL/6 murine primary hepatocytes were isolated by a two-step in situ liver collagenase perfusion technique. The liver of an anaesthetized mouse was perfused in situ through the hepatic portal vein first by  $\text{Ca}^{2+}$  and  $\text{Mg}^{2+}$  free Hank's buffer and then by collagenase medium. The detached hepatocytes were then liberated, washed, and cultured in DMEM/Ham's F12 (1:1) medium supplemented with ITS+ and dexamethasone on collagen coated plates. Primary hepatocytes were harvested either immediately after isolation (0h) or at indicated hours (h) or days (d) post isolation. IFN- $\gamma$  (200U/ml) stimulation for 24 hours was made for primary cells (24h+), L929 cell (+), TIB73 cells (+) as positive controls and unstimulated L929 (-) and TIB-73 (-) were used as negative control. Liver lysates (250 $\mu\text{g}/\text{lane}$ ) were also included. Irga6 mAb 10D7 (A) were applied and Calnexin was also probed as loading control.

The expression of other IRG proteins was also tested. Irgm3 expression in the liver was quite low compared to IFN- $\gamma$  stimulated L929 cells and the expression in primary hepatocytes was even lower, which did not change with time. Irgb6 and Irgm1 had similar expression profile as Irga6 but at much lower level, namely, they were all expressed in liver at a moderate level and also had comparable amount of expression in primary hepatocytes, which stayed at least after 3 hours culture and dropped 24 hours post isolation (Fig. 16). All the IRG proteins in primary hepatocytes were able to be stimulated by IFN- $\gamma$  to a very high level.

In conclusion, Irga6 has high level of expression in primary hepatocytes, which acts as the major contributor to constitutive expression in liver. Similarly, Irgb6, Irgd and Irgm1 also have constitutive expression in liver, which is also conferred primarily by

their expression in hepatocytes. Irgm3 is expressed only at very low level in liver and also in hepatocytes. All the IRG proteins examined here are able to be induced strongly by IFN- $\gamma$  in primary hepatocytes.

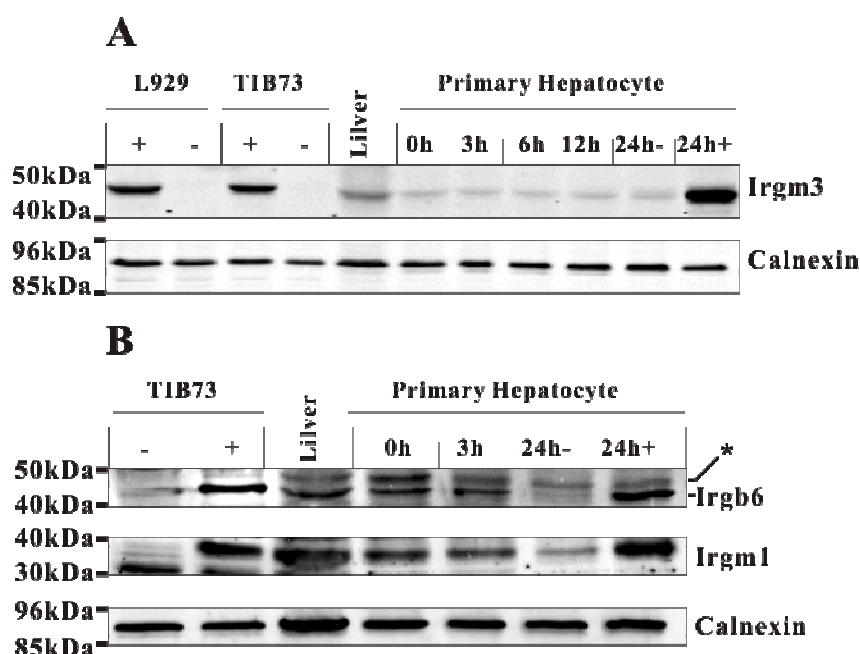


**Figure 16. Some other IRG proteins are also constitutively expressed in murine primary hepatocytes.** Western blot analysis of IRG proteins expression in murine primary hepatocyte was made. Murine primary hepatocytes were isolated cultured and harvested either immediately after isolation (0h) or at indicated hours (h) post isolation. IFN- $\gamma$  (200U/ml) stimulation for 24 hours was made for primary cells (24h+), L929 cell (+), TIB73 cells (+) as positive control and unstimulated L929 (-) and TIB-73 (-) were used as negative control. Liver lysates (250 $\mu$ g/lane) were also included. mAb 168120 (anti-Irgm3 Ab) (A), goat antiserum A20 (anti-Irgb6 Ab), rabbit antiserum L115 (anti-Irgm1 Ab) (B) were applied to detect respective proteins. Calnexin was also probed as loading control. “\*” indicated crossreacting bands of the Irgb6 antiserum.

### 3.4.2 Constitutively expressed Irga6 is localized mainly in ER but not in Golgi in murine primary hepatocytes

IFN- $\gamma$  induced Irga6 is mainly an ER and cytosolic protein (Martens *et al.*, 2005). To test the localization of Irga6 constitutively expressed in primary hepatocytes, immunofluorescence microscopy was applied. In primary hepatocytes cultured for 6 hours after isolation without IFN- $\gamma$  stimulation, double staining for Irga6 and ER marker, calnexin or Golgi marker, Gm130, clearly confirmed that Irga6 is expressed as an ER but not Golgi protein (Fig. 17). Therefore, constitutively expressed Irga6

displays the same localization as the IFN- $\gamma$  stimulated protein.

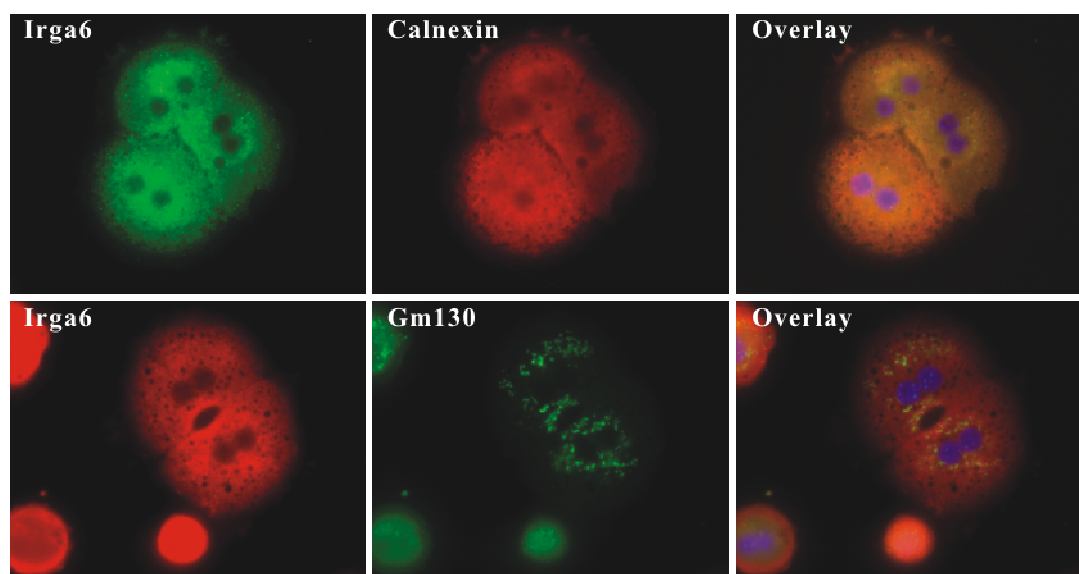


**Figure 17. Irga6 constitutively expressed in primary hepatocytes is localized to ER.** Immunofluorescence analysis of Irga6 expression in murine primary hepatocyte was made. C57BL/6 murine primary hepatocytes were isolated, cultured for 6 hours, fixed and permeabilized for staining. Double staining using either Irga6 mAb 10E7 (green) and calnexin rabbit antiserum (red) or Irga6 rabbit antiserum 165/3 (red) and anti-GM130 mAb (green) was performed. Alexa-546 (red) coupled secondary antibody against rabbit antiserum and FITC (green) coupled secondary antibody against mAb were used. Cell nuclei were stained by DAPI (blue). Pictures were taken using fluorescence microscopy (10x63, ZEISS Axiophot).

### 3.5. IRG proteins participate in IFN- $\gamma$ induced resistance against *Toxoplasma gondii* infection

#### 3.5.1 IFN- $\gamma$ mediates growth inhibition of *Toxoplasma gondii* in murine primary hepatocytes

The replication of intracellular parasite *Toxoplasma gondii* can be strongly inhibited by IFN- $\gamma$  in many cell types (Martens *et al.*, 2005; Könen-Waisman unpublished results). To investigate the IFN- $\gamma$  inhibition effect on *T. gondii* growth in primary hepatocytes, *T. gondii* proliferation assay was carried out. Murine primary hepatocytes were isolated and stimulated with IFN- $\gamma$  for 24 hours or left untreated prior to *T. gondii* infection. The growth of *T. gondii* was monitored by uracil incorporation assay. Primary hepatocytes infected by *T. gondii* using different multiplicity of infection (MOI) all showed similar IFN- $\gamma$  restriction of the parasite

proliferation in primary hepatocytes in a dose dependent manner (Fig. 18). IFN- $\gamma$  does confer primary hepatocytes resistance against *T. gondii*.

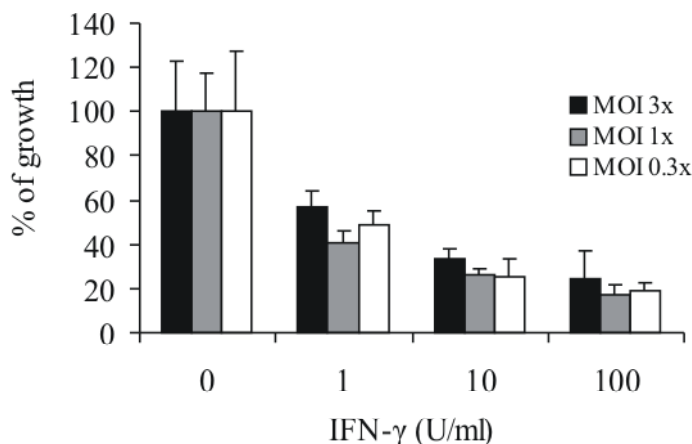


**Figure 18. IFN- $\gamma$  mediates growth inhibition of *T. gondii* in murine primary hepatocytes.** *T. gondii* proliferation assay of primary hepatocyte was carried out. Murine primary hepatocytes were isolated and stimulated with IFN- $\gamma$  (1-200 U/ml) for 24 hours or left untreated prior to *T. gondii* (ME49) inoculation by different multiplicities of infection (MOI). After 48 hours of infection, cultures were labeled with 1 $\mu$ Ci/well [ $^3$ H]-uracil for additional 24 hours. The amount of incorporated uracil, which is directly in proportion to *T. gondii* growth (Pfefferkorn and Pfefferkorn, 1977), was determined by liquid scintillation counting. Percentage of growth was normalized to that of cells uninfected by *T. gondii*.

### 3.5.2 Both constitutively expressed and IFN- $\gamma$ stimulated Irga6 accumulated around *Toxoplasma gondii* vacuoles in murine primary hepatocytes

In IFN- $\gamma$  stimulated cells IRG proteins can accumulate around *T. gondii*, which has been taken as one of the major known IFN- $\gamma$  induced intracellular resistant mechanisms against the parasite in murine cells (Martens *et al.*, 2005).

By immunofluorescence staining for Irga6 and GRA7, which is a *T. gondii* marker (Bonhomme *et al.*, 1998; Fischer *et al.*, 1998), in freshly isolated primary hepatocytes infected by *T. gondii*, the accumulation of the GTPase at parasitophorous vacuoles (PVs) could be clearly detected (Fig. 19A). About 10% of total intracellular parasites were coated by Irga6 in primary cells unstimulated by IFN- $\gamma$  and upon IFN- $\gamma$  stimulation, however, the proportion of Irga6 positive vacuoles rose up to 40% (Fig. 19B).

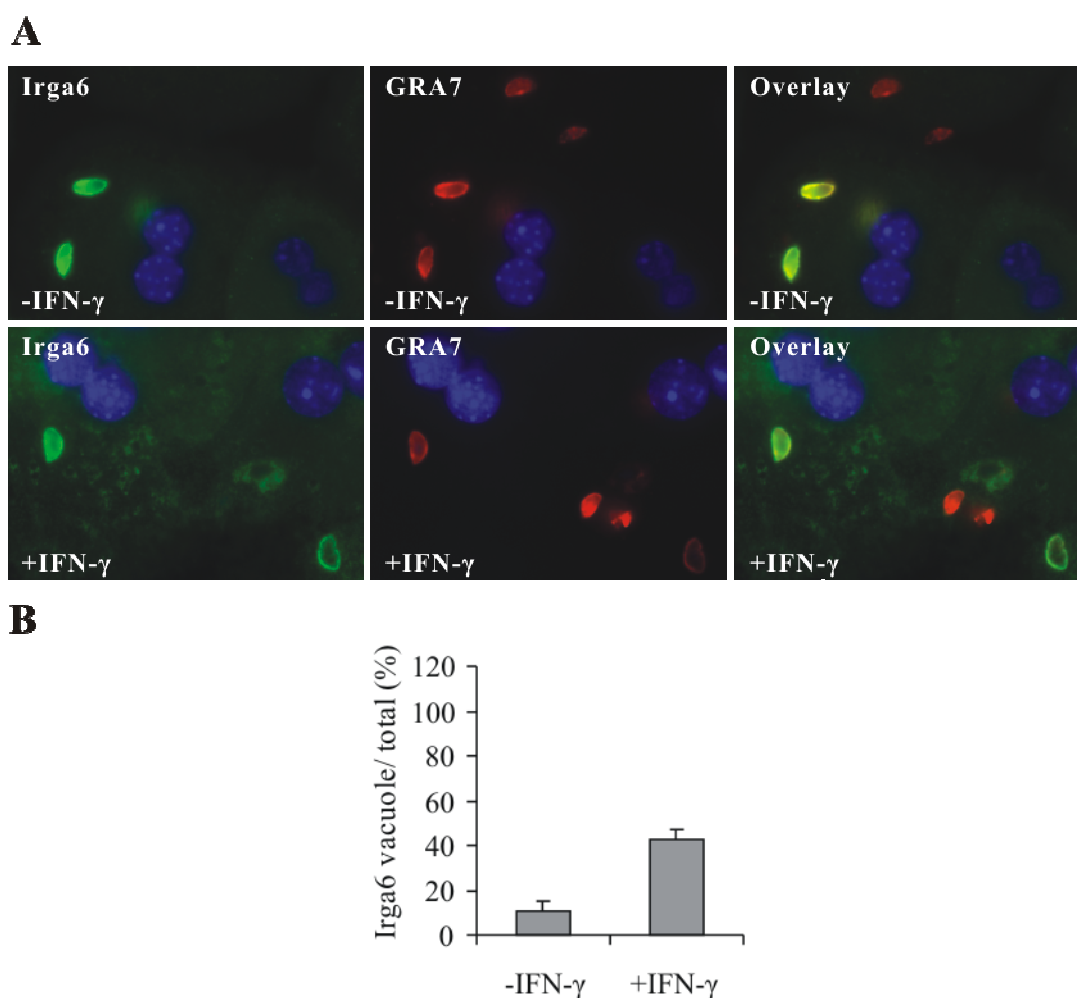


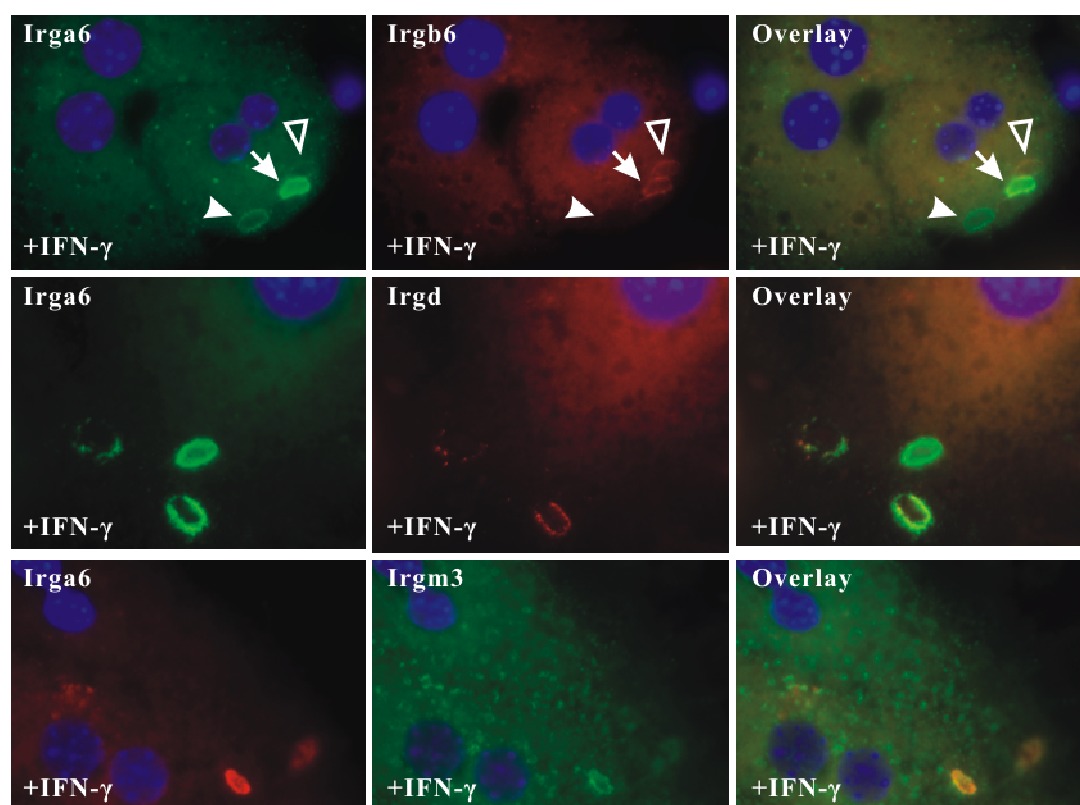
**Figure 19. Constitutive and IFN- $\gamma$  stimulated Irga6 proteins accumulate around *T. gondii* PVs in murine primary hepatocytes.** Immunofluorescence analysis of Irga6 accumulation at *T. gondii* vacuoles in murine primary hepatocytes was made. C57BL/6 murine primary hepatocytes were first isolated and either stimulated (+IFN- $\gamma$ ) for 12 hours with IFN- $\gamma$  (200U/ml) or left untreated and cultured for 3 hours (-IFN- $\gamma$ ). The cells were inoculated with *T. gondii* (ME49) by MOI<sub>x3</sub> for 2 hours, fixed and permeabilized for staining. Double stainings (A) for Irga6 with mAb 10E7 (green) and GRA7 with anti-GRA7 mAb (red) was made. Nuclei were stained by DAPI (blue). Histograms present percentage of Irga6 positive vacuoles in the total intracellular *T. gondii* vacuoles (B). The mean of two or three independent counts representing 200-400 vacuoles were always made for each value. Pictures were taken using fluorescence microscopy (10x63, ZEISS Axiophot).

Irgb6, Irgd, Irgm3 did not accumulate at PVs in primary hepatocytes without IFN- $\gamma$  treatment whereas upon IFN- $\gamma$  induction they could relocate to the vacuoles (Fig. 20A). The accumulation of IRG proteins at the PVs was observed to have an inclusion relationship, namely IRG proteins family members relocate to the PVs in a sequential

order (Könen-Weisman and Khaminets unpublished results). This is also true here for primary hepatocytes. Under IFN- $\gamma$  treated condition, almost all the Irga6 positive vacuoles were also Irgb6 positive only a few (3%) vacuoles are Irga6 positive but Irgb6 negative and vice versa. All Irgd positive vacuoles were also positive for Irga6, but the former accounted for only 40% of the latter (Fig. 20B).

In summary, in primary hepatocytes in contrast to other murine IRG proteins, which accumulate at PVs only upon IFN- $\gamma$  induction, constitutively expressed Irga6 alone can coat vacuoles though with a lower proportion. The coating of PVs by IRG proteins exhibits an inclusion relationship as well.

**A**



**B**

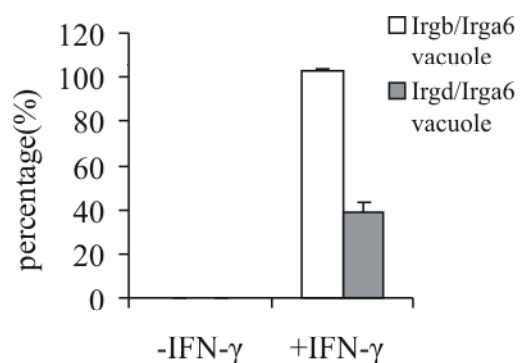


**Figure 20. IFN- $\gamma$  stimulated IRG proteins accumulate around *T. gondii* PVs in murine primary hepatocytes.** Immunofluorescence analysis of IRG proteins accumulation at *T. gondii* vacuoles in murine primary hepatocytes was made. C57BL/6 murine primary hepatocytes were isolated, stimulated (+IFN- $\gamma$ ) for 12 hours with IFN- $\gamma$  (200U/ml) prior to inoculation with *T. gondii* (ME49) by MOI<sub>x3</sub> for 2 hours. The cells were then fixed and permeablized for staining. Several double stainings were performed (A): Irga6 with 10E7 (green) and Irgb6 with goat antiserum A20 (red); Irga6 with 10E7 (green) and Irgd with rabbit antiserum 2078 (red); Irg6 with 165/3 (red) and Irgm3 with mAb 168120 (green). Arrows indicate a vacuole that is both Irga6 and b6 positive; filled arrow heads indicate a vacuole that is only Irga6 positive; empty arrow heads indicate a vacuole that is only Irgb6 positive. Nuclei were stained by DAPI (blue). Histograms present percentage of Irga6 positive vacuoles in the total intracellular *T. gondii* vacuoles and the ratio of Irgb6 positive or Irgd positive vacuole to Irga6 positive vacuole in primary hepatocyte with (+IFN- $\gamma$ ) or without (-IFN- $\gamma$ ) IFN- $\gamma$  stimulation. The mean of two or three independent counts representing 200-400 vacuoles were always made for each value. Pictures were taken using fluorescence microscopy (10x63, ZEISS Axiophot).

### **3.5.3 *Toxoplasma gondii* vacuoles coated by Irga6 mature in murine primary hepatocytes**

*T. gondii* vacuoles accumulating IFN- $\gamma$  induced Irga6 undergo morphology changes, namely from smooth to rough and then to disrupted, implying a gradual disruption of PVs most probably by IRG proteins, which leads to the deterioration of the parasites (Martens *et al.*, 2005).

Here the morphology change of Irga6 coated vacuoles was examined both for IFN- $\gamma$  stimulated and unstimulated primary hepatocytes. In unstimulated cells, 90% of *T. gondii* PVs coated by constitutive Irga6 were smooth and there were however already 10% rough and 1% disrupted vacuoles (Fig. 21). The proportion of rough and disrupted vacuoles increased significantly in IFN- $\gamma$  stimulated cells. Interestingly under IFN- $\gamma$  stimulated condition the Irgd positive vacuoles showed faster maturation, namely higher proportion of rough vacuoles.

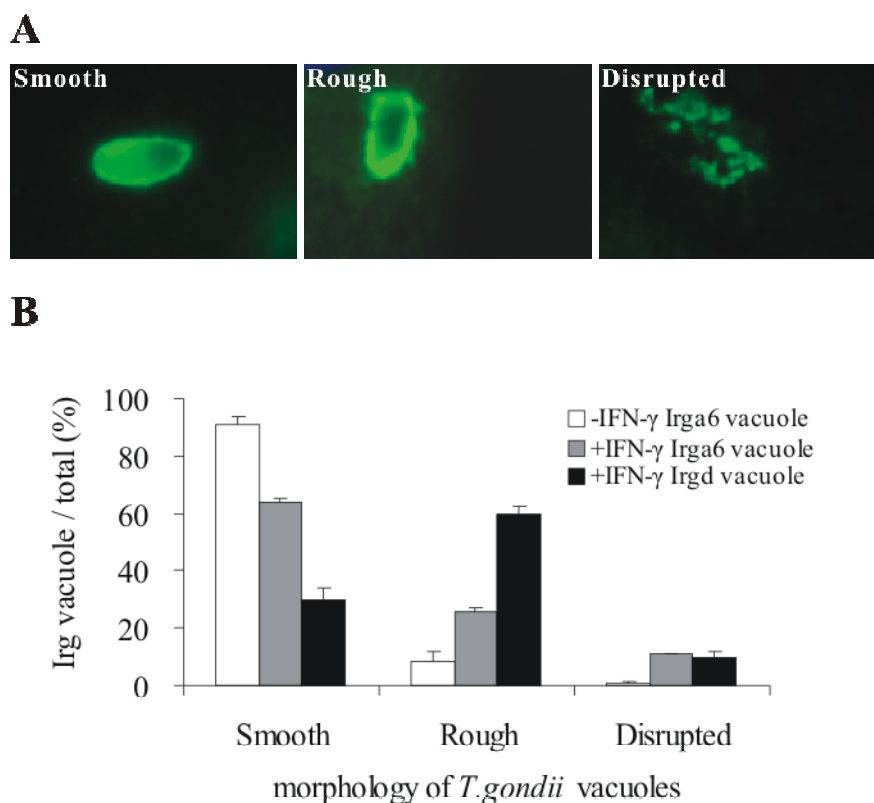


**Figure 21. *Toxoplasma gondii* vacuoles coated by Irga6 mature in murine primary hepatocytes.** Immunofluorescence analysis of the morphology of *T. gondii* vacuoles coated by IRG proteins in murine primary hepatocyte was made. C57BL/6 murine primary hepatocytes were first isolated and either stimulated (+IFN- $\gamma$ ) 12 hours with IFN- $\gamma$  (200U/ml) or left untreated and cultured for 3 hours (-IFN- $\gamma$ ). The cells were inoculated with *T. gondii* (ME49) by MOIx3 for 2 hours, fixed and permeablized for staining. Double stainings were made for Irga6 with 10E7 (green) and Irgd with rabbit antiserum 2078 (red). Smooth, rough and disrupted vacuoles (A) were counted for Irga6 and Irgd under IFN- $\gamma$  stimulated and unstimulated conditions. Diagram represents percentages of each type of vacuole for Irga6 and Irgd (B). Two or three independent counts representing 200-400 vacuoles were always made for each staining.

### 3.6. Irga6 focal expression in liver and kidney exploits interferon pathway

#### 3.6.1 The focal expression of Irga6 in liver and kidney is developmentally regulated

Except for general constitutive expression, Irga6 also has intense focal expression in liver. Immunohistochemical staining of liver sections establishes two types of Irga6 focal expression.

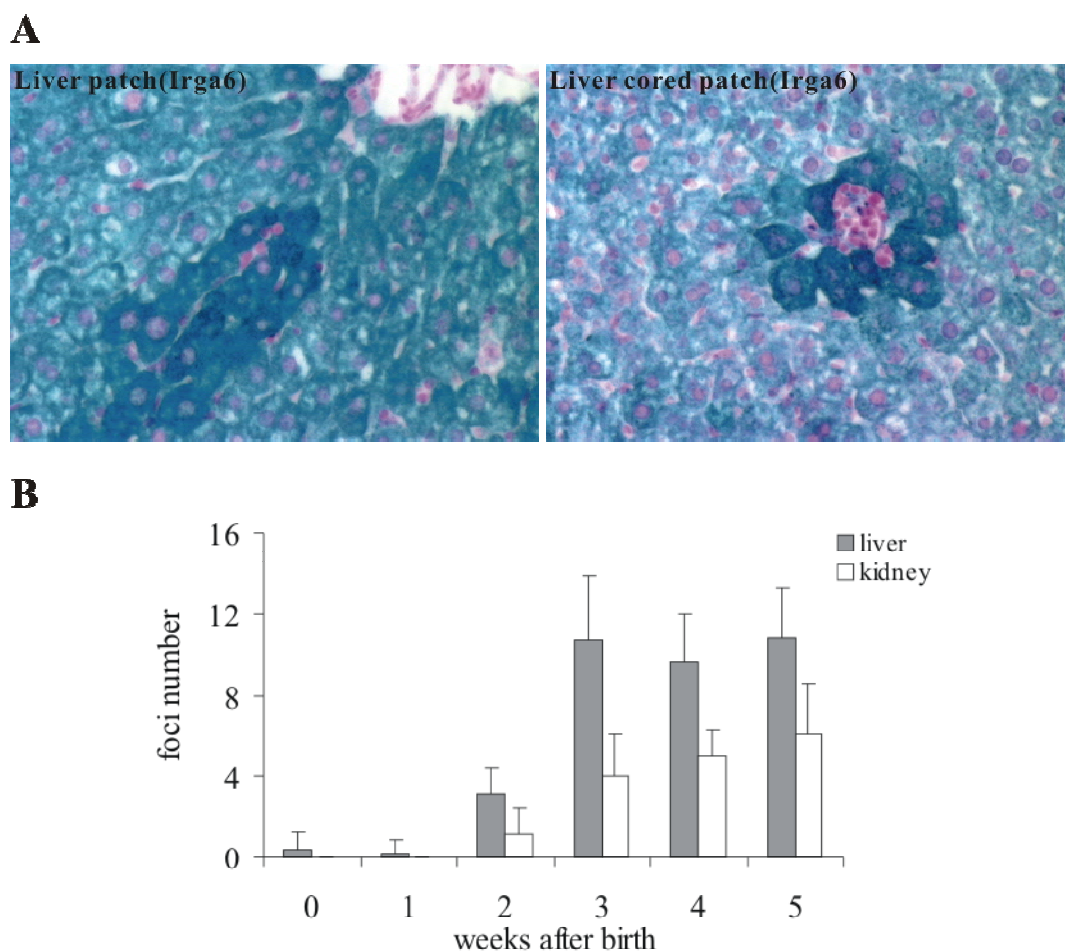


**Figure 22. Irga6 has two types of focal expression in liver and the focal expression in liver and kidney is developmentally regulated.** Immunohistochemical analysis of Irga6 expression in mouse liver was performed (A). C57BL/6 adult mice liver paraffin section (6 $\mu$ m) was stained for Irga6 with 165/3 (green). Nucleus counter stain was in red with NFR. Picture was taken using light microscopy (10x40). Quantification of Irga6 focal expression in liver from mice of different ages was made. Liver and kidney from C57BL/6 new born mice and mice aged as indicated after birth were embedded in paraffin and sections (6 $\mu$ m) were cut through the whole organ with an interval of 300  $\mu$ m between adjacent sections. The sections were then stained for Irga6 with 165/3 and Irga6 expression foci were counted separately within a microscopic view field (10x10, ZEISS Axiophot). Each value in the histogram represents the mean of 20 such counts for organs from 2 mice of each age.

One type is represented by a group of liver parenchymal cells, which express much higher amounts of Irga6 than the surrounding cells forming clear-cut boundaries and take the shape of patches. The other kind of focal expression exhibits exactly the same features except that they always have in the center a group of small mononuclear cells, which are Irga6 negative. Those mononuclear cells have small condensed nuclei and few cytoplasm, characteristic of lymphocytes or leukocytes (Fig. 22A). In the

following study, the former is named “patch or P” and the latter “cored patch or CP”. In order to test how early Irga6 focal expression occurs in liver, liver from C57BL/6 mice of different ages were examined. Irga6 expression foci (including P and CP) on stained liver sections were counted under the microscopic view field (10x10 Zeiss Axiophot). In newborn and very young (1 week) mouse liver there were only very few Irga6 expression foci. The number of foci started to rise in 2-week liver and reached a constant level (10-12 foci/microscopic view field) from 3 weeks on. Irga6 expression in kidney was also quantified in the same way showing a similar profile (Fig. 22B). The Irga6 focal expression seems to be developmentally regulated in liver and kidney.

### **3.6.2 Irgm3 is coexpressed at Irga6 expression foci in liver and kidney.**

To determine whether other IRG proteins are also expressed at Irga6 expression foci in liver, immunohistological staining of mouse liver for Irgm3 was performed. Since an Irga6 focal expression staining on the liver section represents the cross-section of a group of parenchymal cells in a ball shape, in consecutive liver sectioning the cross-section of the same group of cells should be present at the same position on adjacent liver sections. Consecutive serial liver paraffin sections were cut. Two adjacent serial sections were probed by Irga6 and Irgm3 antibodies respectively, and the same position on Irgm3 stained section, where on the adjacent section Irga6 expression foci were localized, was monitored. While Irgm3 had almost no general expression in liver, it did co-express at Irga6 expression foci, strongly indicating that the focal expression originates from interferon activation (Fig. 23). Interestingly, intensive expression of Irgm3 could also be detected in a certain type of small cells of unknown origin. In kidney Irgm3 was also expressed at Irga6 expression foci.

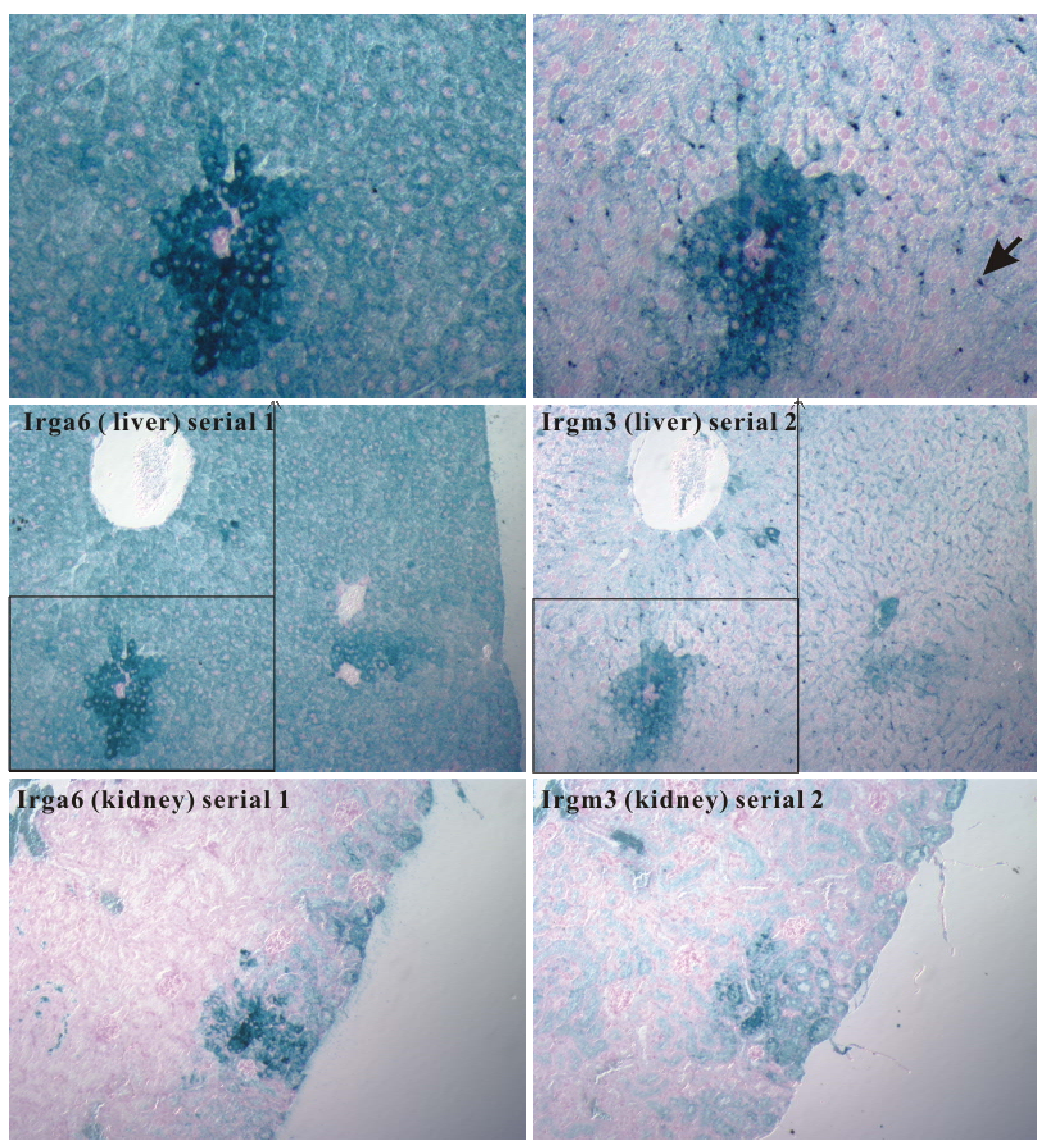
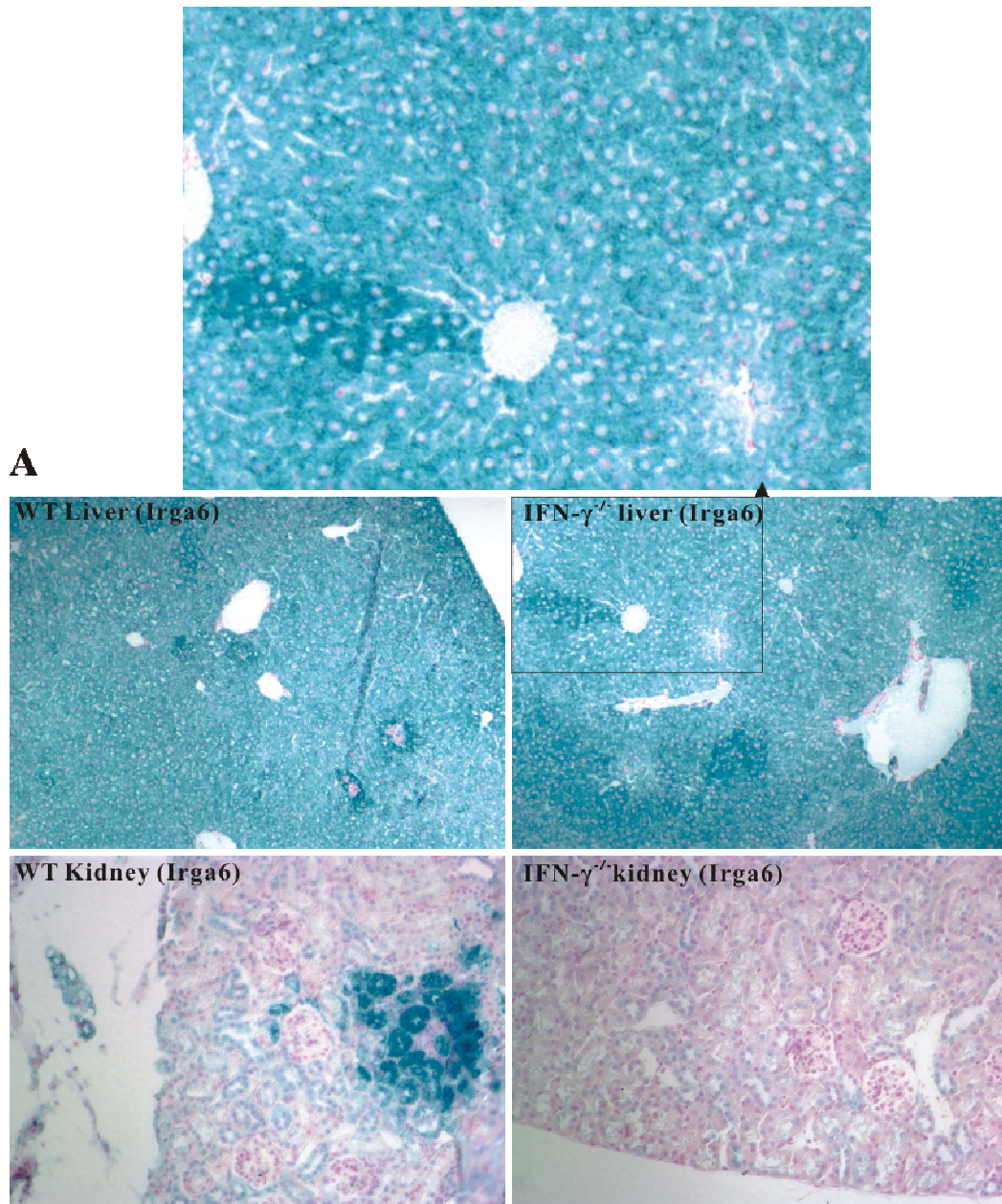


**Figure 23. Irgm3 is coexpressed at Irga6 expression foci in liver and kidney.** Analysis of Irgm3 coexpression with Irga6 in mouse liver and kidney was made with immunohistochemical methods. C57BL/6 adult mice liver and kidney paraffin sections (6 $\mu$ m) were prepared in a consecutive serial. The two adjacent serial sections were probed by Irga6 (serial 1, green) and Irgm3 (serial 2, green) antibodies respectively. Frames show enlarged images. Arrow indicates a small cells expressing Irgm3. Nucleus counter-staining was NFR (red). Pictures were taken using light microscopy (10X10, ZEISS Axiophot)

### 3.6.3 Irga6 cored patch in liver and patch in kidney is dependent on interferons.

IFN- $\gamma$  deficient mice were examined for the purpose of defining the relationship between Irga6 focal expression and IFN- $\gamma$ . Liver and kidney paraffin sections from C57BL/6 WT and IFN- $\gamma^{-/-}$  mice were stained for Irga6 and the focal expression was quantified. In contrast to WT mouse liver, though IFN- $\gamma^{-/-}$  mouse liver did have Irga6



**B**

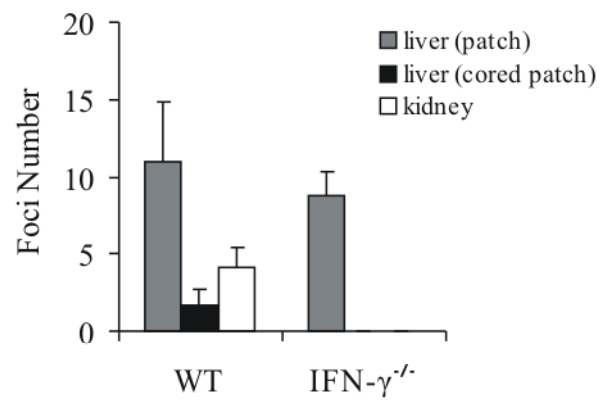


**Figure 24. Irga6 liver cored expression patches and kidney expression patches disappear in IFN- $\gamma$ <sup>-/-</sup> mice.** Immunohistochemical analysis of Irga6 expression in IFN- $\gamma$ <sup>-/-</sup> mice liver and kidney was made (A). Adult mice liver and kidney from C57BL/6 WT and IFN- $\gamma$ <sup>-/-</sup> mice were embedded in paraffin and sections (6 $\mu$ m) were cut through the whole organ with an interval of 300  $\mu$ m between adjacent sections. stained for Irga6 (green). Frame shows enlarged images. Nucleus counter-staining was NFR (red). Irga6 patch, cored patch in liver and patch in kidney were counted separately within a microscopic view field (10x10, ZEISS Axiophot). Each value in the histogram represents the mean of 20 such counts for organs from 2 mice of each genotype (B). Pictures were taken using light microscopy (10X10, ZEISS Axiophot).

patches, there were no cored patches. Irga6 expression foci also disappeared in the knock out kidney (Fig. 24). Therefore, Irga6 cored patches in liver and patches in kidney had an IFN- $\gamma$  origin.

Analysis of interferon receptor knock out mouse kidney was undertaken to verify the role of interferon activation in Irga6 focal expression. Kidney paraffin sections from 129/sv WT, type I interferon receptor knock out (IFNAR), type II interferon receptor knock out (IFNGR), and double receptor knock out (IFNAGR) mice were stained for Irga6 and the focal expression was quantified. WT 129/sv mouse kidney had Irga6 expression foci, though at lower amount. In both single interferon receptor and double receptor knock out kidney there were no expression foci at all, establishing the effect of interferon on Irga6 focal expression (Fig. 25).

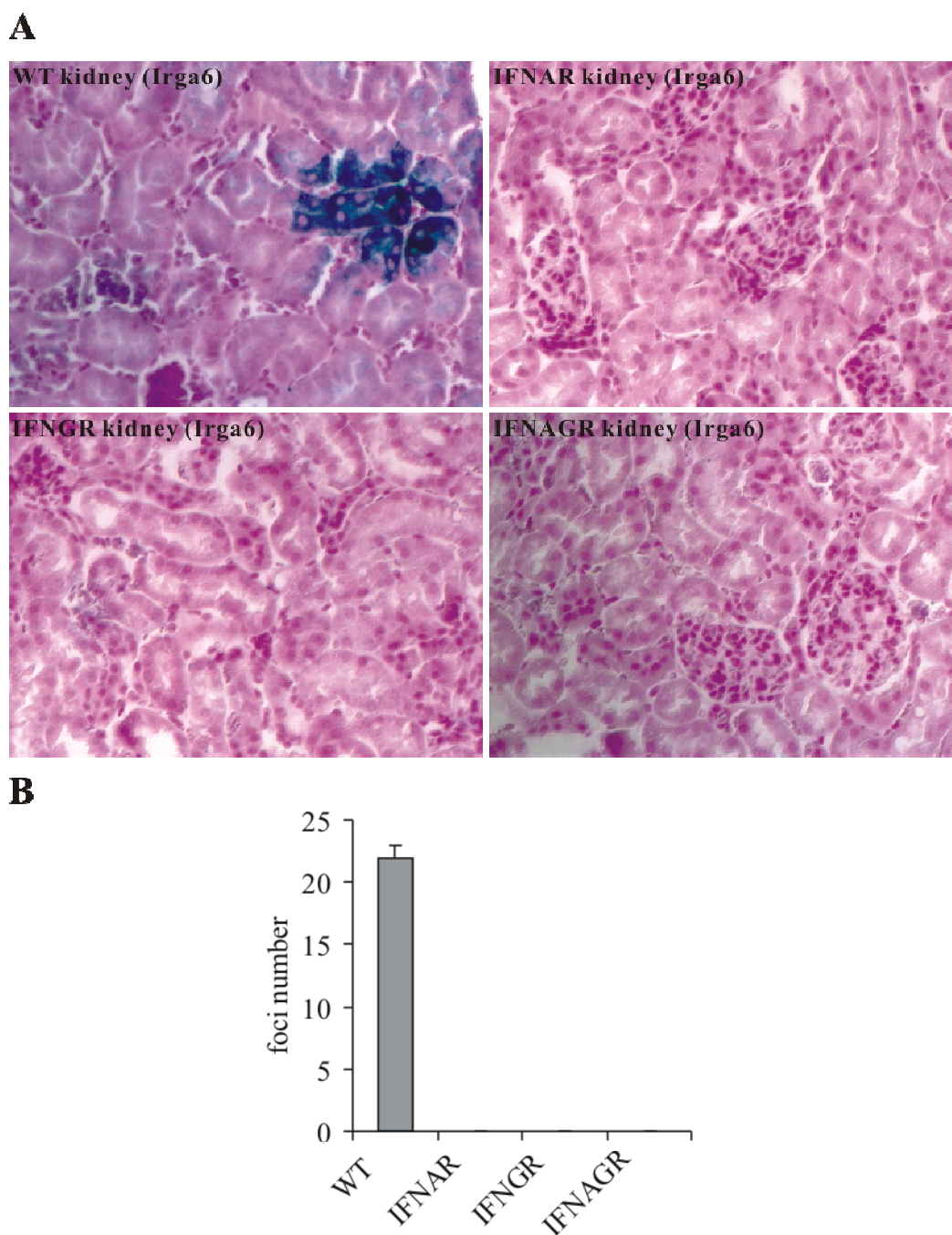


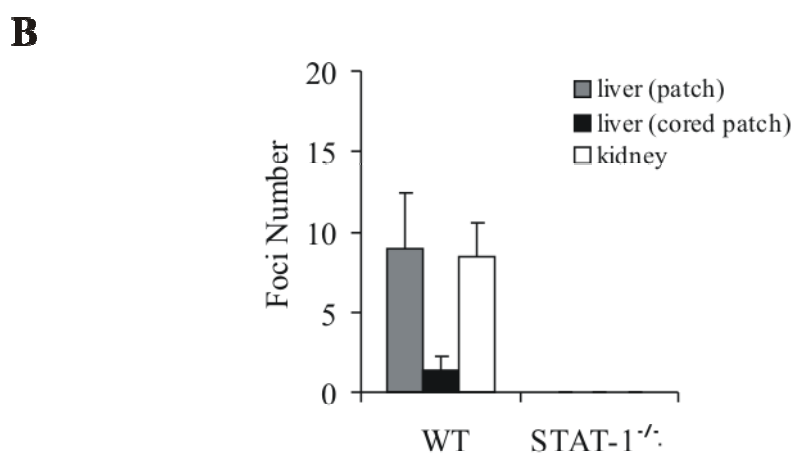
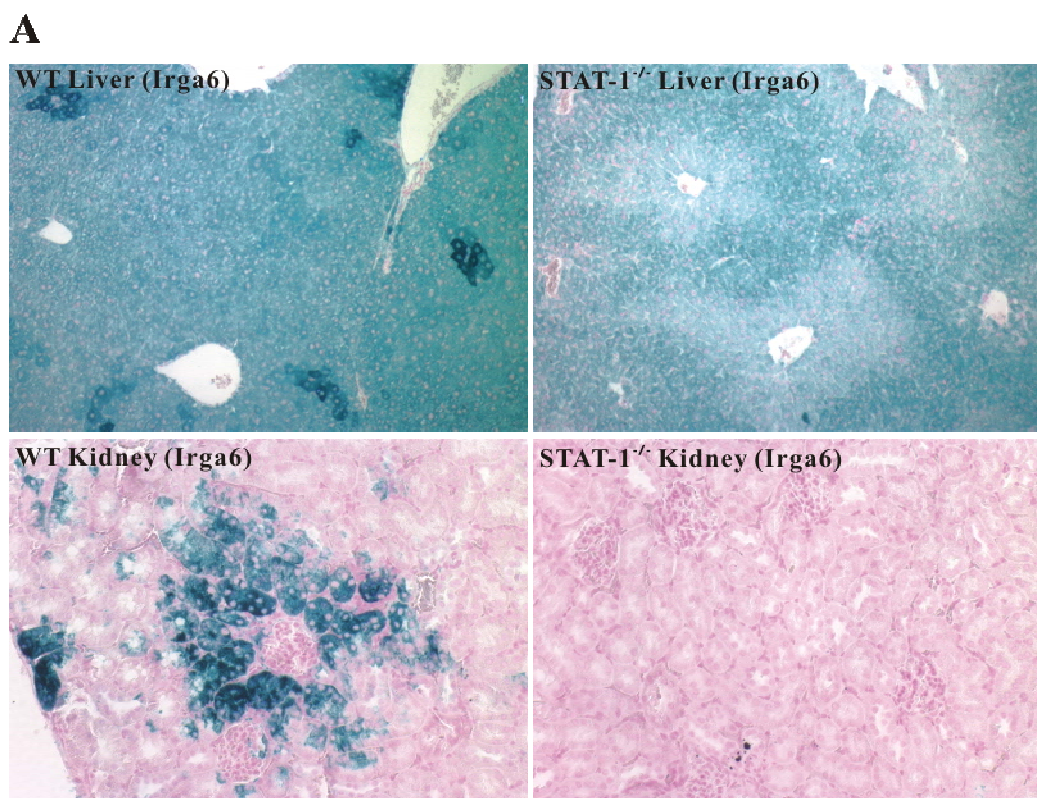
**Figure 25. Irga6 focal expression is absent in interferon receptor knock out mice kidney.** Immunohistochemical staining of Irga6 expression in interferon receptor knock out mice kidney was made (A). Paraffin sections (6 $\mu$ m) of adult mice kidney from 129/sv WT, type I interferon receptor knock out (IFNAR), type II interferon receptor knock out (IFNGR), and double receptor knock out (IFNAGR) mice were cut through the whole organ with an interval of 300  $\mu$ m between adjacent sections. The sections were stained for Irga6 (green) and the focal expression was quantified. Nucleus counter-staining was NFR (red). Irga6 patch in kidney were counted for each 5 sections from 2 kidneys of 2 mice. (B). Pictures were taken using light microscopy (10X40, ZEISS Axiophot).

### **3.6.4 Irga6 focal expression is eliminated in STAT-1<sup>-/-</sup> but not gp130<sup>-/-</sup> liver and kidney**

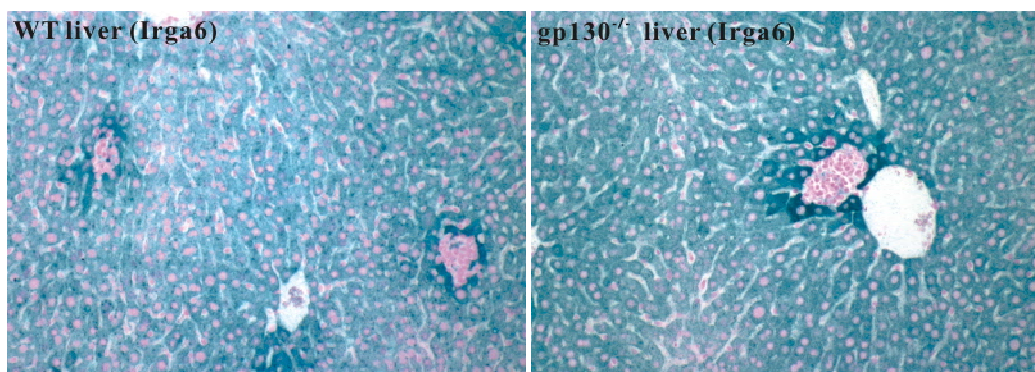
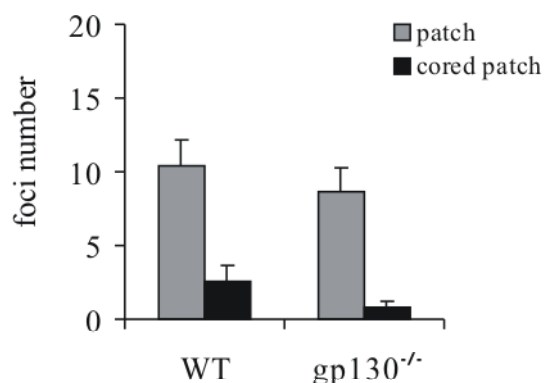
In order to further prove the importance of interferon to Irga6 focal expression, STAT-1 deficient mice were examined. STAT-1 is a transcription factor used both by type I interferon and type II interferon signaling, the deletion of which leads to the blockage of both interferon pathways (Durbin *et al.*, 1996; Meraz *et al.*, 1996). Paraffin sections of liver and kidney from C57BL/6 WT or STAT-1<sup>-/-</sup> mice were stained for Irga6 and the focal expression was quantified (Fig. 26). While the general expression of Irga6 in liver was intact, all the Irga6 focal expression is completely abolished both in liver and in kidney. The expression of Irga6 in heart was also tested and showed no change in the knock out mice (Data not shown).

IL-6 is a pro-inflammatory cytokine secreted by T cells and macrophages to stimulate immune response to trauma and pathogen invasion (van der Poll *et al.*, 1997). Gp130 is the essential signaling receptor component and the deficiency in gp130 abolished IL-6 signaling (Yoshida *et al.*, 1996). gp130<sup>-/-</sup> mice were sampled and exhibited normal Irga6 expression in liver and kidney (Fig. 27).

In conclusion, Irga6 focal expression is dependant on interferon signaling pathways. The Irga6 cored patch in liver and patch in kidney are of IFN- $\gamma$  origin, whereas the Irga6 patch is induced most probably by type I interferon.



**Figure 26. Irga6 focal expression is eliminated in STAT-1<sup>-/-</sup> mice liver and kidney.** Immunohistochemical staining of Irga6 expression in STAT-1<sup>-/-</sup> mice liver and kidney was made (A). Paraffin sections (6 $\mu$ m) of adult mice liver and kidney from C57BL/6 WT and STAT-1<sup>-/-</sup> mice were cut through the whole organ with an interval of 300  $\mu$ m between adjacent sections and stained for Irga6 (green) and the focal expression was quantified. Nucleus counter-staining was NFR (red). Irga6 patch, cored patch in liver and patch in kidney were counted separately within a microscopic view field (10x10, ZEISS Axiophot). Each value in the histogram represents the mean of 20 such counts for organs from 2 mice of each genotype (B). Pictures were taken using light microscopy (10X10, ZEISS Axiophot).

**A****B**

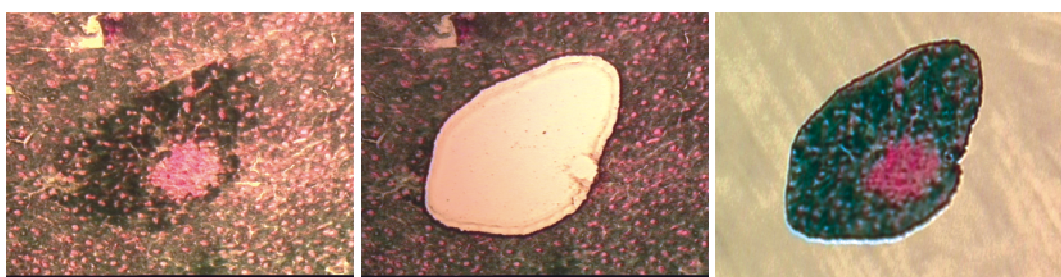
**Figure 27. Irga6 focal expression is normal in gp130<sup>-/-</sup> mice liver and kidney.** Immunohistochemical staining of Irga6 expression in gp130<sup>-/-</sup> mice liver and kidney was made (A). Paraffin sections (6 $\mu$ m) of adult mice liver and kidney from C57BL/6 WT and gp130<sup>-/-</sup> mice were cut through the whole organ with an interval of 300  $\mu$ m between adjacent sections and stained for Irga6 (green) and the focal expression was quantified. Nucleus counter-staining was NFR (red). Irga6 patch, cored patch in liver and patch in kidney were counted separately within a microscopic view field (10x10, ZEISS Axiophot). Each value in the histogram represents the mean of 20 such counts for organs from 2 mice of each genotype (B). Pictures were taken using light microscopy (10X10, ZEISS Axiophot).

### 3.7. Two transcriptional forms of Irga6 are expressed differentially in liver

Irga6 gene has 2 alternative transcriptional forms, namely 1A which has an interferon promoter and 1B which is expressed under a hepatocyte specific promoter. It is tantalizing to speculate that the general expression in liver be mainly 1A form of Irga6, whereas the focal expression mainly make use of the 1B form. To test this speculation, detailed investigation of the expression of Irga6 1A and 1B forms in liver was carried out using Laser Microdissection (LMD) and quantitative Real-Time PCR (qRT-PCR)

techniques.

Cryo-sections of liver were stained for Irga6 and the expression foci were cut by laser and collected for RNA extraction and RTPCR (Fig. 28). Since direct immunostaining of the sections always resulted in very low RNA yield, the following method was developed. C57BL/6 mouse liver were cut in to consecutive cryo-sections and numbered (e.g. 1, 2, 3....). The odd-numbered sections were stained for Irga6 and photos of Irga6 expression foci were taken. The even-numbered sections were then only counter stained with NFR and the position of Irga6 focal expression was defined by using photos of Irga6 expression foci from adjacent odd-numbered sections as reference. Subsequently the positioned Irga6 expression foci on the even-numbered sections were cut using Laser Microdissection technique.



**Before dissection -- on slide    After dissection -- on slide    After collection -- in cap**

**Figure 28. Irga6 expression foci were collected by Laser Microdissection.** Immunohistochemical staining of Irga6 expression in C57BL/6 mice liver was made. Cryo-sections (6µm) of adult mice liver were stained for Irga6 (green) Nucleus counter-staining was NFR (red). Laser microdissection (PALM) was carried out using sharp focused low power laser to cut the Irga6 expression foci. 50 of such laser sections were collected by pulse of high power laser strike onto a drop of oil in a 500µl tube cap and stored in liquid nitrogen for further RNA extraction.

### 3.7.1 Irga6 1B form is more abundant in liver

In the first place, Irga6 1A and 1B transcripts level in mouse liver was determined by quantitative Real-Time PCR. Same amount of liver cDNA was used as template and Irga6 1A and 1B exon specific 5' primers were designed, which together with a common 3' primer on the coding exon are capable of detecting the 2 transcripts, as shown by the melting curves (Fig. 29A). Though it is not easy to compare precisely the amount of 2 products, since they originated from different primer pairs, with a

difference of 5 to 6 in CP values (5 to 6 cycles), 1B transcript should be much more abundant than 1A in whole liver (Fig. 29B).

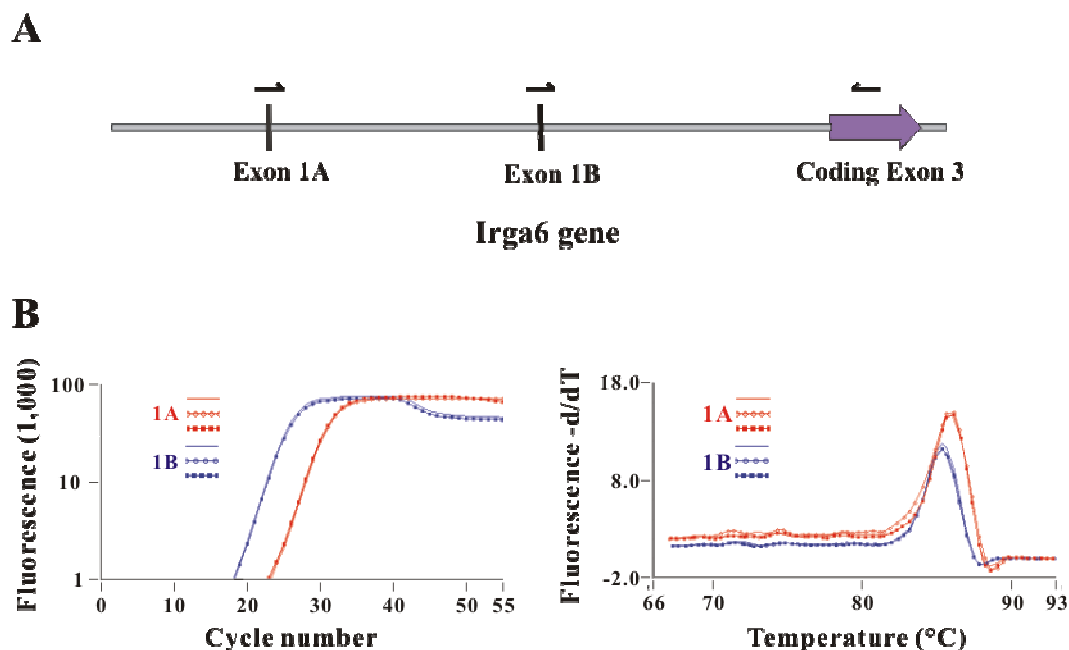


**Figure 29. Irga6 1B form is more abundant in liver.** A. Scheme of primers design for detection of 2 different transcript forms of Irga6. 5' primers specific for Irga6 1A and 1B exon together with one common 3' primer specific for the coding exon generate specific products for both forms of transcripts. B. Quantitative Real-Time PCR analysis of Irga6 1A and 1B transcripts in liver was performed. Liver total RNA was isolated (RNAeasy Mini, QEAGEN), and transcribed into cDNA (Superscript II system, Invitrogen). Equal amounts of liver cDNA were taken as template for Real-Time PCR (SYBR Green I Light Cycler, Roche) using 1A and 1B specific primers. For each gene 3 replicate reactions were made. SYBR green I fluorescence history versus cycle number of 1A and 1B (A) was used to determine ct values (B left). Fluorescence changing rate versus temperature--the melting curve (B right) showed the specificity of the products.

### 3.7.2 Irga6 1A form is remarkably more abundant in Irga6 expression foci in liver

Irga6 1A and 1B expression levels were compared between Irga6 expression foci (F) and the non-foci (NF) using Real-Time PCR. More than 50 Irga6 foci and comparable amount of non-foci were cut and collected (Laser Microdissection, PALM). Total RNA was extracted, and cDNA was synthesized.

Real-Time PCR (SYBR Green I LightCycler, Roche) demonstrated that while Irga6 1B form in foci was only slightly (2 times) higher than non-foci, 1A in the foci is

increased up to 30 folds compared to non-foci (Fig. 30A and C). The melting curve of 1A in Irga6 non-foci at the 1A specific melting temperature always displayed a very small peak, which was barely higher than the noise peak (Fig. 30 B). Final products of both 1A foci and non-foci PCR reaction were cloned and sequenced. It turned out that only 10% of the 1A non-foci products were specific for 1A, whereas 100% of the 1A foci products were specific (Fig. 30D). Since the calculation was based on fluorescence of total products, the ratio for 1A level of foci to non-foci should be much higher than 30.

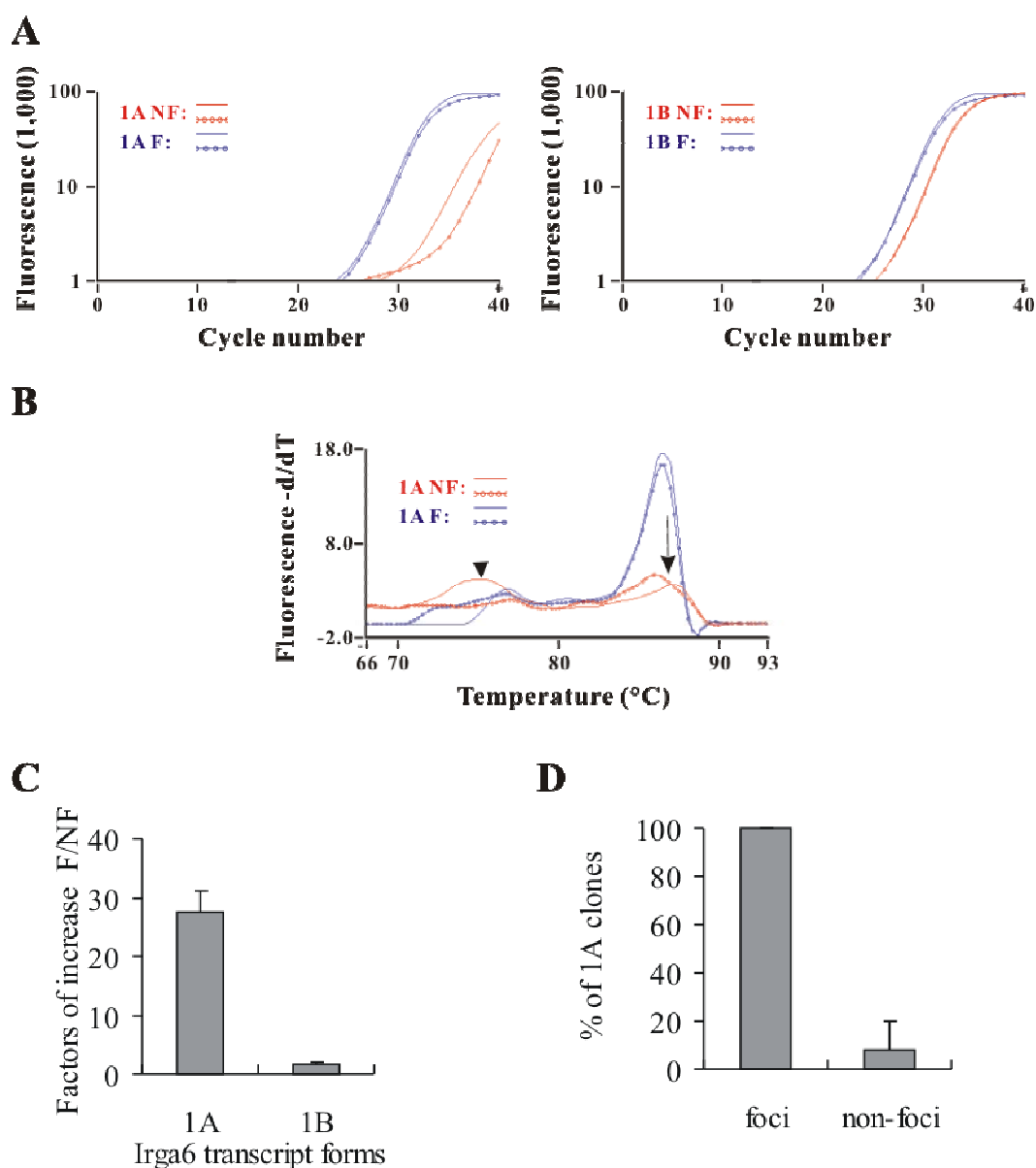


**Figure 30. Irga6 1A form is much more abundant in Irga6 expression foci in liver.** Quantitative Real-Time PCR was performed to determine Irga6 1A and 1B transcripts level in Irga6 1A expression foci or non-foci in liver. More than 50 Irga6 foci and comparable number of non-foci laser sections were collected (Laser Microdissection, PALM). Total RNA was extracted (RNAeasy Micro, QIAGEN), and cDNA was synthesized (Superscript II system, Invitrogen). Real-Time PCR (SYBR Green I Light Cycler, Roche) was carried out using foci (NF, red) or non-foci (F, blue) cDNA as templates, looking for Irga6 1A and 1B as target genes. GAPDH was also included as reference gene. For each gene 2 replicate reactions were made in every experiment. SYBR green I fluorescence history versus cycle number of 1A and 1B (A) was used to determine ct values.  $\Delta$ ct (NF-F) values for target and reference genes were calculated. The primer efficiencies were determined by Real-Time PCR using template (liver cDNA) titration (Pfaffl, 2001). The ratio of F/NF of 1A and 1B (C) were determined then using PFAFFL method (Pfaffl *et al.*, 2001). Histogram (C) represents the mean values of 2 independent experiments. Fluorescence changing rate versus temperature is the melting curve (B right) showing the specificity of the products (B right). Arrow points to 1A specific product, arrow head points to unspecific noise. 1A foci and non-foci products were ligated to pGEM-T Easy vector (Promega), transformed into E. coli. (DH5 $\alpha$ ). 20 clones were sequenced and percentage of 1A sequences were calculated (D).

### 3.7.3 Irga6 1A form in cored patch is expressed at similar level as in patch in liver

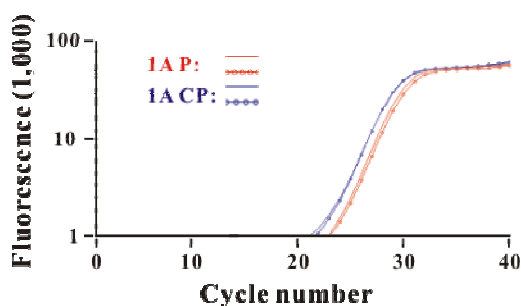


**Figure 31. Irga6 1A form expression level in cored patch is similar to that of patch in liver.** Quantitative Real-Time PCR was performed to determine Irga6 1A transcript level in Irga6 1A cored patch and patch in liver. More than 50 Irga6 cored patch and comparable number of non-cored patch laser sections were collected (Laser Microdissection, PALM). Total RNA was extracted (RNAeasy Micro, QIAGEN), and cDNA was synthesized (Superscript II system, Invitrogen). Real-Time PCR (SYBR Green I Light Cycler, Roche) was carried out using patch (P, red) or non-patch (CP, blue) cDNA as templates, looking for Irga6 1A as target genes. GAPDH was also included as reference gene. For each gene 2 replicate reactions were made in every experiment. SYBR green I fluorescence history versus cycle number of 1A (A) was used to determine ct values.  $\Delta$ ct (NF-F) values for target and reference genes were calculated. The ratio of CP/P of 1A (B) were determined then using PFAFFL method (Pfaffl *et al.*, 2001).

Type I interferons were reported to be weaker inducers of IRG proteins (Carlow *et al.*, 1998; Taylor *et al.*, 1996). To determine whether there are more Irga6 1A form in cored patch, expression levels of 1A were compared between Irga6 expression cored patch and patch. More than 50 Irga6 cored patch (CP) and comparable amount of patch (P) were cut and collected for Real-Time PCR. Irga6 1A expression in cored patch is only slightly higher than that of patch (Fig. 31).

#### 3.7.4 IFN- $\gamma$ is expressed in Irga6 cored patch but not in patch in liver

Semi-quantitative Reverse-Transcriptase PCR was performed searching for IFN- $\gamma$  mRNA in both Irga6 cored patch and patch. cDNA from Irga6 cored patch and patch were used as template and Nest-PCR for IFN- $\gamma$  was performed, using internal primer pairs within the PCR product of the first round PCR to do the second round PCR. Clearly IFN- $\gamma$  mRNA could only be detected in cored patch (CP) but not in patch (P) (Fig. 32).

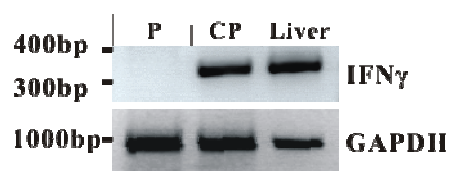
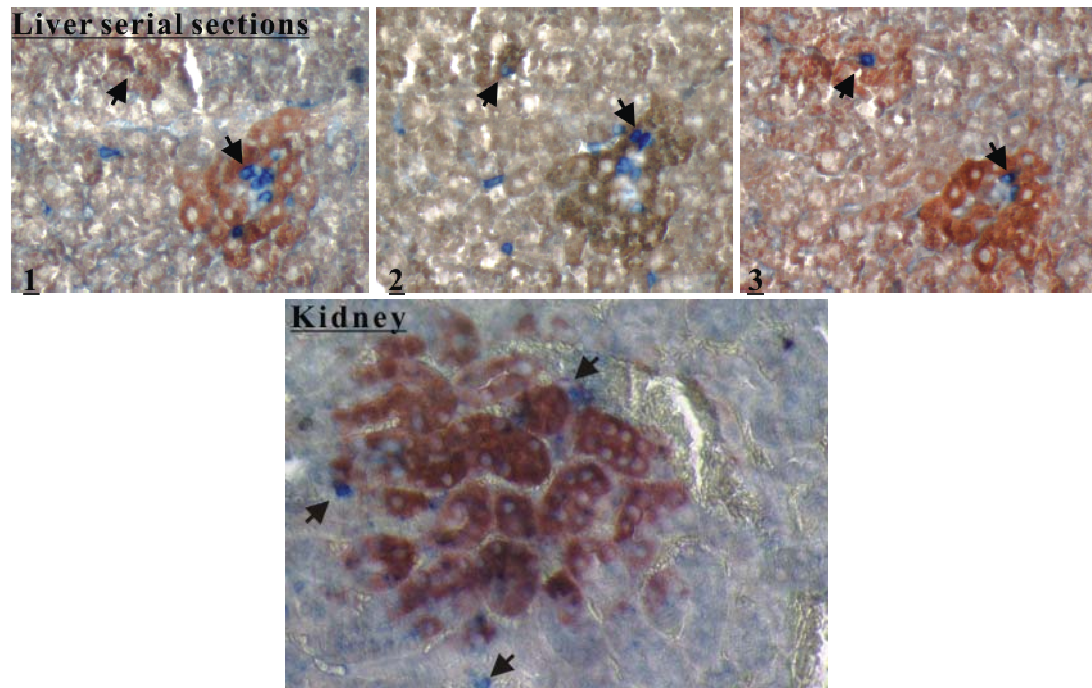


**Figure 32. IFN- $\gamma$  is expressed in Irga6 cored patch but not in patch in liver.** Semi-quantitative Reverse-Transcription PCR was performed to determine IFN- $\gamma$  expression in Irga6 1A cored patch and patch in liver. More than 50 Irga6 cored patch and comparable number of non-cored patch laser sections were collected (Laser Microdissection, PALM). Total RNA was extracted (RNAeasy Micro, QIAGEN), and cDNA was synthesized (Superscript II system, Invitrogen) as templates for IFN- $\gamma$  Nest-PCR. 5' Primer specific for IFN- $\gamma$  exon1 (IFNG fw2) and 3' primer (IFNG bw2) for exon 4 was designed for the first round of amplification of 45 cycles. The product length was 507 bp, which was then taken as template for the second round of PCR of 45 cycles using another 5' primer specific for exon 2 and 3 junction (IFNG sp2) and the same 3' primer. The final product length is 332 bp. Liver cDNA (Liver) was also included and GAPDH was amplified as loading control. The sequencing of CP product demonstrated that the product is indeed IFN- $\gamma$ .

### 3.8. T cells are essential for Irga6 cored focal expression in liver

#### 3.8.1 T cells and macrophages are present in the center of Irga6 cored focal expression in liver and kidney

##### **A** Irga6(red) and CD3 (blue)



##### **B** Irga6 (red) and F4/80 (blue)

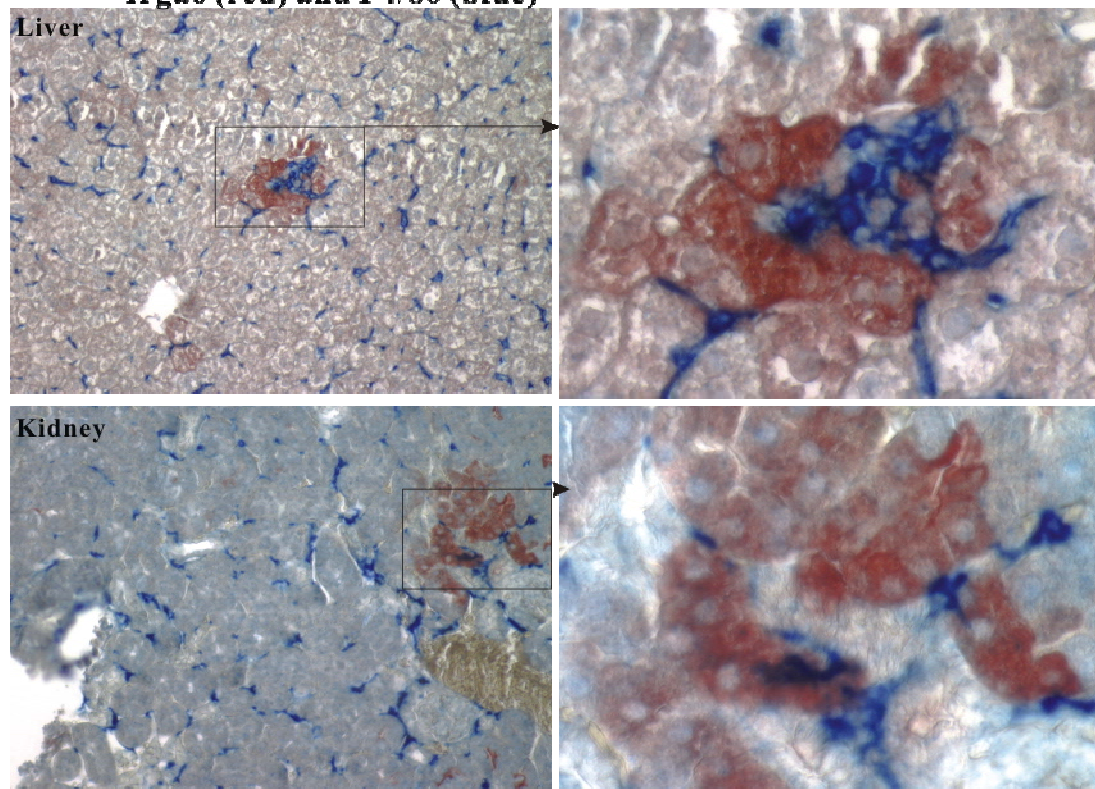


**Figure 33. T cells and macrophages are present in the center of Irga6 cored expression in liver and kidney.** Immunohistological double staining of mice liver and kidney was made for Irga6 and T cell or macrophage marker. Paraffin sections (6µm) of adult C57BL/6 mice liver and kidney were stained for Irga6 (red) with 165/3 and CD3 with anti-CD3 mAb (A, blue) or anti-F4/80 mAb (A, blue). For Irga6 and CD3 double staining, consecutive serial sections were made and arrows point to CD3 positive T cells. For detection of Irga6 the horseradish peroxidase substrate AEC was used and for CD3 or F4/80 the Alkaline Phosphatase Substrate Kit III (Vector, Linaris) was used. Pictures were taken using light microscopy (10X10, ZEISS Axiophot).

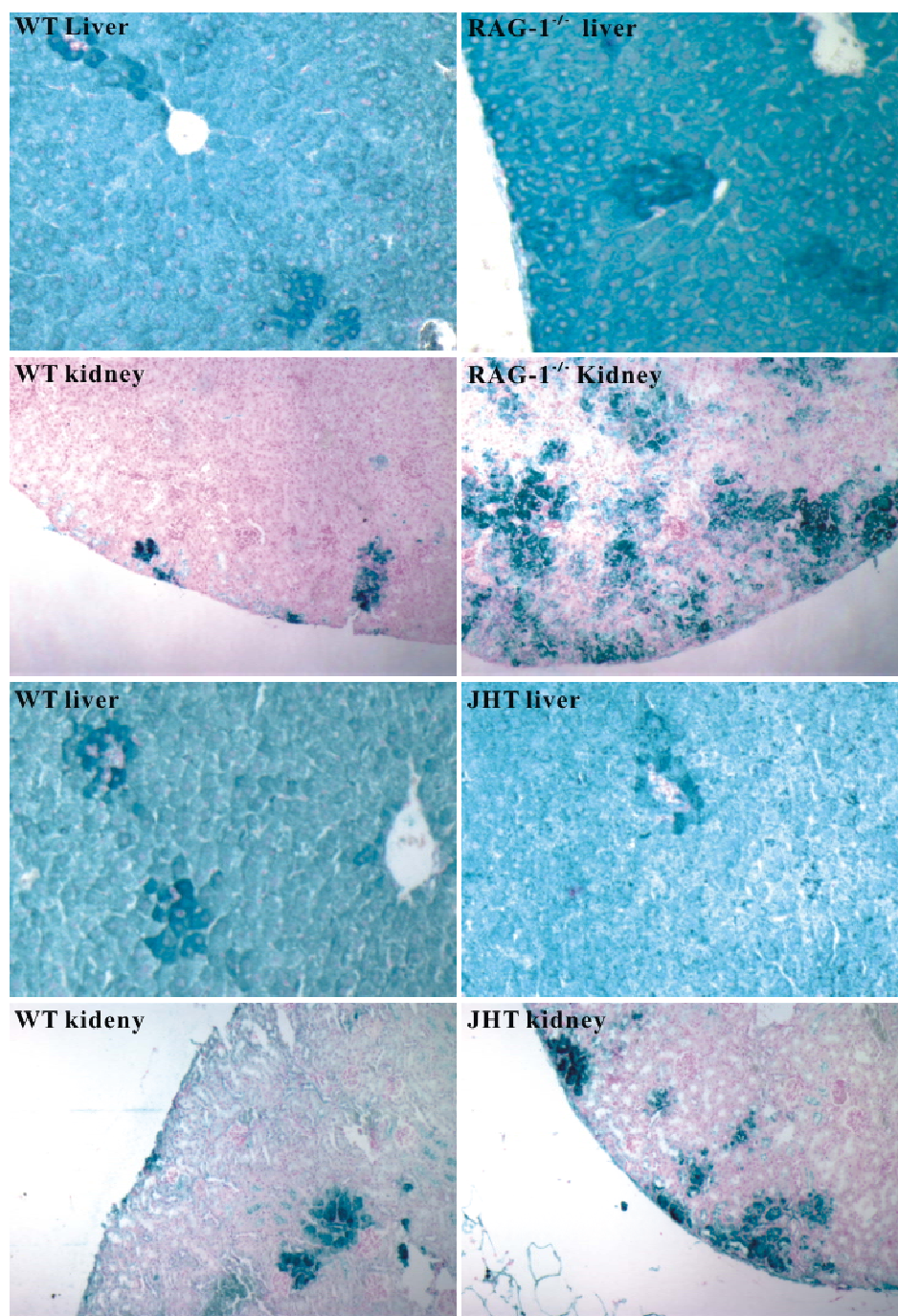
In order to identify the sources of IFN- $\gamma$  for Irga6 cored patch expression, the cell type composition of the “core” were analyzed. Double staining of C57BL/6 mouse liver paraffin sections were made for Irga6 (red) and CD3 (blue), which is a T cell marker, or Irga6 (red) and F4/80 (blue), which is a macrophage cell surface marker. Serial sections explicitly demonstrated that T cells were present in the center of Irga6 cored patch. T cells were found in the Irga6 expression foci in kidney as well (Fig. 33A). In addition macrophages were also localized to the “core” of Irga6 expression patch in liver and kidney (Fig. 33B).

### **3.8.2 Irga6 cored patch expression in liver is eliminated in RAG-1<sup>-/-</sup> mice**

RAG-1<sup>-/-</sup> mice are genetic altered strains lacking T and B lymphocytes (Mombaerts *et al.*, 1992). These mice were examined to establish the relationship of T cells to Irga6 focal expression. Paraffin sections of C57BL/6 WT and RAG-1<sup>-/-</sup> mouse liver and kidney were stained for Irga6 (green) and the focal expression was quantified. No Irga6 cored patch expression was found in RAG-1<sup>-/-</sup> liver and the patch expression was reduced additionally (Fig. 34). Interestingly, kidneys from knock out mice were almost full of Irga6 expression foci, indicating an over-expression of interferon (Fig. 34A).

JHT mice are deficient of B cells because of the loss of functional H chain locus (Chen *et al.*, 1993). Analysis of JHT mice showed normal presence of all types of Irga6 focal expression (Fig. 34). The number Irga6 cored patch liver and patch in kidney were elevated in the knock out mice.

**A**



**B**

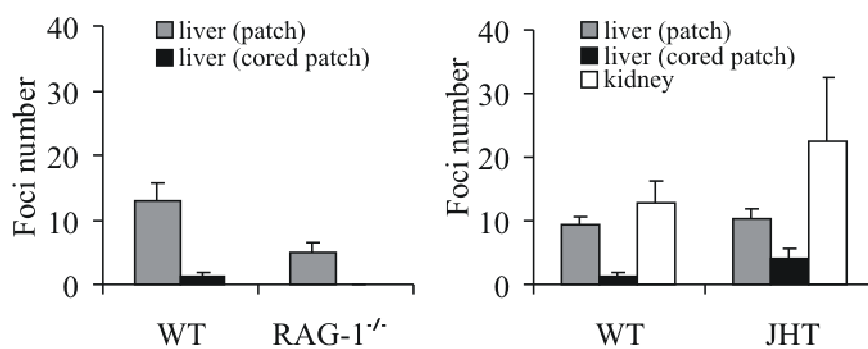


**Figure 34. Irga6 cored patch expression is eliminated in liver of RAG-1<sup>-/-</sup> but not JHT mice.** Immunohistochemical staining of Irga6 expression in RAG-1<sup>-/-</sup> and JHT mice liver and kidney was made (A). Paraffin sections (6µm) of adult mice liver and kidney from C57BL/6 WT, RAG-1<sup>-/-</sup> and JHT mice were stained for Irga6 (green) with 165/3 and the focal expression was quantified. Nucleus counter-staining was NFR (red). Irga6 patch, cored patch in liver and patch in kidney were counted separately within a microscopic view field (10x10, ZEISS Axiophot). Each value in the histogram represents the mean of 20 such counts for organs from 2 mice of each genotype (B). Pictures were taken using light microscopy (10X10, ZEISS Axiophot).

In brief, T cells are essential for Irga6 cored patch expression, which is most probably induced by IFN- $\gamma$  secreted by T cells in the middle.

### **3.9. V $\beta$ 8 V $\alpha$ 14 NK T cell is the major T cell population in Irga6 cored expression patch in liver**

In many immune responses, like the immune responses elicited by superantigens and many autoimmune diseases, there exist biased uses of certain subsets of T cell receptors. Therefore examination of TCR repertoire sometimes may reveal the nature of immune responses.

#### **3.9.1 T cell receptor V $\beta$ 8 subfamily is preferentially used by T cells in Irga6 cored expression patch in liver**

T cell receptor V $\beta$  (TCR V $\beta$ ) usage was analyzed for T cells existing in the Irga6 focal expression cores. More than 50 Irga6 cored patches in liver were first collected by Laser Microdissection, and cDNA was then synthesized as template for Nested-PCR. The first PCR was carried out using V $\beta$  consensus primer (DVB1S) as 5' primer and a 3' C $\beta$  primer (C $\beta$  outer). The product was then taken as template for another round of PCR using another 3' C $\beta$  primer (C $\beta$  inner) to produce fragments around 280 bp, which were then cloned and sequenced. The clones with TCR V $\beta$  sequences were identified using an online tool IMGT/V-QUEST, which can identify V $\beta$  sequences by comparing given sequences to those in the data base, (<http://imgt.cines.fr/>). T cells from cervical and mesenteric lymph nodes were used as control (Fig. 35A and B). In contrast to control T cell clones which exhibited a wide range of TCR V $\beta$  distribution,

including 8, 5, 14, 15, 2, 10, 11, all clones from Irga6 cored patch belonged to V $\beta$ 8 subfamilies, especially V $\beta$ 8.2 which was the most abundant. This indicates that there was a biased TCR V $\beta$  usage in Irga6 cored patch (Fig. 35C).

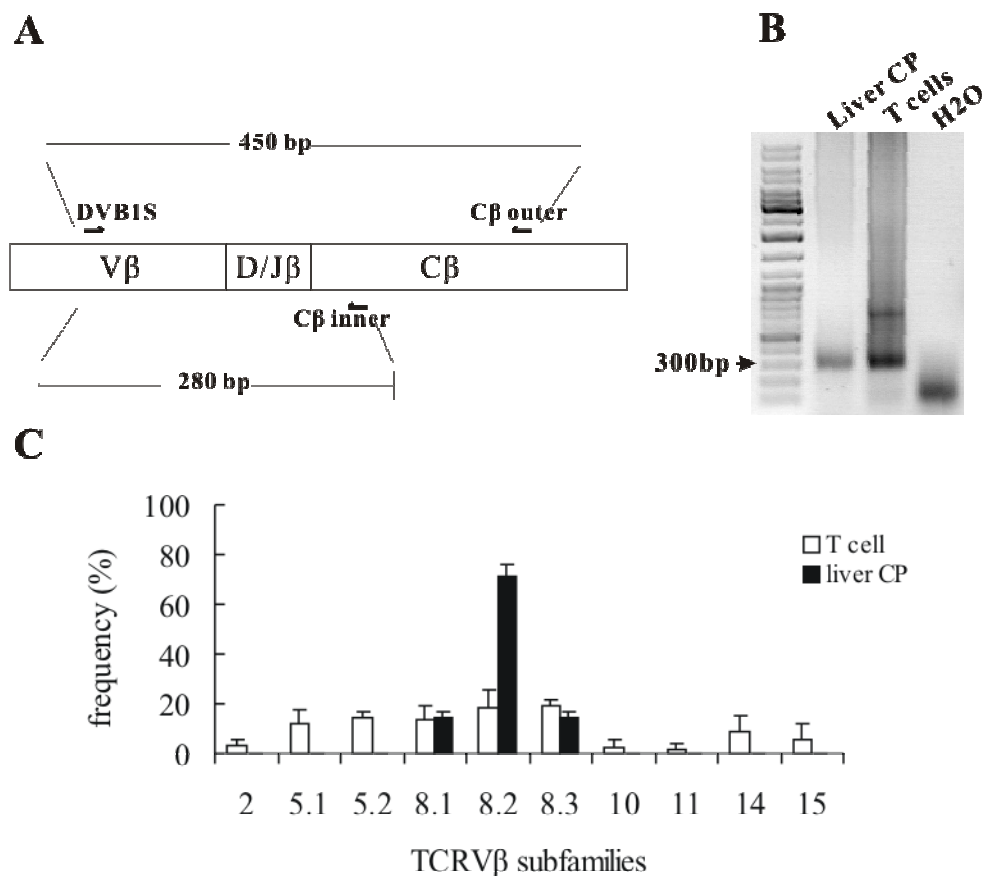


**Figure 35. TCR V $\beta$ 8 subfamily is preferentially used by T cells in Irga6 cored expression patch.** More than 50 Irga6 cored patches were collected by laser sections, total RNA was extracted, and cDNA was synthesized as template for Nested-PCR. The first PCR was carried out by V $\beta$  consensus primer (DVB1S) as 5' primer and a 3' C $\beta$  primer (C $\beta$  outer). The second round of PCR used the same 5' primer and another 3' C $\beta$  primer (C $\beta$  inner) (A). T cells from cervical and mesenteric lymph nodes were used as control. The length of final products was around 280bp (B). The products were subsequently ligated to pGEM-T Easy vector (Promega), transformed into *E. coli*. (DH5 $\alpha$ ) and clones were sequenced. The sequences were compared to classical TCR V $\beta$  sequences online using IMGT/V-QUEST (<http://imgt.cines.fr/>), and the clones with a sequence identity of more than 95% to known V $\beta$  sequences were identified as V $\beta$  clones. In total 132 and 68 V $\beta$  clones for control T cells and Irga6 cored patch respectively were identified and the percentage of each V $\beta$  subfamily was displayed by the histogram(C).

## A

Junction Type	Clone number	D $\beta$	J $\beta$	V 8.1 region	N(D)N region	J region
1)	4	-	1.4	ATTTCTGTGCCAGCAGTGAT	<u>AGGCAG</u>	AACGAAAGATTATTTTCGG
2)	1	-	1.4	ATTTCTGTGCCAGCAGTGAT	<u>GTCCAG</u>	AACGAAAGATTATTTTCGG

Junction Type	Clone number	D $\beta$	J $\beta$	V8.2 region	N(D)N region	J region
1)	2	1.1	1.1	GTGTACTTCTGTGCCAGCGGTG	<u>GGGGGCTTG</u>	CAAACACAGAAGTCTCTTT
2)	14	1.1	2.7	GTGTACTTCTGTGCCAGCGG	<u>GGACAGC</u>	GAACAGTACTTCGGTCCCGG
3)	3	1.1	2.7	GTGTACTTCTGTGCCAGCGGTGATG	<u>CGGACAA</u>	CTCCTATGAACAGTACTTCGGTCCCGG
4)	2	2.1	2.3	GTGTACTTCTGTGCCAGCGG	GGGGACATCT	AGTGCAGAAACGCTGTATT
5)	1	1.1	2.1	GTGTACTTCTGTGCCAGCGGTGA	<u>GACAGGGGT</u>	CTATGCTGAGCAGTCTCTCG
short	3					

Junction Type	Clone number	D $\beta$	J $\beta$	V8.3 region	N(D)N region	J region
1)	1	1.1	1.1	TTGTACTTCTGTGCCAGCAG	<u>GGACAG</u>	CACAGAAGTCTCTTTGGTA
2)	3	1.1	2.1	TTGTACTTCTGTGCCAGCAG	<u>AAGGACAGGGG</u>	CTATGCTGAGCAGTCTCTCG
short	1					

## B

V $\beta$  8.1

- 1) : ATTTCTGTGCCAGCAGTGATAGGCAGAACGAAAGATTATTTTCGGTCATGGAACCAAGCTGTCTGTCTGGAGGATCTGAGAAAT  
 2) : ATTTCTGTGCCAGCAGTGATGTCCAGAACGAAAGATTATTTTCGGTCATGGAACCAAGCTGTCTGTCTGGAGGATCTGAGAAAT

V $\beta$  8.2

- 1) : TTCTGTGCCAGCGGTGGGGGCTTGCAAACACAGAAGTCTTCTTTGGTAAAGCAACAGACTCAGACTTGTAGAGGATCTGAGAAA  
 2) : TTCTGTGCCAGCGGTGACAGCGAACAGTACTTCGGTCCCGGCACCAGGCTCACGGTTTT-----AGAGGATCTGAGAAA  
 3) : TTCTGTGCCAGCGGTGATGGGACAACCTCTATGAACAGTACTTCGGTCCCGGCACCAGGCTCACGGTTTT-----AGAGGATCTGAGAAA  
 4) : TTCTGTGCCAGCGGTGGACATCTAGTGCAGAAACGCTGTATTTGGCTCAGCAACAGACTGACTGTCTCTCGAGGATCTGAGAAA  
 5) : TTCTGTGCCAGCGGTGAGACAGGGGGTCTATGCTGAGCAGTTCCTCCGACCAAGGACACGACTCACCGTCTAGAGGATCTGAGAAA

V $\beta$  8.3

- 1) : TTCTGTGCCAGCAG--GGACAGCA-----CAGAAGTCTTCTTTGGTAAAGCAACAGACTCAGACTTGTAGAGGATCTGAGAAAT  
 2) : TTCTGTGCCAGCAGAAAGACAGGGGGCTATGCTGAGCAGTCTTTCGGACCAAGGACACGACTCACCGTCTAGAGGATCTGAGAAAT

**Figure 36. TCR V $\beta$ 8 clones of Irga6 cored patch had variety of junctions.** A. Sequences of identified TCR V $\beta$ 8 clones of Irga6 cored patch were compared, classified into different junction types and the number of clones for each type are listed. D $\beta$ , J $\beta$  subfamily names are also labeled ('-' means not identified) and TCR V $\beta$ -N(D)N-J $\beta$  junctional sequences are shown. D $\beta$  elements flanked by the template independent (N) sequences are underlined. 'Short' indicates V $\beta$ 8 clones that are too short to have complete junctional regions. B. Sequence alignment of identified TCR V $\beta$ 8 clones of Irga6 cored patch. Sequences shaded in black are identical sequences. Sequences shaded in gray or without shade show sequences that are not identical.

Detailed analysis of the sequences of clones from Irga6 cored patch revealed that they possessed various junctions. For example, there were 4 J regions and 5 junction types for V $\beta$ 8.2 clones (Fig. 36A). Sequence alignments demonstrated that they also had differences in length (Fig. 36B).

### 3.9.2 T cells carrying V $\beta$ 8 TCR exist in Irga6 cored expression patch in liver

To prove that V $\beta$ 8 TCR bearing T cells are really present in the center of Irga6 cored

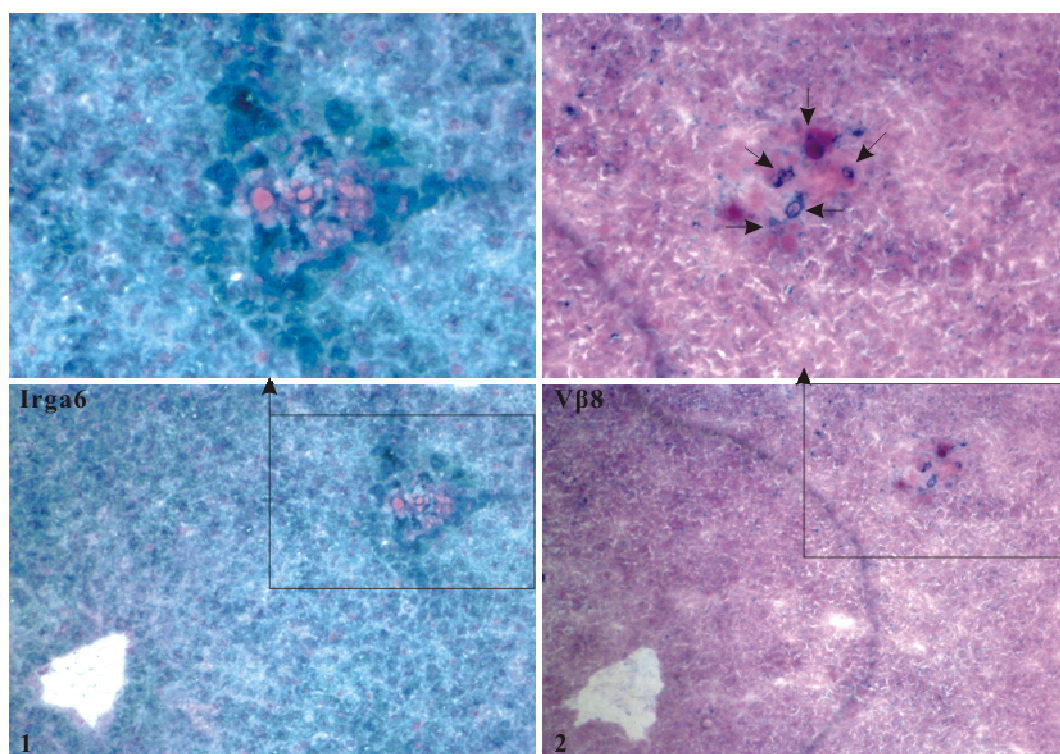


**Figure 37. T cells bearing V $\beta$ 8 TCR are present in the center of Irga6 cored patch in liver.** Immunohistochemical analysis of V $\beta$ 8 TCR expression in mouse liver was carried out. Cryo-sections (6 $\mu$ m) from C57BL/6 adult mice liver were prepared in a consecutive serial. The two adjacent serial sections were probed by Irga6 mAb 165/3 (1, green) and TCR V $\beta$ 8 mAb name (2, blue) respectively. Frames show enlarged images. Arrows indicate T cells expressing V $\beta$ 8 TCR. Nucleus counter-staining was NFR (red). Pictures were taken using light microscopy (10X10, ZEISS Axiophot).

patch in liver, immunostaining for V $\beta$ 8 TCR in mouse liver was carried out. C57BL/6 mice livers were cut into consecutive cryo-sections and immunostaining for Irga6 and

anti-V $\beta$ 8 TCR was made on two adjacent sections respectively. Comparison of the staining at the same position on the two sections demonstrated V $\beta$ 8 TCR positive T cells obviously existed right in the center of Irga6 cored patch (Fig. 37).

### 3.9.3 T cell receptor V $\alpha$ 14-J $\alpha$ 18 is preferentially used by T cells in Irga6 cored expression patch in liver

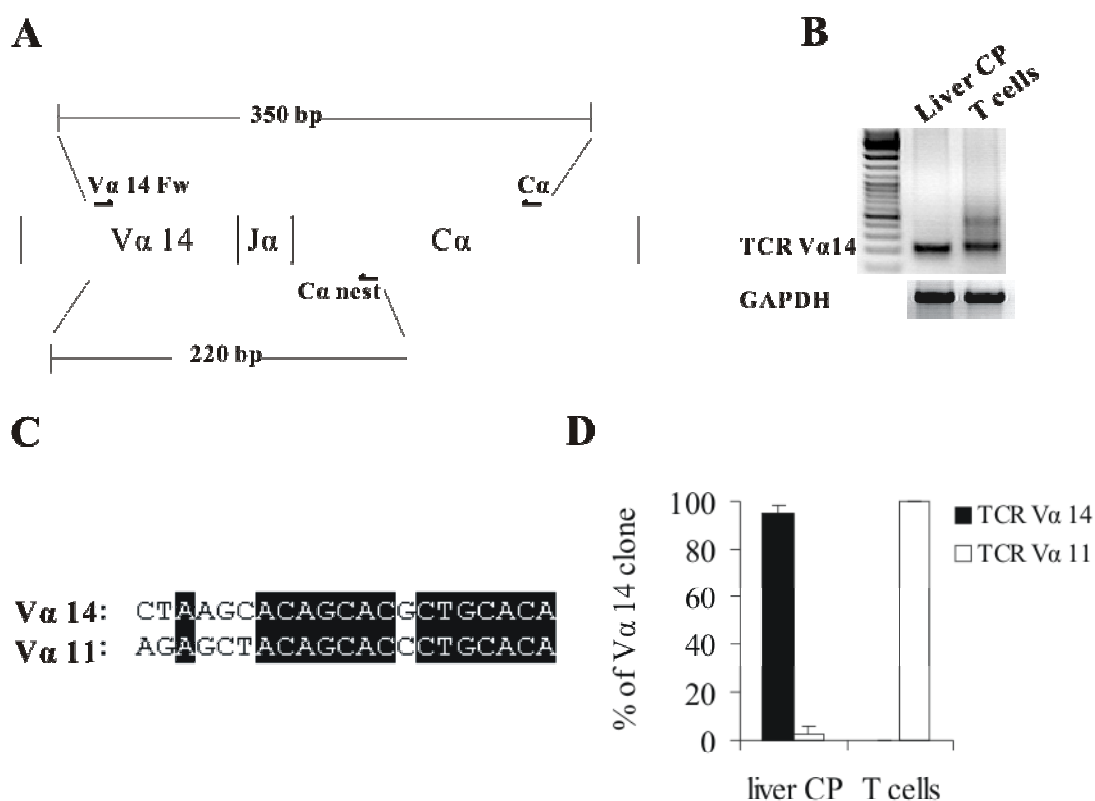


**Figure 38. TCR V $\alpha$ 14-J $\alpha$ 18 is preferentially used by T cells in Irga6 cored expression patch.**

More than 50 Irga6 cored patches were collected by laser sections, total RNA was extracted, and cDNA was synthesized as template for Nested-PCR. The first PCR was carried out by V $\alpha$ 14 specific 5' primer and a 3' primer for C $\alpha$  (C $\alpha$ ), and the second PCR was done using another 3' primer for C $\alpha$  (C $\alpha$  nest) (A). T cells from cervical and mesenteric lymph nodes were used as control and the length of final products was around 280bp. GAPDH was used as loading control (B). The products were sequenced and the sequences were compared to classical TCR V $\alpha$  sequences online using IMGT/V-QUEST (<http://imgt.cines.fr/>), and the clones with a sequence identity of more than 95% to known V $\alpha$  sequences were identified as V $\alpha$  clones. In total 40 and 71 V $\alpha$  clones for control T cells and Irga6 cored patch were identified respectively and the percentage of each V $\alpha$  subfamily was displayed by the histogram (D). Alignment of V $\alpha$ 14 primer and the corresponding region on V $\alpha$ 11 was made (C).

## A

Junction type	Clone number	V $\alpha$	J $\alpha$	V region	N region	J region
1)	14	14	18	ACCTACATCTGTGTGGTGGG		AGATAGAGGTT CAGCCTTAG
2)	3			ACCTACATCTGTGTGGTG	TC	AGATAGAGGTT CAGCCTTAG
3)	18			ACCTACATCTGTGTGGTGGG	G	GATAGAGGTT CAGCCTTAG
4)	8			ACCTACATCTGTGTGGTGGG	T	GATAGAGGTT CAGCCTTAG
5)	24			ACCTACATCTGTGTGGTGGG	C	GATAGAGGTT CAGCCTTAG
6)	3			ACCTACATCTGTGTGGTG	TC	GATAGAGGTT CAGCCTTAG
	2	11	49	TTACTTCTGTGCTGCTGAGG	TCTT	CACGGGTTACCAGAACTTCT

Clone number	J $\alpha$	V $\alpha$ 1 region	N region	J region
1	12	ACTTACTTCTGTGCTGCTGA	AACC	GGGACTGGAGGCTATAAAGT
5	40	ACTTACTTCTGTGCTGCTG	GTG	ATACAGGAAACTACAAATAC
4	22	ACTTACTTCTGTGCTG	TGCTGCCG	CATCTTCTGCCAGCTGGCAA
5	48	ACTTACTTCTGTGCTGCTG	CCAAT	CCAACTATGGAAATGAGAAA
2	31	ACTTACTTCTGTGCTGCTG	GGCTTT	AATCTTCTTTGGTGATGGGA
2	45	ACTTACTTCTGTGCTGC	CTC	GAATACAGAAGGTGCAGATA
2	13	ACTTACTTCTGTGCTGCTGAGG	CGGGG	ATCTGGGACTTACCAGAGG
3	23	ACTTACTTCTGTGCTGCTGAGG	CC	TATAACCAGGGGAAGCTTAT
5	33	ACTTACTTCTGTGCTGTTGAG	CTC	GATAGCAACTATCAGTTGAT
1	21	ACTTACTTCTGTGCTGCTGAG	AG	GTCTAATTACAACGTGCTTT
5	21	ACTTACTTCTGTGCTGTTGAG	GCGTA	TGCTAATTACAACGTGCTTT
5	21	ACTTACTTCTGTGCTGCTGAGG	CGG	CTAATTACAACGTGCTTT
1	short			

## B

V $\alpha$ 14

1) : TACATCTGTGTGGTGGGATAGAGGTT CAGCCTTAGGGAGGCTGCATTTTGG  
2) : TACATCTGTGTGGTGT CAGATAGAGGTT CAGCCTTAGGGAGGCTGCATTTTGG  
3) : TACATCTGTGTGGTGGGGATAGAGGTT CAGCCTTAGGGAGGCTGCATTTTGG  
4) : TACATCTGTGTGGTGGGTGATAGAGGTT CAGCCTTAGGGAGGCTGCATTTTGG  
5) : TACATCTGTGTGGTGGGCATAGAGGTT CAGCCTTAGGGAGGCTGCATTTTGG  
6) : TACATCTGTGTGGTGGTCATAGAGGTT CAGCCTTAGGGAGGCTGCATTTTGG

**Figure 39. T cells from Irga6 cored patch use invariant TCR V $\alpha$ 14-J18.** A. Sequences of identified TCR V $\alpha$ 14 and 11 clones were compared, classified into different junction types and the number of clones for each type is listed. V $\alpha$  and J $\alpha$  subfamily names are also labeled and TCR V $\alpha$ -N-J $\alpha$  junctional sequences are shown. 'Short' indicates V $\beta$ 8 clones that are too short to have complete junctional regions. B. Sequences alignment of identified TCR V $\beta$ 14 clones of Irga6 cored patch. Sequences shaded in black are identical sequences. Sequences shaded in gray or without shade show sequences that are not completely identical.

NKT cells are a lineage of T cells, which have a V $\beta$ 8 usage bias for TCR $\beta$  chain and also mostly an invariant V $\alpha$ 14-J $\alpha$ 18 TCR  $\alpha$  rearrangement (Bendelac *et al.*, 2007). Therefore, TCR V $\alpha$ 14 was analyzed in Irga6 cored patch.

Irga6 cored patches in liver were first collected by Laser Microdissection, from which RNA was extracted and cDNA synthesized as template for Nested-PCR. The first PCR was carried out using V $\alpha$ 14 specific 5' primer and a 3' C $\alpha$  primer (C $\alpha$ ). The product was taken as template for a second round of PCR using another 3' C $\alpha$  primer (C $\alpha$  nest) to produce fragments around 220 bp, which were then cloned, sequenced and identified (Fig. 38A and B).

It turned out that V $\alpha$  positive clones fell into 2 groups, V $\alpha$ 14 and V $\alpha$ 11. Sequence comparison revealed that the V $\alpha$ 14 primer sequence has a quite high identity with one region of V $\alpha$ 11 (Fig. 38C). For Irga6 cored patch in liver 97% of the V $\alpha$  clones are V $\alpha$ 14 and only 3% are V $\alpha$ 11. In the case of T cells, however, 100% of the clones are V $\alpha$ 11 (Fig. 38D). This indicates that the V $\alpha$ 14 T cells were much more concentrated in Irga6 cored patch.

Detailed analysis of the sequences of clones from Irga6 cored patch demonstrated that they all share a common J segment, namely J $\alpha$ 18, in spite of which small variations of only 1 or 2 nucleotides right at the V-J junction could be observed (Fig. 39A). Clones from T cells that are only positive for V $\alpha$ 11 displayed a great variety of junctional types using 10 different J $\alpha$  segments (Fig. 39B).

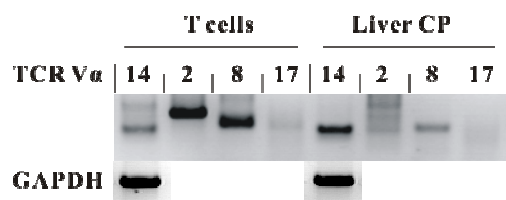


**Figure 40. T cells bearing TCR V $\beta$ 14 are more abundant in Irga6 cored expression patch.**

More than 50 Irga6 cored patches were collected by laser sections, total RNA was extracted, and cDNA was synthesized as template for Nest-PCR. The first PCR was carried out by 5' primer specific for V $\alpha$ 14, 2, 8 or 17 and a 3' primer for C $\alpha$  (C $\alpha$ ), and the second PCR was done using another 3' primer for C $\alpha$  (C $\alpha$  nest). T cells from cervical and mesenteric lymph nodes were used as control. GAPDH was used as loading control.

Several other TCR V $\alpha$  members were also examined in the same context using RTPCR. For periphery T cells V $\alpha$  2, 8, 17 are among the most frequently used TCR V $\alpha$  subfamilies (Yoshida *et al.*, 2000b). The expression of these V $\alpha$  subfamily members were tested for Irga6 cored patch and control T cells. TCR V $\alpha$  2, 8 had very strong expression for control T cells, which was very weak or almost absent for Irga6 cored patch, and TCR V $\alpha$  17 also was expressed to a lesser extend for T cells but not at all for Irga6 cored patch (Fig. 40).

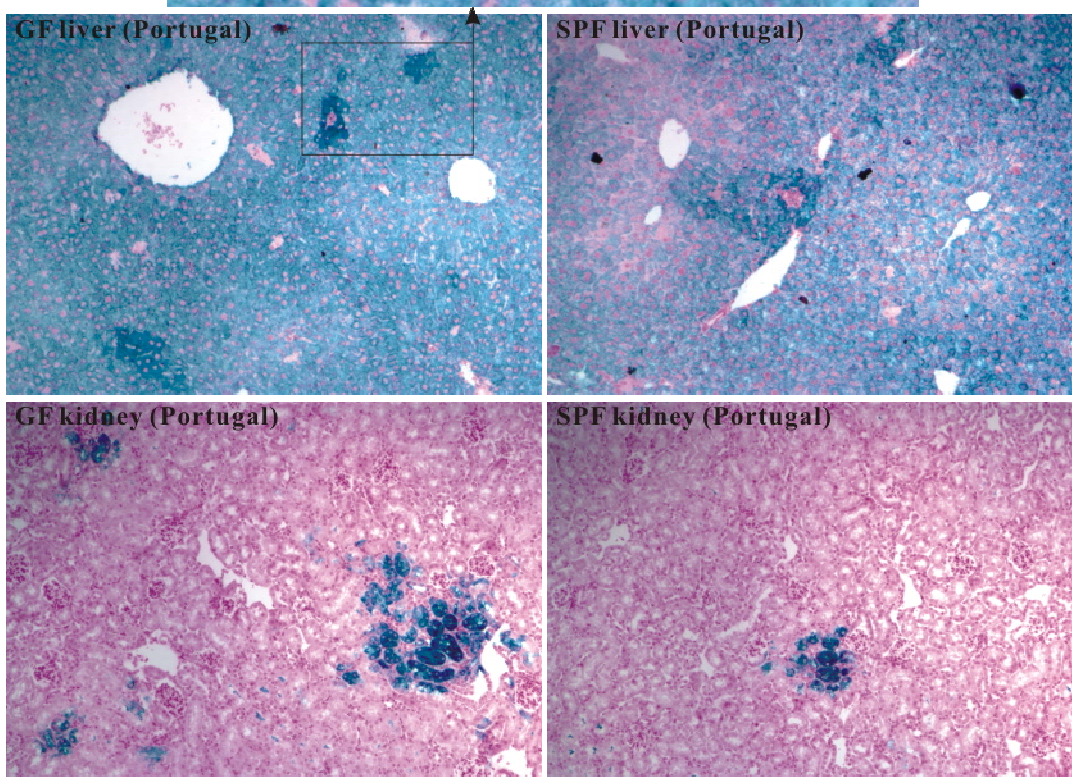
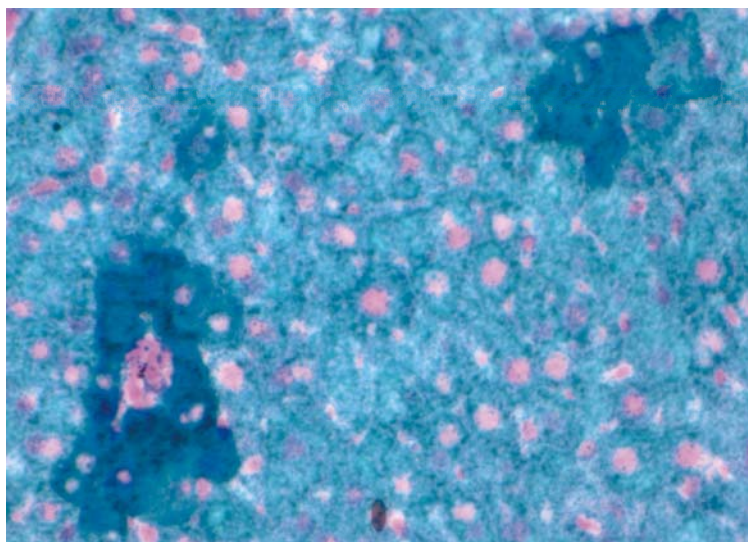
In summary, NKT cells are most probably the major T cell type in Irga6 cored patch.

### **3.10. Irga6 focal expression is not caused by bacteria and endotoxin**

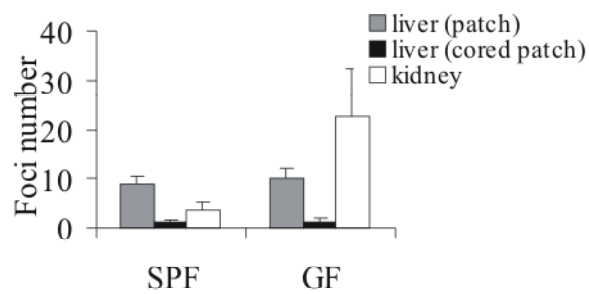
#### **3.10.1 Irga6 focal expression is intact in germ free mice**

In order to determine the causes of Irga6 focal expression Germ free mice, which are free of bacteria and common infectious viruses, were analyzed, (Wagner *et al.*, 1959). Germ free (GF) mice and specific pathogen free (SPF) C57BL/6 mice were obtained from the Instituto Gulbenkian de Ciência (Portugal). Liver and kidney were cut into paraffin sections (6 $\mu$ m), stained for Irga6 (green) and Irga6 focal expression was then quantified (Fig 41). Surprisingly, Irga6 focal expression was present also in GF mouse liver and kidney. The Irga6 focal expression was even much elevated in GF kidney (Fig. 41B). GF mice from two other sources, Institut für Labortierkunde Uni. Zürich (Switzerland) and the Karolin's Institute (Sweden), were also examined, and in both cases the normal existence of Irga6 focal expression was also confirmed (Fig. 41C).

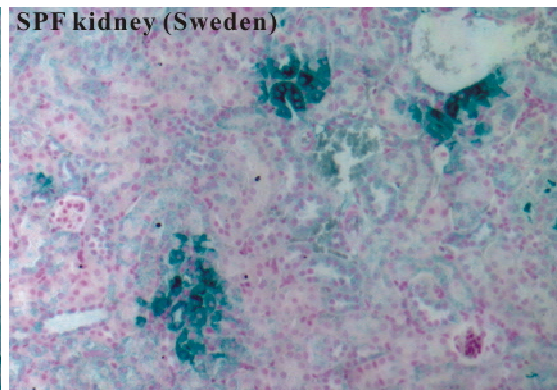
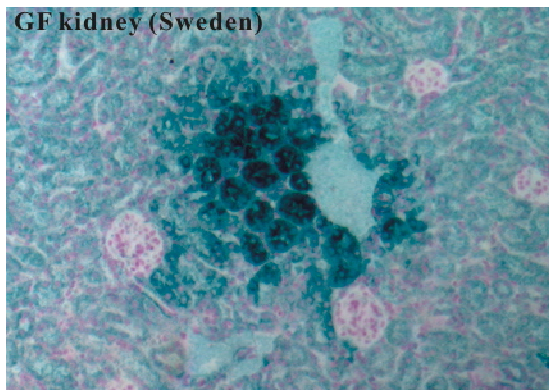
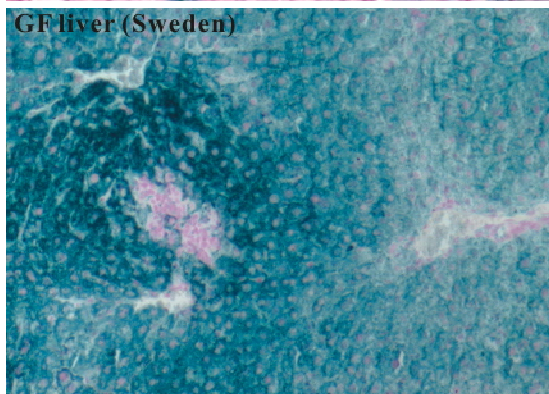
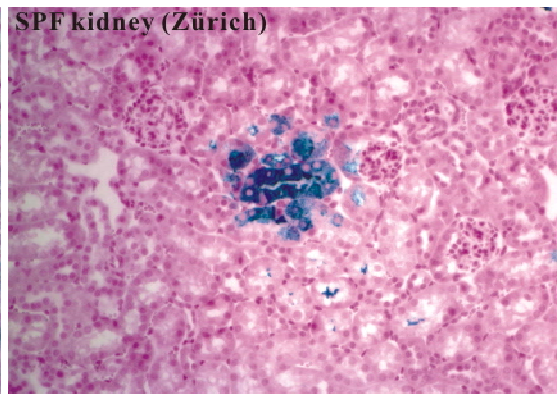
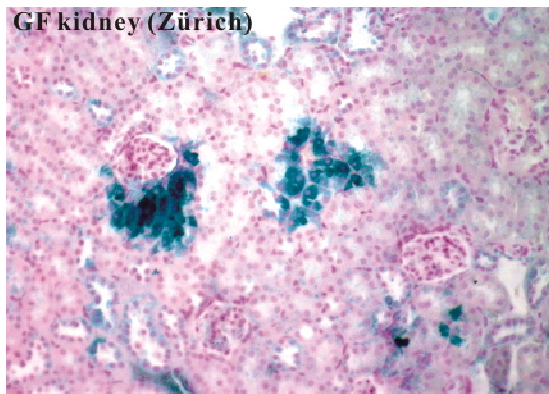
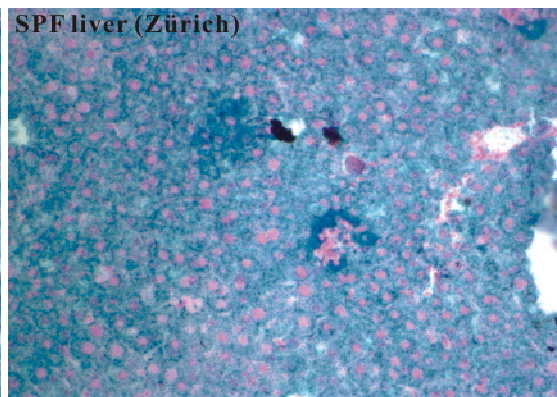
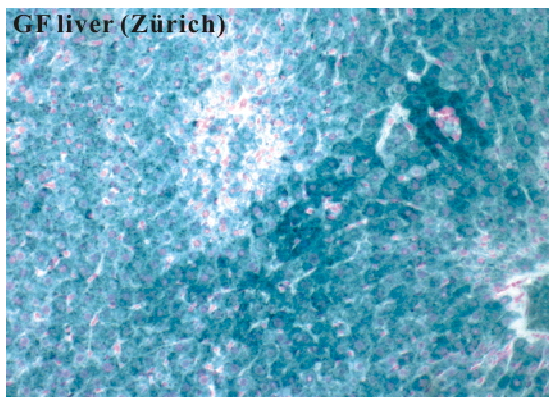
**A**



**B**



**C**

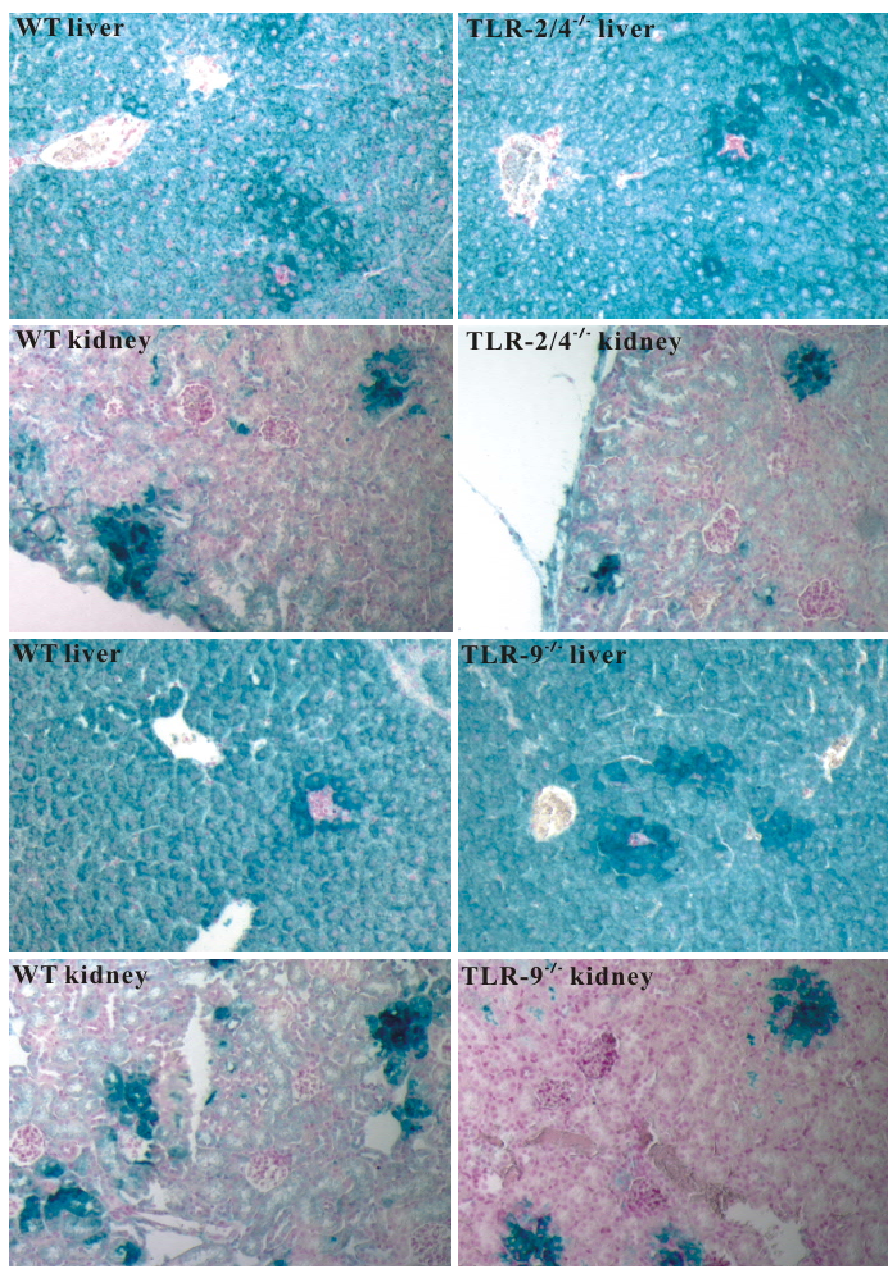
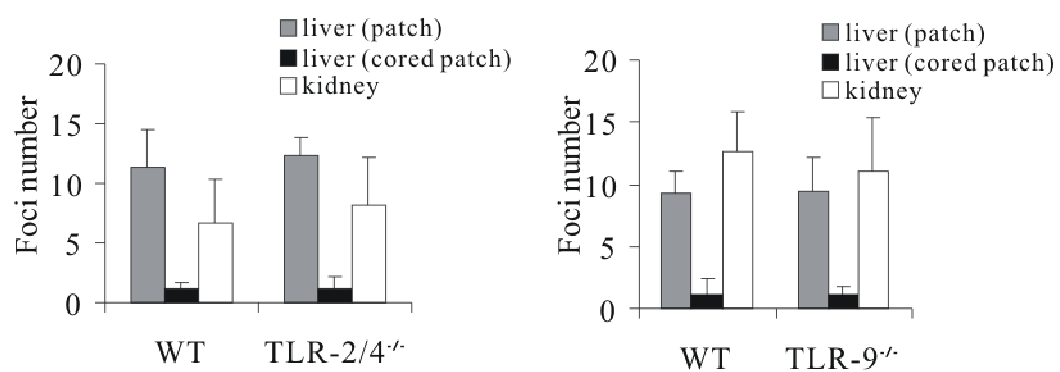


**Figure 41. Irga6 cored patch expression exist in GF mice.** GF and SPF mice from the Instituto Gulbenkian de Ciência (Portugal), Institut für Labortierkunde Uni. Zürich (Switzerland) and the Karolin's Institute (Sweden) were obtained. Paraffin sections (6µm) of liver and kidney were prepared from these mice. Immunohistochemical staining for Irga6 (green) was made (A and C) and the focal expression was quantified. Nucleus counter-staining was NFR (red). Frame show enlarged image (A). For Portugal tissues Irga6 patch, cored patch in liver and patch in kidney were counted separately within a microscopic view field (10x10, ZEISS Axiophot). Each value in the histogram represents the mean of 20 such counts for organs from 2 mice of each type (B). Pictures for mice from Portugal (10x10), Switzerland and Sweden (10x20) were taken using light microscopy (ZEISS Axiophot).

### 3.10.2 Irga6 focal expression persists in TLR pathway deficient mice

Mice deficient in TLR pathway were examined to establish the possible relationship between Irga6 focal expression and endotoxins. C57BL/6 WT and TLR-2/4 double knock out or TLR-9<sup>-/-</sup> mice were obtained. Paraffin sections of liver and kidney from these mice were stained for Irga6 (green) and Irga6 focal expression was then quantified (Fig. 42). No significant differences could be detected between the WT and knock out mice.

MyD88 is one of the most important adaptor proteins down stream in TLR signaling (Fitzgerald *et al.* 2001). MyD88<sup>-/-</sup> mice were also tested. C57BL/6 WT and MyD88<sup>-/-</sup> mouse liver paraffin sections were prepared and stained for Irga6 (green). Irga6 focal expression was also quantified. Again no big effect can be observed (Fig. 43).

**A****B**

**Figure 42. Irga6 cored patch expression is not affected in TLR-2/4 double knock out and TLR-9<sup>-/-</sup> mice.** C57BL/6 WT, TLR-2/4 double knock out and TLR-9<sup>-/-</sup> mice were obtained. From these mice liver and kidney paraffin sections (6µm) were cut through the whole organ with an interval of 300µm between 2 adjacent sections. Immunohistochemical staining for Irga6 (green) was made (A) and the focal expression was quantified (B). Nucleus counter-staining was NFR (red). Irga6 patch, cored patch in liver and patch in kidney were counted separately within a microscopic view field (10x10, ZEISS Axiophot). Each value in the histogram represents the mean of 20 such counts for organs from 2 mice of each genotype (B). Pictures were taken using light microscopy (10X10, ZEISS Axiophot).

### 3.11 Irga6 expression after *Listeria monocytogenes* infection

It is intriguing to learn how Irga6 expresses in *Listeria* infection. C57BL/6 mice were infected by *Listeria monocytogenes* and sacrificed at different time points and Irga6 expression in liver and kidney was examined by western blot and immunohistochemistry.

In contrast to liver inoculated by heat-killed *Listeria monocytogenes*, which had a comparable level of expression as uninfected liver in western blot, in liver infected by live bacteria, Irga6 expression was already much elevated 24 hours post infection and rose even higher in the following days. The situation was similar in the case of infected kidney (Fig. 44)

Immunostaining of Irga6 of liver and kidney infected for 24 hours still exhibited normal pattern of Irga6 focal expression with a more intensive staining both for the general and focal expression. In livers infected for more than 2 days, Irga6 general expression was greatly elevated and focal expression disappeared consequently. Instead, huge unstained foci occurred, which started to appear from the second day on and accumulated in a greater number in the following days. The expression of Irga6 in

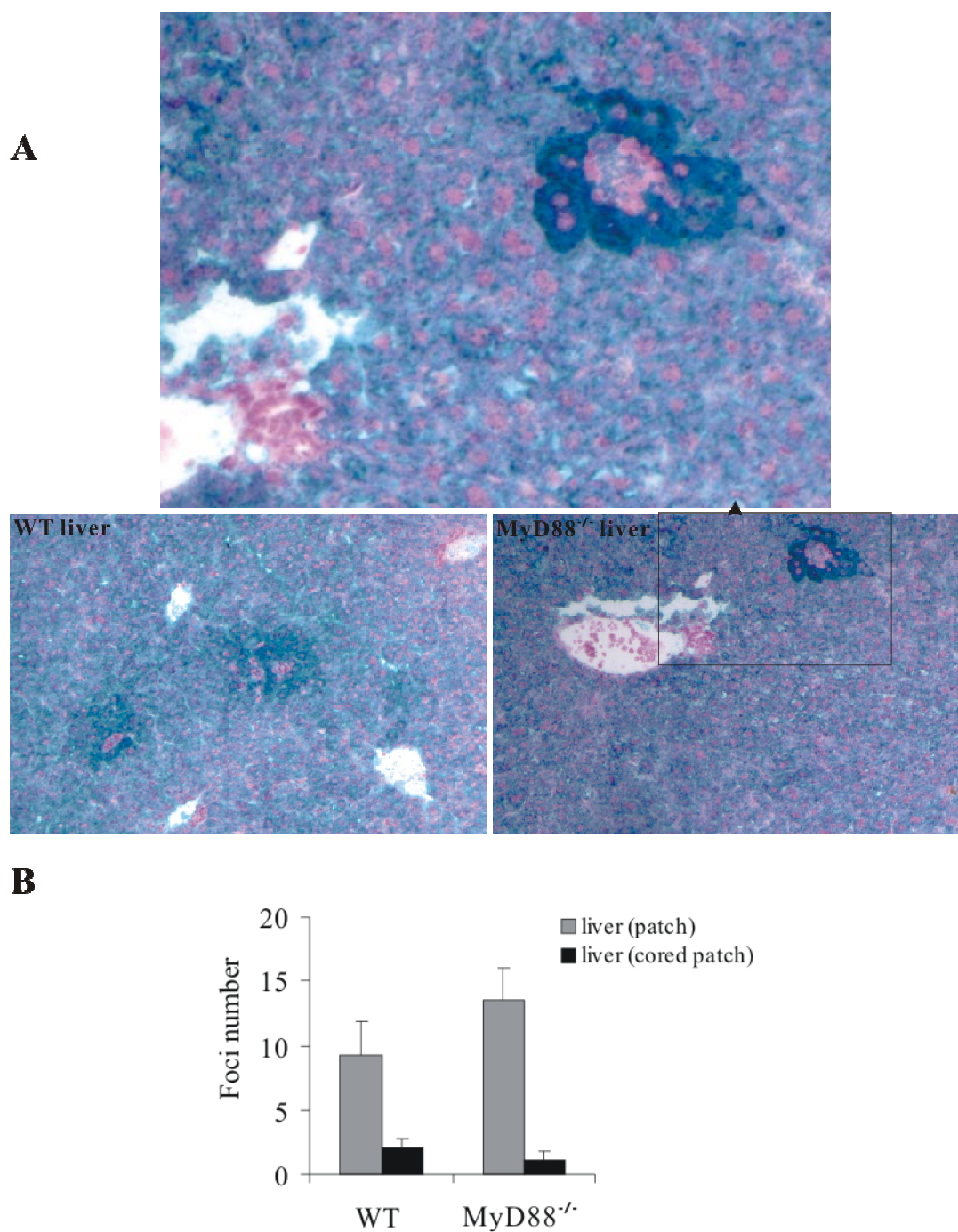


**Figure 43. Irga6 cored patch expression is normal in MyD88<sup>-/-</sup> mice.** C57BL/6 WT and MyD88<sup>-/-</sup> mice were obtained. From these mice paraffin sections (6 $\mu$ m) of liver and kidney were cut through the whole organ with an interval of 300 $\mu$ m between 2 adjacent sections. Immunohistological staining for Irga6 (green) was made (A) and the focal expression was quantified (B). Nucleus counter-staining was NFR (red). Irga6 patch, cored patch in liver and patch in kidney were counted separately within a microscopic view field (10x10, ZEISS Axiophot). Each value in the histogram represents the mean of 20 such counts for organs from 2 mice of each genotype (B). Pictures were taken using light microscopy (10X10, ZEISS Axiophot).

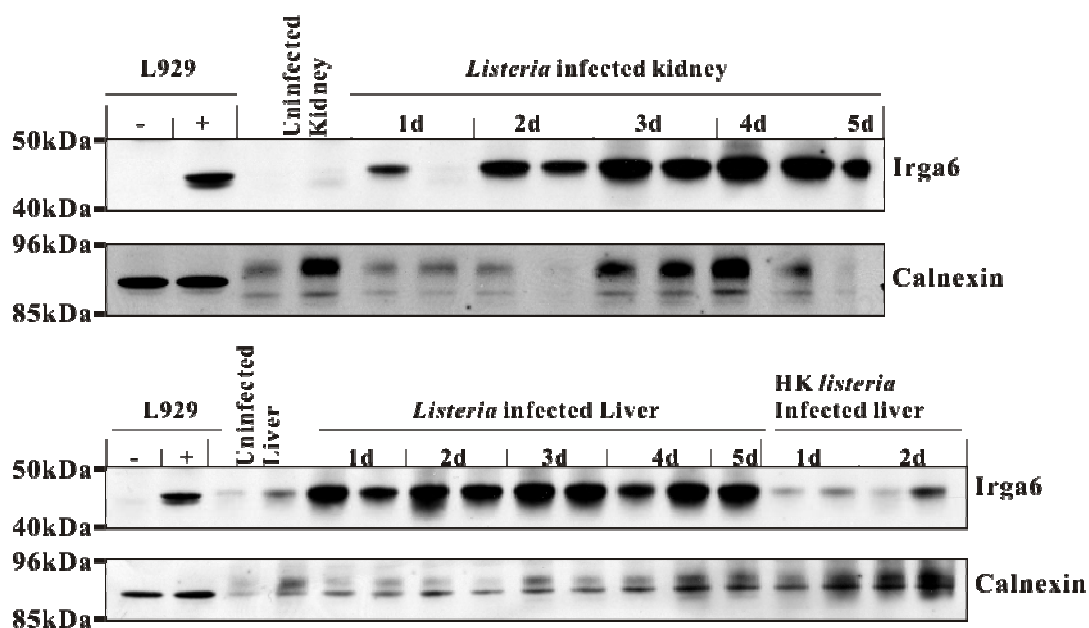


**Figure 44. Irga6 expression in liver and kidney infected by *listeria monocytogenes* in western blot.** Western blot analysis of Irga6 expression in liver and kidney infected by *Listeria monocytogenes* was made. C57BL/6 adult mice were either infected by *Listeria monocytogenes* at LD<sub>50</sub> or inoculated by same amount of heat-killed bacteria or left untreated. Liver and kidney were taken at indicated time points post infection (p.i.), ground in liquid nitrogen, weighed and then lysed in RIPA buffer. L929 cells stimulated (+) by IFN- $\gamma$  (200U/ml) for 24 hours were used as positive control. Irga6 mAb 10D7 was used for detecting protein expression. Calnexin was also probed as loading control.

infected kidney also started to become intensified 24 hours post infection and from the second day post infection on the whole kidney was overall filled with extremely intense Irga6 expression, indicating a strong overall IFN- $\gamma$  response (Fig. 45).

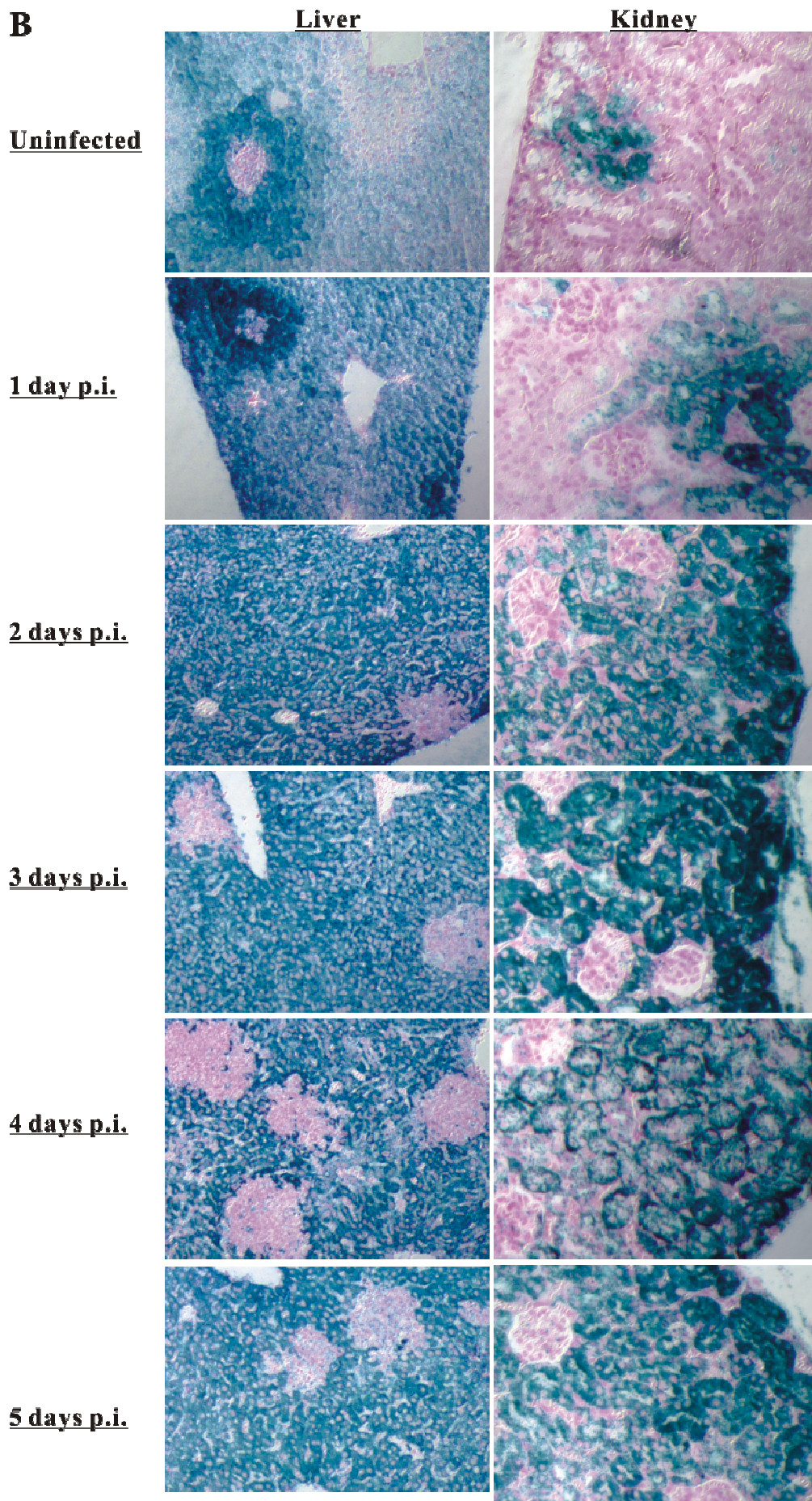


**Figure 45. Irga6 expression in liver and kidney infected by *listeria monocytogenes*.** Immunohistochemical analysis of Irga6 expression in liver and kidney infected by *Listeria monocytogenes* was carried out. Liver and kidney were embedded in paraffin and cut into 6µm sections and stained for Irga6 (green) by 165/3 antiserum. Nuclear counter-stain was NFR. Pictures were taken using light microscopy (10X10, ZEISS Axiophot).

## 4. Discussion

IRG proteins are a family of IFN-inducible GTPases, which confer resistance to a varied group of bacterial and protozoan pathogens correlating to the resistance dependent on IFN- $\gamma$ . The expression of IRG has been widely investigated and a consensus that IRG GTPases are expressed under the tight regulation of IFNs, has been reached. Our unexpected findings that IRG proteins do have significant constitutive as well as IFN-inducible expression *in vivo*, and in liver at least for one member, Irga6, achieved by selective usage of distinct alternative promoters, would not only change our current understanding of the expression pattern but also shed a new light on the resistance functions of this family of IFN-inducible GTPases. Peculiar Irga6 focal expression in liver as well as in kidney was also observed and proved to be induced by local production of IFNs. The production of IFN- $\gamma$  that induces Irga6 focal expression in liver surprisingly represents the local activation of NKT cells even in the absence of microbial environment (germ-free mice). Even though the causes of this NKT cell activation are still elusive, we speculate that this stimulation of NKT cells may stand for an ongoing process required for the maintenance of peripheral NKT cell effector phenotype.

### 4.1 IRG proteins are constitutively expressed in mice liver

Previous analysis of expression for IRG proteins *in vivo* revealed a predominant IFN-esp. IFN- $\gamma$ -dependent expression in liver, spleen or lung during infection with intracellular pathogens like *Listeria monocytogenes*, *Toxoplasma gondii* or *Mycobacterium tuberculosis* (Boehm *et al.*, 1998; Collazo *et al.*, 2001; Gavrilescu *et al.*, 2004; Taylor *et al.*, 2000). For instance, the mRNA expression of all the six well-known members of *Irg* genes could be induced to a very high level in the liver infected by *Listeria monocytogenes* in an IFN- $\gamma$  dependent manner, but in the absence of infection there was no basal expression observed (Fig. 5) (Boehm *et al.*, 1998). However, we observed that, when a proper control such as L929 cells induced with

IFN- $\gamma$  was included in the same experiment setup, compared to the induced cells very high level of basal mRNA expression of *Irga6* gene was discovered in uninfected liver (Fig. 6). The otherwise overlooked basal expression in uninfected liver was surprisingly high, much higher than that in the fibroblast cell line stimulated with IFN- $\gamma$ . Furthermore this basal expression is only mildly decreased in animals deficient in both type I and type II interferon receptors (Fig. 12).

*Irgm3* gene expression has also not been detected in liver in a non-quantitative way (Taylor *et al.*, 1996). Again, however, in an experiment quantitatively normalized to IFN- $\gamma$ -induced L929 cells we could easily detect an expression of Irgm3 protein in liver, though in this case at a much lower level than in induced L929 cells (Fig. 7&16). *Irgb6*, *Irgm1* and *Irgd* are all also expressed in the liver at a significant level, though the IFN influence on these GTPases are not yet tested (Fig. 16).

The question rises why IFN-inducible resistance GTPases should be constitutively expressed in the liver? In the special case of *Irga6*, where the basal liver expression is extremely high, we have shown that the tissue specific expression in the liver and IFN-induction of *Irga6* are independently controlled by distinct promoters.

#### **4.2 The expression of *Irga6* in liver was under the control of alternative activation of distinct promoters**

The open reading frame of *Irga6* gene is encoded on a single 3' long exon behind two alternatively used 5' exons, exon 1A and exon 1B that are spliced to the long coding exon producing two *Irga6* transcripts (Fig. 13). The promoter region of *Irga6* 1A is a strong IFN-inducible promoter, containing 3 ISRE and 2 GAS sites, whereas *Irga6* 1B promoter is much weaker harboring only 1 ISRE and 1 GAS sites (Bekpen *et al.*, 2005). Our analysis of putative promoter binding sites in the promoter regions of both *Irga6* transcripts led to the discovery of multiple hepatocyte nuclear factor binding sites only in the proximal promoter region of *Irga6* 1B (Fig. 13&14).

Hepatocyte-specific gene transcription requires simultaneous binding of multiple, distinct hepatocyte nuclear factors (HNFs) to the gene regulatory region providing synergistic transcriptional activation (Fig. 46) (Costa *et al.*, 2003). Among HNFs, one

of the most important is HNF4, which, interacting with multiple proteins that act at distinct steps during transcription (Green *et al.*, 1998), can activate transcription by facilitating the assembly of transcription initiation machinery (Schrem *et al.*, 2002). Similar to other hepatocyte-specific genes such as transthyretin (TTR) (Fig. 46), putative binding sites of multiple HNFs in Irga6 1B promoter region fall into two clusters, both of which include a HNF-4 site (Fig. 13&14), strongly suggesting that it is a hepatocyte specific promoter. Consistently, Irga6 was found to be expressed in freshly isolated primary hepatocytes at very high level, which was comparable to that in liver. Interestingly this expression decreased very rapidly when the primary cells were cultured for certain time (Fig. 15). It is well acknowledged that when hepatocytes are removed from the animal and cultured *in vitro*, the transcription rates of many liver-specific genes decrease dramatically, due to rapid dedifferentiation of primary hepatocytes (Clayton and Darnell, 1983; Clayton *et al.*, 1985). The fast decline of Irga6 expression in primary hepatocytes is in line with our assumption that Irga6 constitutive expression in liver is driven by a tissue specific promoter.

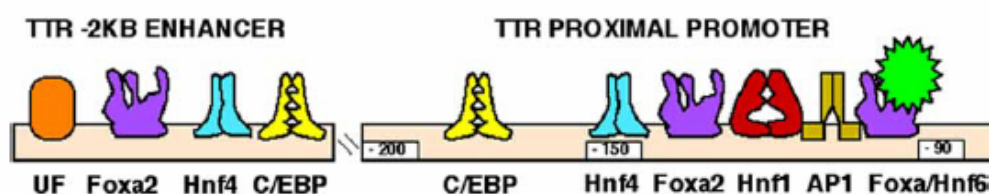


**Figure 46. Transcription factors that regulate expression of the TTR and FoxA2 genes and their binding sites.** Schematically shown are the FoxA2 (HNF3 $\beta$ ) and TTR promoter constructs and their corresponding transcription factors. Members of 4 different liver-enriched transcription factors HNF1, Foxa, HNF4, HNF6, and C/EBP (Samadani and Costa, 1996) and the growth factor inducible AP-1 rotein (Qian *et al.*, 1995) bind the TTR regulatory regions. The strong affinity FoxA binding site (-106 to -96 bp) overlaps with the HNF6 binding site in the TTR promoter (Samadani and Costa, 1996). The TTR enhancer is also recognized by an uncharacterized ubiquitous factor (UF) and contains one FoxA binding site, which is selectively recognized by the FoxA2 isoform (Samadani *et al.*, 1996). (Modified from Costa *et al.*, 2003)

Systematic analysis of the expression of Irga6 1A and 1B transcript forms in liver and primary hepatocytes performed by Parvanova (Ph.D thesis), revealed that 1B transcript was exceptionally more abundant (50 to 100 fold) than 1A both in normal

liver and primary hepatocytes. Upon stimulation however, such as infection for liver or IFN- $\gamma$  induction for primary hepatocytes, the Irga6 1A transcript was upregulated more than 1,000 fold whereas the 1B transcript was only slightly elevated (Parvanova, Ph.D thesis). These observations validated our speculation that the expression of Irga6 in liver is controlled by differential activation of different promoters.

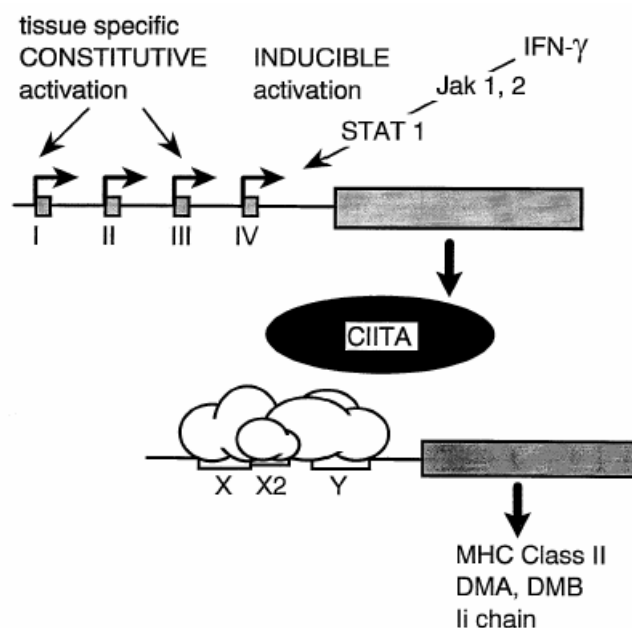


**Figure 47.** Schematic representation of the complexity of promoterspecific control of CIITA and MHC-II expression. (Modified from Muhlethaler-Mottet *et al.*, 1997)

Among the numerous IFN-regulated genes, only CIITA and ADAR1 were reported to modulate gene expression utilizing multiple promoters and alternative exon1 splicing to a shared exon2 (George *et al.*, 2005; Muhlethaler-Mottet *et al.*, 1997). The biological relevance of the expression regulation of ADAR1 gene by alternative usage of type I IFN-inducible promoter and embryonic specific promoter is not clear (George *et al.*, 2005). In the case of CIITA however, distinct CIITA promoters control either MHC<sub>II</sub> constitutive expression in dendritic cells and B lymphocytes, or IFN- $\gamma$ -inducible expression in a variety of MHC-II-negative cell types (Muhlethaler-Mottet *et al.*, 1997) (Fig. 47). Thus a hierarchy is involved in the control of the cellular, temporal and functional diversity of MHC-II expression by differential activation of different promoters of a single transactivator gene. Alternative promoters have also been identified in several other non-IFN-inducible eukaryotic genes

(Ayoubi and Van De Ven, 1996; Schibler and Sierra, 1987). Their differential usage can afford an extra level of flexibility in the regulation of these genes, for example, one promoter can be functional in a given tissue or during a particular developmental stage.

It is unlikely that Irga6 functions in such a way as CIITA or in a tissue- or developmental specific manner since Irga6 obviously does not serve as a transactivator nor a normal tissue- or developmental specific gene. Mice deficient for individual members of IRG GTPases have dramatic susceptibility phenotypes to many infectious intracellular bacteria and protozoa correlating well with the loss of IFN- $\gamma$  dependent resistance in mice, implicating IRG proteins as IFN-inducible resistant factors (Collazo *et al.*, 2001; MacMicking, 2004; MacMicking, 2005; Taylor *et al.*, 2000). Tissue-specific expression of resistant GTPases in the absence of IFN is possibly due to special immune milieu in liver. Liver is an organ of immune privilege, namely immune tolerance, since immunologically, the liver is an extreme environment, exposed to a constant flux of antigens and bacterial molecules from the intestine. As in the intestine, tolerance in such an environment may be preferable to immunity. However, the liver is also a favorable place of infection for many pathogens such as malarial parasite or *Listeria* (Crispe *et al.*, 2006). Constant expression of resistance molecules such as immunity-related GTPases in the absence of IFNs may be a preferable solution to prepare liver cells in a state of greater competence in resistance to pathogens in such an immune tolerant environment.

#### **4.3 Constitutively expressed IRG proteins participate in cell-autonomous resistance to *Toxoplasma gondii* in primary hepatocytes**

There is growing evidence favoring the idea that IRG proteins exert their resistance function in a cell-autonomous manner. It has been demonstrated under IFN- $\gamma$  stimulation conditions that five of the known IRG proteins were concentrated very fast at the parasitophorous vacuoles (PVs) in *T.gondii* infected primary astrocytes (Martens *et al.*, 2005) or various of other cell types (Hunn and Könen-Waisman unpublished results). Parasites labeled by IRG proteins then underwent disruption

probably due to vesiculation of the PV membrane and consequent exposure of the parasite to the cytosol (Martens *et al.*, 2005). Our data add primary hepatocytes to the list of cell types which can control *T.gondii* growth by stimulation with IFN- $\gamma$  (Fig. 18). The behavior of IFN- $\gamma$ -induced IRG proteins in infected cells, including accumulation to the PV membrane, hierarchy of PV coating by different IRG family members is essentially the same as observed in primary astrocytes (Martens *et al.*, 2005); Könen-Waisman unpublished results) (Fig. 19&20&21). This reinforces the argument that accumulation of IRG GTPases onto the *T.gondii* vacuoles is a common resistance mechanism shared by cells under stimulation of IFN- $\gamma$  *in vivo*. To our great interest, in freshly isolated primary hepatocytes constitutively expressed Irga6 was able to accumulate at the *T.gondii* vacuoles in the absence of IFN- $\gamma$ , though a smaller portion of *T.gondii* vacuoles was coated than under IFN- $\gamma$  stimulated conditions (Fig. 19). Obviously, tissue-specifically expressed Irga6 is able to launch a similar anti-*T.gondii* program as in IFN- $\gamma$ -induced cells. This observation further strengthens our speculation that the preexistence of IRG proteins, which are normally highly induced upon infection, in an immune suppression environment like liver would be advantageous for host resistance to various intracellular pathogens which may make use of this immune privileged milieu. Surprisingly, no other IRG proteins could be detected at *T.gondii* vacuoles, although most of them showed considerable level of expression in primary hepatocytes (Fig. 20). For this, we do not have an explanation yet, nevertheless one plausible reason could be that it is a stoichiometrical effect. Given the fact that the presence of GMS proteins is essential for correct localization and activation of GKS proteins (Hunn unpublished results), the low expression level observed for some IRG members such as Irgm3 in primary hepatocytes (Fig. 16), is likely to contribute to the lower efficiency of GKS protein accumulation at *T.gondii* vacuoles in comparison to the optimal situation of IFN- $\gamma$ -induction.

#### **4.4 IRG proteins are constitutively expressed in many other tissues**

The constitutive expression of *Irgm3* gene in mouse tissues such as thymus, spleen, small intestine and lung was reported in a non-quantitative way (Taylor *et al.*, 1996),

and the protein expression of Irgm3 and Irgd in thymus and spleen was subsequently detected (Collazo *et al.*, 2001). In line with these observations, in our quantitative analysis, Irga6 protein also exhibited significant constitutive expression in thymus and spleen, and to lesser extent in skin, intestine, lung, kidney and testis (Fig. 10). Nevertheless, the expression levels of Irga6 in these tissues were incomparable to that in the liver. Irga6 was expressed at a high level in the heart as well. No IRG protein expression could be found in brain. In the case of Irgm3, however, the expression in tissues other than liver was hardly detectable using western blot. Only under highly over-exposed conditions, Irgm3 protein expression could be detected, which shared the similar expression profile as Irga6 (Fig. 10).

The expression of Irga6 in heart is not very much affected in IFN receptor deficient mice. This recalls the Irga6 expression in liver driven by a hepatocyte specific promoter. However in contrast to liver, where, the ratio of liver-specific Irga6 1B transcript to 1A is up to 100, in heart 1A form is 5 times more abundant than 1B form, in addition to the fact that the absolute expression level of Irga6 1B is scores of times higher than that in the heart (Parvanova, Ph.D thesis). Furthermore Irga6 in heart is not ubiquitously expressed which is not similar to that in liver, rather only in certain cardiac myocytes (Fig. 11). These observations are not in favor of the argument that Irga6 expression in heart is also controlled by a heart-specific promoter which should promote an overall expression of only one form of transcript.

Irga6 is expressed in spleen, thymus, skin and intestine in an IFN-dependent manner (Fig. 12). For spleen and thymus developmentally regulated bursts of IFN synthesis may contribute to the expression of IRG proteins in these organs, since a constitutive expression of Irga6 was also reported in hematopoietic stem cells (Terskikh *et al.*, 2001; Venezia *et al.*, 2004). Skin and intestine are constantly exposed to external microbial environment as well as other immune stimuli such as lesions. Therefore it may be that local IFN bursts in responses to such unexpected stimulations induce the expression of IRG proteins. This hypothesis can be tested by examining germ-free mice.

The weak expression of Irga6 in kidney turned out to exist in a focal pattern (Fig. 11).

This focal expression similar to that in liver (Fig. 8&9) is dependent on IFNs, which will be discussed in more detail later.

#### **4.5 Irga6 focal expression in liver and kidney exploits interferon pathway**

Immunohistochemical staining of liver always showed a general expression of Irga6 in hepatocytes, and in addition exceptional intense focal expression also in hepatocytes (Fig. 22). In kidney though Irga6 is not expressed ubiquitously, the focal expression of Irga6 appears very similar to that in liver (Fig. 11). Through the genetic analysis of IFN signaling pathway, it turned out that focal expression in both liver and kidney represents local IFN activation (Fig. 24, 25 and 26). This argument was further strengthened by the detection of coexpression of Irgm3 in Irga6 expression foci both in liver and kidney (Fig. 23).

The IFN signaling pathway starts from binding of IFNs to corresponding receptors on the cell surface. All IFN- $\alpha/\beta$  subtypes interact with the same receptor complex, termed the IFN- $\alpha/\beta$  receptor (IFNAR) and IFN- $\gamma$  binds to the IFN- $\gamma$  receptor complex (IFNGR) (Bach *et al.*, 1997; Darnell *et al.*, 1994; Stark *et al.*, 1998; Uze *et al.*, 1990). The binding of both types of IFNs to IFNAR or IFNGR results in the cross-activation of these Jak protein kinases, which then phosphorylate their downstream substrates, Stat1 and Stat2 (signal transducers and activators of transcription) (Darnell *et al.*, 1994; Ihle and Kerr, 1995; Schindler and Darnell, 1995; Stark *et al.*, 1998), causing the formation of STAT1-STAT2 heterodimers for type I IFNs, and STAT1 homodimers for IFN- $\gamma$ . Thereafter, STAT1-STAT2 heterodimers associate with a third protein, IRF9, and bind one class of type I IFN response elements, the ISRE, whereas STAT1 homodimers activate gene expression by binding to another class of IFN response elements, the GAS (Bluyssen *et al.*, 1996; Darnell *et al.*, 1994; Decker *et al.*, 1991; Haque and Williams, 1994; Lew *et al.*, 1991). Type III IFN signaling is very similar to that of type I IFN (Kotenko *et al.*, 2003; Sheppard *et al.*, 2003; Vilcek, 2003).

Therefore, STAT1 is essential for both all types of IFN signaling, and STAT1 deficient mice are unresponsive to all types of IFN (Durbin *et al.*, 1996; Meraz *et al.*, 1996).

Our data showed that the focal expression of Irga6 in liver and kidney from STAT1 deficient mice was completely abolished (Fig. 26), strongly suggesting the local induction of Irga6 by IFNs. This argument was reinforced by the observation that Irga6 1A form, which is driven by an IFN-inducible promoter, is much more abundant in the expression foci than non-foci in liver (Fig. 30).

Immunohistochemical staining of liver sections establishes two types of Irga6 focal expression. One type is represented by a group of liver parenchymal cells, which express much higher amounts of Irga6 than the surrounding cells forming clear-cut boundaries and take the shape of patches. The other kind of focal expression exhibits exactly the same features except that they always have in the center a group of small mononuclear cells, which are Irga6 negative. Those mononuclear cells have small condensed nuclei and few cytoplasm, characteristic of lymphocytes or leukocytes (Fig. 22).

Among the two types of focal expression of Irga6 in liver, only cored patch expression was abolished in IFN- $\gamma$  knock out mice (Fig. 24), implying an IFN- $\gamma$ -induced expression of Irga6 in cored patches. Demonstration of the existence of IFN- $\gamma$  within the 'cores' of cored patches but not in the patches without cores (Fig. 32) further established the role of IFN- $\gamma$  as the inducer of Irga6 local expression in cored patches. In the case of Irga6 expression patch without cores, although no direct evidence is available, it is extremely likely that this type of expression is induced by type I IFN, since it is dependent on STAT1 signaling but obviously not IFN- $\gamma$ .

The origin of focal expression of Irga6 in kidney is somehow baffling, since it is dependent on both type I and II IFN receptors, implying a dual control from both types of IFN. It is well acknowledged that type I IFN signaling can cross talk with the signaling of type II IFN (Takaoka *et al.*, 2000). One interpretation is therefore that type I IFN is required to synergize the activation of type II IFN to achieve an optimal focal induction of Irga6 in kidney. A very recent report demonstrated that stimulated myeloid dendritic cells (DCs) were able to activate NKT cells to produce IFN- $\gamma$  (Paget *et al.*, 2007). Furthermore, this process was dependent on type I IFN synthesis in dendritic cells as well as de novo production of glycosphingolipid of DCs. In view

of the fact that NKT cells are the major activators in the cored patch expression of Irga6 in liver, it is a plausible argument that activation of NKT cells in a type I IFN dependent manner is the cause of the Irga6 expression foci in kidney.

#### **4.6 NKT cell activation in Irga6 cored expression patch in liver**

Unlike type I IFN, which theoretically can be produced by almost all types of cells, the capacity of IFN- $\gamma$  production is normally limited to a few types of immunocompetent cells such as activated NK cells and activated subsets of T cells (Mosmann and Coffman, 1989; Perussia, 1991; Sad *et al.*, 1995). The small mononuclear cells in the cores of Irga6 expression patches are perfect candidates for IFN- $\gamma$  secretion. Indeed, we demonstrated cells with macrophage and T cell markers in the center of the cored expression patch of Irga6 in liver (Fig. 33), and the indispensability of T cells for the formation of Irga6 cored patches was also demonstrated by examining T cell deficient mice (Fig. 34). This requirement of a functional immune system is in line with the fact that, unlike the overall constitutive expression in liver, which is launched already in neonatal mice and persists constantly high later on, the focal expression is hardly detectable in the post neonatal mice and the number of foci rises to a constant level from three weeks on. This correlates well with the development of the immune system of neonatal mice, which have T cells with limited capacity of cytokine production right after birth (Riley, 1998).

A systematic analysis of T cell receptor repertoire used by T cells in the cores of Irga6 patches revealed that NKT cells are most likely the major T cell subset responsible for the local IFN- $\gamma$  activity in liver. NKT cells are defined as a T cell lineage expressing NK lineage receptors, in addition to semi-invariant CD1d-restricted  $\alpha\beta$  TCRs. More than 80% of these TCRs are V $\alpha$ 14-J $\alpha$ 18/V $\beta$ 8, V $\beta$ 7, and V $\beta$ 2 in mouse (or V $\alpha$ 24-J $\alpha$ 18/V $\beta$ 11 in human), and the remaining are V $\alpha$ 3.2-J $\alpha$ 9/V $\beta$ 8, V $\alpha$ 8/V $\beta$ 8, and other TCRs (Cardell *et al.*, 1995; Park *et al.*, 2001). Among the three V $\beta$  segments used by V $\alpha$ 14-J $\alpha$ 18 NKT cells, V $\beta$ 8 (mainly V $\beta$ 8.2) is predominantly employed at a proportion of more than 50% (Bendelac *et al.*, 1994; Lantz and Bendelac, 1994). In view of the fact that non-V $\alpha$ 14-J $\alpha$ 18 NKT cells mainly make use of V $\beta$ 8 segment as

well, a biased usage of V $\beta$ 8 by NKT cells is apparently consistent. Our data showed that T cells in the cores of Irga6 expression patches carried only TCR V $\beta$ 8 (predominantly V $\beta$ 8.2) (Fig. 35). Furthermore, all the V $\alpha$ 14 TCR carried by T cells in the cores of Irga6 expression patches only employed the V $\alpha$ 14-J $\alpha$ 18 junction, while the TCR V $\alpha$ 11, which was an unspecific product in the attempt to amplify V $\alpha$ 14 from the peripheral T cells displayed a variety of junctional variations (Fig. 38 and 39). The V $\alpha$ 14-J $\alpha$ 18 junction described here actually was also polyclonal but with only a few substitution right at the junction between V $\alpha$ 14 and J $\alpha$ 18. This narrowly defined junction for T cells in the cores of Irga6 patches, compared to its highly variable counterpart for peripheral T cells implies a highly selective clustering of a specific subset of T cells in the cores of Irga6 expression foci. TCR V $\alpha$ 14 has been reported not being frequently used by peripheral T cells (Yoshida *et al.*, 2000a), which is rather consistent with our observation. However, TCR V $\alpha$ 14 was very abundantly used by T cells in the cores of Irga6 expression foci in comparison to other V $\alpha$  family members. Taken together, these observations demonstrate that V $\alpha$ 14-J $\alpha$ 18/V $\beta$ 8 NKT cells are the near exclusive population of T cells in the cores of Irga6 expression foci in liver. In Irga6 cored patches V $\alpha$ 8 could also be found at a relatively lower level (Fig. 40), suggesting the presence of non-V $\alpha$ 14-J $\alpha$ 18 NKT cells in the cores.

NKT cells are activated upon presentation of their ligands by dendritic cells (DCs) and secrete IL4 and IFN- $\gamma$ , which probably also requires type I IFN secretion by DCs. A following reciprocal activation of NKT cells and DCs can in turn enhance NKT cell activation and cytokine production (Kitamura *et al.*, 1999; Tomura *et al.*, 1999). Propagation of this reaction involves the activation of NK cell cytotoxicity and IFN- $\gamma$  production (Carnaud *et al.*, 1999; Eberl and MacDonald, 2000) and priming of robust adaptive immune responses (Fujii *et al.*, 2004; Fujii *et al.*, 2003; Gonzalez-Aseguinolaza *et al.*, 2002). In view of the fact that cytokine secretion esp. that of IFN- $\gamma$  is characteristic of NKT cells activation, the IFN- $\gamma$  dependent Irga6 expression foci with cores enriched in NKT cells, are very likely to represent local activation of NKT cells in liver. This argument is reinforced by our observation that TLR signaling is not essential for the Irga6 cored patch formation (Fig. 42 and 43)

since TLR signaling is shown not to be involved in the direct NKT cell activation via its ligand representation (Bendelac *et al.*, 2007). In the mouse the liver is the organ most enriched in NKT cells, making up 30% of the local T cell population (Matsuda *et al.*, 2000). NKT cells normally patrol the liver sinusoids through CXCR6/CXCL16 interaction to provide immune surveillance (Geissmann *et al.*, 2005). Furthermore, NKT cells stop patrolling and become fixed upon TCR activation (Geissmann *et al.*, 2005). Hence it is tempting to imagine that, when NKT cells are activated locally in liver, chemokines and cytokines such as IFN- $\alpha/\beta$  and IFN- $\gamma$  are produced, which in turn recruit leukocytes like macrophages, NK cells and probably more NKT cells to aggregate and to produce even more IFN- $\gamma$ , which subsequently induces the expression of Irga6 in the hepatocytes around. The direct involvement of NKT cells in this process need to be further clarified for instance by CD1d-Gal: Cer tetramer labeling of NKT cell in the cores of Irga6 expression and by examining CD1d- or  $\beta$ -hexosaminidase-B-deficient mice, both of which are devoid of NKT cells (Coles *et al.*, 2000; Zhou *et al.*, 2004).

#### **4.7 What are the causes of local NKT cell activation?**

The causes of local NKT cell activation in the liver remain elusive. It is known that NKT cells are activated when their TCR are engaged by their ligands loaded on MHC-like antigen presentation molecule, CD1d (Bendelac *et al.*, 2007).

$\alpha$ -GalCer, a glycosphingolipid derived from marine sponges, is a strong agonist ligand that can initiate NKT cell-dependent immune response, leading to enhanced immunity to tumors and infectious organisms and suppression of certain autoimmune diseases (Godfrey *et al.*, 2004; Joyce *et al.*, 1998). The activation of NKT cells by marine sponge  $\alpha$ -GalCer obviously lacks direct physiological relevance. Recently closely related structures that substitute for LPS have been discovered in the cell wall of *Sphingomonas*, a Gram-negative, LPS-negative member of  $\alpha$ -proteobacteria (Kawahara *et al.*, 2000; Kawasaki *et al.*, 1994). These sphingolipids can strongly stimulate NKT cells, which leads to the clearing of the infection (Kinjo *et al.*, 2005; Mattner *et al.*, 2005; Wu *et al.*, 2005). Our data showing unaltered Irga6 focal

expression patterns in germ-free mice rule out the possibility of such an activation of NKT cells by bacterial sphingolipid in a microbial environment (Fig. 41).

Three years ago, a report from Zhou *et al.* offered strong evidence that isoglobotrihexosylceramide (iGb3), a mammalian glycosphingolipid (GSL) produced for cellular membrane sphingolipids, is an endogenous CD1d-dependent agonist for NKT cells from mice and humans (Zhou *et al.*, 2004). It is known that endogenous lipid ligands are involved in a stage of positive selection at which the endogenous ligand presentation by CD1d expressed on double positive T cells in the thymic cortex is indispensable (Wei *et al.*, 2005). In this report, it was showed that  $\beta$ -hexosaminidase-B (*Hexb*<sup>-/-</sup>) deficient mice, which lack the ability to degrade iGb4 into iGb3 in the lysosome, had a great decrease in thymic NKT cell production, and of the known degradation products resulting from the activity of these enzymes, only (iGb3) showed *in vitro* stimulatory activity toward iNKT cells (Zhou *et al.*, 2004). Therefore, it was concluded that iGb3 is the endogenous ligand mediating positive selection of iNKT cells in the thymus. A subsequent study using an iGb3-blocking lectin then implicated iGb3 in peripheral activation of iNKT cells by dendritic cells (DCs) (Mattner *et al.*, 2005). However, the role of iGb3 as an endogenous CD1d lipid ligand determining thymic NKT cell selection has recently been challenged by the latest report demonstrating that mice deficient in mice deficient in iGb3 synthase and consequently totally lacking iGb3, have normal NKT cell development (Porubsky *et al.*, 2007). The authors argued that other GSLs instead of iGb3 may serve as physiological selecting ligands *in vivo* since the NKT cell loss is not specific to *Hexb*<sup>-/-</sup> mice but rather a general property of other mouse models of glycosphingolipid storage disorder (Gadola *et al.*, 2006; Sagiv *et al.*, 2006). The consensus, however, that the interactions between NKT cell TCR and endogenous sphingolipid ligands in CD1d expressing bone marrow-derived cells in thymus is essential for NKT cell thymic differentiation, is not changed, since both thymic CD1d and intact glycolipid lysosomal degradation and storage are crucial for the normal selection of NKT cells in thymus (Gadola *et al.*, 2006; Wei *et al.*, 2005). In thymus positively selected NKT cell precursors undergo several round of division and acquire an effector phenotype and

then migrate to periphery (Pellicci *et al.*, 2002; Stetson *et al.*, 2003). It was proposed that, in peripheral tissues the effector status of NKT cells characterized by their explosive cytokine release upon TCR stimulation (Yoshimoto and Paul, 1994) and their basal low-level transcription of cytokine genes (Stetson *et al.*, 2003) must be maintained by repeated TCR engagement presumably by their endogenous ligands presented by CD1d. In line with this hypothesis, CD1d is not only expressed by antigen presenting cells but also strikingly on cells like Kupffer cells, sinusoid endothelial cells and hepatocytes in mice liver, where the highest frequencies of NKT cells are found in mice (Geissmann *et al.*, 2005). Surprisingly however, CD1d is not required for survival and effector phenotype maintenance of terminally differentiated NKT cells (Matsuda *et al.*, 2002; Wei *et al.*, 2005). In view of the fact that the Irga6 expression foci also exist normally in germ-free mice, which have been shown to have unaltered NKT cell distribution and effector phenotype (Park *et al.*, 2000), it is tantalizing to speculate that the Irga6 expression foci represent a continuous process of local activation of NKT cells in order to maintain an effector phenotype. The involvement of CD1d in this local activation of NKT cells could be tested by examining mice that have normal NKT cell thymic development but are deficient in CD1d in liver or kidney.

#### **4.8. Where does Irga6 focal expression without cores originate?**

The origin of Irga6 expression foci without cores remains mysterious. Why there are local type I IFN activities independent of the presence of lymphocytes and also in the absence of microbial environment? One possibility is local responses to virus infection since germ-free mice are not completely virus-free. Virtually all cell types are able to produce IFN- $\alpha/\beta$  in response to viral exposure. The most efficient producer of IFN- $\alpha$ , however, is one of two principle subsets of dendritic cells, Plasmacytoid dendritic cell (pDC) (Fitzgerald-Bocarsly *et al.*, 1988). IFN- $\alpha/\beta$  are produced by pDCs in response to a wide range of enveloped viruses, including herpes simplex virus (HSV), human immunodeficiency virus type I (HIV-1), influenza viruses etc. (Coccia *et al.*, 2004; Jarrossay *et al.*, 2001), as well as parasites (*Plasmodium*

falciparum) (Pichyangkul *et al.*, 2004), bacteria (e.g. SAC) (Svensson *et al.*, 1996). Although TLRs esp. TLR 7 and 9 that are expressed by pDCs (Hemmi *et al.*, 2002; Krug *et al.*, 2001) and MyD88 are demonstrated to be involved in the activation and the IFN- $\alpha/\beta$  production of pDCs in response to viruses, MyD88 independent pathways leading to IFN- $\alpha$  production by pDCs have also been described (Tabeta *et al.*, 2004). The MyD88 independent Irga6 focal expression without cores (Fig. 43) may represent the local activation of pDCs and the consequent production of type I IFN by pDCs.

## 5. Summary

Immunity-related GTPases (IRG) are essential, interferon-inducible resistant factors in mice that are actively against a broad spectrum of important intracellular pathogens. IRGs are represented by 25 genes in the mouse and also in almost all mammals and many other vertebrates, but surprisingly not in human. Structurally IRGs all share canonical GTP-binding domains and the crystal structure of one representative family member, Irga6, possesses an H-Ras-1-like GTP-binding domain. The biochemical properties of Irga6 are reminiscent of dynamins. Though the resistance mechanisms are still obscure, there is growing evidence supporting the role of IRG proteins as cell-autonomous resistant factors most probably through their direct targeting to intracellular pathogen-containing membrane compartments.

IRGs are expressed under the tight regulation of IFNs. We found in this work unexpectedly that IRG proteins do have significant constitutive as well as IFN-induced expression *in vivo*. In liver at least for one member of IRG, Irga6, this differential expression is achieved by alternative activation of a liver-specific promoter and an IFN-inducible promoter. The constitutively expressed Irga6 in the presence of other constitutively expressed IRG proteins in primary hepatocytes is able to launch a similar anti-*T.gondii* program as IFN-induced protein, implying the role of IRG proteins as sentinel in the resistance against intracellular pathogens in liver that is an organ of immune privilege. Peculiar Irga6 focal expression in liver as well as in kidney is also observed and proved to be induced by local production of IFNs. This production of IFN- $\gamma$  that induces Irga6 focal expression in liver surprisingly represents the local activation of NKT cells even in the absence of microbial environment (germ-free mice). Even though the causes of this NKT cell activation are still elusive, we speculate that this stimulation of NKT cells may stand for an ongoing process required for the maintenance of the effector status for peripheral NKT cells.

## Zusammenfassung

Interferon- induzierbare IRGs (immunity- related GTPases) spielen eine bedeutende Rolle als Resistenzfaktoren in Mäusen gegen ein breites Spektrum intrazellulärer Parasiten. In der Maus kodieren 25 Gene für IRGs, ebenso lassen sie sich in fast allen Säugern sowie in vielen anderen Vertebraten finden, erstaunlicherweise jedoch nicht im Menschen. Strukturell teilen sich alle IRGs eine konservierte GTP-Bindungsdomäne, diese zeigt bei einem Vertreter der Proteinfamilie, Irga6, eine H-Ras-1- gleiche Kristallstruktur. Ihrer biochemischen Eigenschaften nach erinnert Irga6 an Dynamine. Obwohl die Abwehrmechanismen immer noch nicht genau bekannt sind, mehren sich die Anzeichen welche für eine Funktion der IRG- Proteine als zellautonome Resistenzfaktoren, wahrscheinlich über eine direkte Lokalisation an die Membran intrazellulärer pathogenhaltiger Kompartimente, sprechen.

Die Expression der IRGs unterliegt der Regulation durch IFNs. Überraschenderweise fanden wir im Zuge dieser Arbeit heraus, dass IRG- Proteine sowohl ein signifikante konstitutive wie auch eine IFN- induzierte Expression zeigen. Diese unterschiedliche Expression wird z.B. in der Leber für zumindest ein IRG- Mitglied, Irga6, dadurch erreicht, das alternativ ein leberspezifischer Promoter oder ein IFN- induzierbarer Promoter aktiviert wird. Konstitutiv exprimiertes Irga6, in Anwesenheit weiterer konstitutiv exprimierter IRG- Proteine, vermag in primären Hepatocyten ein vergleichbares anti- *T.gondii*- Programm zu starten wie die IFN- induzierten Proteine, und deutet darauf hin, dass die konstitutiv exprimierten IRG Proteine in der immunprivilegierten Leber einen jederzeit verfügbaren Resistenz Mechanismus bilden. Charakteristische fokale Irga6- Expression ist in der Leber wie auch in den Nieren zu beobachten und auf lokale Produktion von Interferonen zurück zu führen. Diese durch die Produktion von IFN-g induzierte fokale Expression in der Leber spiegelt erstaunlicherweise genau die lokale Aktivierung von NKT- Zellen wieder, selbst in Abwesenheit eines mikrobiellen Umfelds (keimfreie Mäuse). Obwohl die Gründe für diese Aktivierung von NKT- Zellen noch schwer nachvollziehbar sind,

vermuten wir dass diese Stimulation von NKT- Zellen vielleicht einen fortlaufenden Prozess darstellt und dass dieser benötigt wird um den Effektorzustand für periphere NKT- Zellen aufrecht zu erhalten.

## 6. References

- Altschul, S. F., Gish, W., Miller, W., Myers, E. W. and Lipman, D. J.** (1990). Basic local alignment search tool. *J Mol Biol* **215**, 403-10.
- Anderson, S. L., Carton, J. M., Lou, J., Xing, L. and Rubin, B. Y.** (1999). Interferon-induced guanylate binding protein-1 (GBP-1) mediates an antiviral effect against vesicular stomatitis virus and encephalomyocarditis virus. *Virology* **256**, 8-14.
- Arnheiter, H. and Meier, E.** (1990). Mx proteins: antiviral proteins by chance or by necessity? *New Biol* **2**, 851-7.
- Ayoubi, T. A. and Van De Ven, W. J.** (1996). Regulation of gene expression by alternative promoters. *Faseb J* **10**, 453-60.
- Bach, E. A., Aguet, M. and Schreiber, R. D.** (1997). The IFN gamma receptor: a paradigm for cytokine receptor signaling. *Annu Rev Immunol* **15**, 563-91.
- Baek, K. J., Thiel, B. A., Lucas, S. and Stuehr, D. J.** (1993). Macrophage nitric oxide synthase subunits. Purification, characterization, and role of prosthetic groups and substrate in regulating their association into a dimeric enzyme. *J Biol Chem* **268**, 21120-9.
- Banchereau, J. and Steinman, R. M.** (1998). Dendritic cells and the control of immunity. *Nature* **392**, 245-52.
- Baxter, A. G., Kinder, S. J., Hammond, K. J., Scollay, R. and Godfrey, D. I.** (1997). Association between alphabetaTCR+CD4-CD8- T-cell deficiency and IDDM in NOD/Lt mice. *Diabetes* **46**, 572-82.
- Bekpen, C., Hunn, J. P., Rohde, C., Parvanova, I., Guethlein, L., Dunn, D. M., Glowalla, E., Leptin, M. and Howard, J. C.** (2005). The interferon-inducible p47 (IRG) GTPases in vertebrates: loss of the cell autonomous resistance mechanism in the human lineage. *Genome Biol* **6**, R92.
- Bendelac, A.** (1995). Positive selection of mouse NK1+ T cells by CD1-expressing cortical thymocytes. *J Exp Med* **182**, 2091-6.
- Bendelac, A., Hunziker, R. D. and Lantz, O.** (1996). Increased interleukin 4 and

- immunoglobulin E production in transgenic mice overexpressing NK1 T cells. *J Exp Med* **184**, 1285-93.
- Bendelac, A., Killeen, N., Littman, D. R. and Schwartz, R. H.** (1994). A subset of CD4+ thymocytes selected by MHC class I molecules. *Science* **263**, 1774-8.
- Bendelac, A., Lantz, O., Quimby, M. E., Yewdell, J. W., Bennink, J. R. and Brutkiewicz, R. R.** (1995). CD1 recognition by mouse NK1+ T lymphocytes. *Science* **268**, 863-5.
- Bendelac, A., Savage, P. B. and Teyton, L.** (2007). The biology of NKT cells. *Annu Rev Immunol* **25**, 297-336.
- Benlagha, K., Kyin, T., Beavis, A., Teyton, L. and Bendelac, A.** (2002). A thymic precursor to the NK T cell lineage. *Science* **296**, 553-5.
- Benlagha, K., Wei, D. G., Veiga, J., Teyton, L. and Bendelac, A.** (2005). Characterization of the early stages of thymic NKT cell development. *J Exp Med* **202**, 485-92.
- Beretta, L., Gabbay, M., Berger, R., Hanash, S. M. and Sonenberg, N.** (1996). Expression of the protein kinase PKR is modulated by IRF-1 and is reduced in 5q-associated leukemias. *Oncogene* **12**, 1593-6.
- Biron, C. A., Nguyen, K. B., Pien, G. C., Cousens, L. P. and Salazar-Mather, T. P.** (1999). Natural killer cells in antiviral defense: function and regulation by innate cytokines. *Annu Rev Immunol* **17**, 189-220.
- Bluyssen, A. R., Durbin, J. E. and Levy, D. E.** (1996). ISGF3 gamma p48, a specificity switch for interferon activated transcription factors. *Cytokine Growth Factor Rev* **7**, 11-7.
- Boehm, U., Guethlein, L., Klamp, T., Ozbek, K., Schaub, A., Futterer, A., Pfeffer, K. and Howard, J. C.** (1998). Two families of GTPases dominate the complex cellular response to IFN-gamma. *J Immunol* **161**, 6715-23.
- Bonhomme, A., Maine, G. T., Beorchia, A., Burlet, H., Aubert, D., Villena, I., Hunt, J., Chovan, L., Howard, L., Brojanac, S. et al.** (1998). Quantitative immunolocalization of a P29 protein (GRA7), a new antigen of toxoplasma gondii. *J Histochem Cytochem* **46**, 1411-22.

- Borowski, C. and Bendelac, A.** (2005). Signaling for NKT cell development: the SAP-FynT connection. *J Exp Med* **201**, 833-6.
- Brigl, M., Bry, L., Kent, S. C., Gumperz, J. E. and Brenner, M. B.** (2003). Mechanism of CD1d-restricted natural killer T cell activation during microbial infection. *Nat Immunol* **4**, 1230-7.
- Brossay, L., Chioda, M., Burdin, N., Koezuka, Y., Casorati, G., Dellabona, P. and Kronenberg, M.** (1998). CD1d-mediated recognition of an alpha-galactosylceramide by natural killer T cells is highly conserved through mammalian evolution. *J Exp Med* **188**, 1521-8.
- Brossay, L., Jullien, D., Cardell, S., Sydora, B. C., Burdin, N., Modlin, R. L. and Kronenberg, M.** (1997). Mouse CD1 is mainly expressed on hemopoietic-derived cells. *J Immunol* **159**, 1216-24.
- Brozovic, S., Nagaishi, T., Yoshida, M., Betz, S., Salas, A., Chen, D., Kaser, A., Glickman, J., Kuo, T., Little, A. et al.** (2004). CD1d function is regulated by microsomal triglyceride transfer protein. *Nat Med* **10**, 535-9.
- Butcher, B. A., Greene, R. I., Henry, S. C., Annecharico, K. L., Weinberg, J. B., Denkers, E. Y., Sher, A. and Taylor, G. A.** (2005). p47 GTPases regulate *Toxoplasma gondii* survival in activated macrophages. *Infect Immun* **73**, 3278-86.
- Cannons, J. L., Yu, L. J., Hill, B., Mijares, L. A., Dombroski, D., Nichols, K. E., Antonellis, A., Koretzky, G. A., Gardner, K. and Schwartzberg, P. L.** (2004). SAP regulates T(H)2 differentiation and PKC-theta-mediated activation of NF-kappaB1. *Immunity* **21**, 693-706.
- Cardell, S., Tangri, S., Chan, S., Kronenberg, M., Benoist, C. and Mathis, D.** (1995). CD1-restricted CD4+ T cells in major histocompatibility complex class II-deficient mice. *J Exp Med* **182**, 993-1004.
- Carlow, D. A., Marth, J., Clark-Lewis, I. and Teh, H. S.** (1995). Isolation of a gene encoding a developmentally regulated T cell-specific protein with a guanine nucleotide triphosphate-binding motif. *J Immunol* **154**, 1724-34.
- Carlow, D. A., Teh, S. J. and Teh, H. S.** (1998). Specific antiviral activity demonstrated by TGTP, a member of a new family of interferon-induced GTPases. *J*

*Immunol* **161**, 2348-55.

**Carnaud, C., Lee, D., Donnars, O., Park, S. H., Beavis, A., Koezuka, Y. and Bendelac, A.** (1999). Cutting edge: Cross-talk between cells of the innate immune system: NKT cells rapidly activate NK cells. *J Immunol* **163**, 4647-50.

**Carter, C. C., Gorbacheva, V. Y. and Vestal, D. J.** (2005). Inhibition of VSV and EMCV replication by the interferon-induced GTPase, mGBP-2: differential requirement for wild-type GTP binding domain. *Arch Virol* **150**, 1213-20.

**Cassatella, M. A., Hartman, L., Perussia, B. and Trinchieri, G.** (1989). Tumor necrosis factor and immune interferon synergistically induce cytochrome b-245 heavy-chain gene expression and nicotinamide-adenine dinucleotide phosphate hydrogenase oxidase in human leukemic myeloid cells. *J Clin Invest* **83**, 1570-9.

**Chen, J., Trounstein, M., Alt, F. W., Young, F., Kurahara, C., Loring, J. F. and Huszar, D.** (1993). Immunoglobulin gene rearrangement in B cell deficient mice generated by targeted deletion of the JH locus. *Int Immunol* **5**, 647-56.

**Chen, J., Baig, E. and Fish, E. N.** (2004). Diversity and relatedness among the type I interferons. *J Interferon Cytokine Res* **24**, 687-98.

**Cheng, Y. S., Becker-Manley, M. F., Chow, T. P. and Horan, D. C.** (1985). Affinity purification of an interferon-induced human guanylate-binding protein and its characterization. *J Biol Chem* **260**, 15834-9.

**Cheng, Y. S., Colonna, R. J. and Yin, F. H.** (1983). Interferon induction of fibroblast proteins with guanylate binding activity. *J Biol Chem* **258**, 7746-50.

**Cheng, Y. S., Patterson, C. E. and Staeheli, P.** (1991). Interferon-induced guanylate-binding proteins lack an N(T)KXD consensus motif and bind GMP in addition to GDP and GTP. *Mol Cell Biol* **11**, 4717-25.

**Chiu, Y. H., Jayawardena, J., Weiss, A., Lee, D., Park, S. H., Dautry-Varsat, A. and Bendelac, A.** (1999). Distinct subsets of CD1d-restricted T cells recognize self-antigens loaded in different cellular compartments. *J Exp Med* **189**, 103-10.

**Clayton, D. F. and Darnell, J. E., Jr.** (1983). Changes in liver-specific compared to common gene transcription during primary culture of mouse hepatocytes. *Mol Cell Biol* **3**, 1552-61.

- Clayton, D. F., Harrelson, A. L. and Darnell, J. E., Jr.** (1985). Dependence of liver-specific transcription on tissue organization. *Mol Cell Biol* **5**, 2623-32.
- Coccia, E. M., Severa, M., Giacomini, E., Monneron, D., Remoli, M. E., Julkunen, I., Cella, M., Lande, R. and Uze, G.** (2004). Viral infection and Toll-like receptor agonists induce a differential expression of type I and lambda interferons in human plasmacytoid and monocyte-derived dendritic cells. *Eur J Immunol* **34**, 796-805.
- Coles, M. C., McMahon, C. W., Takizawa, H. and Raulet, D. H.** (2000). Memory CD8 T lymphocytes express inhibitory MHC-specific Ly49 receptors. *Eur J Immunol* **30**, 236-44.
- Collazo, C. M., Yap, G. S., Sempowski, G. D., Lusby, K. C., Tessarollo, L., Woude, G. F., Sher, A. and Taylor, G. A.** (2001). Inactivation of LRG-47 and IRG-47 reveals a family of interferon gamma-inducible genes with essential, pathogen-specific roles in resistance to infection. *J Exp Med* **194**, 181-8.
- Costa, R. H., Grayson, D. R., Xanthopoulos, K. G. and Darnell, J. E., Jr.** (1988). A liver-specific DNA-binding protein recognizes multiple nucleotide sites in regulatory regions of transthyretin, alpha 1-antitrypsin, albumin, and simian virus 40 genes. *Proc Natl Acad Sci U S A* **85**, 3840-4.
- Costa, R. H., Kalinichenko, V. V., Holterman, A. X. and Wang, X.** (2003). Transcription factors in liver development, differentiation, and regeneration. *Hepatology* **38**, 1331-47.
- Crispe, I. N., Giannandrea, M., Klein, I., John, B., Sampson, B. and Wuensch, S.** (2006). Cellular and molecular mechanisms of liver tolerance. *Immunol Rev* **213**, 101-18.
- Darnell, J. E., Jr., Kerr, I. M. and Stark, G. R.** (1994). Jak-STAT pathways and transcriptional activation in response to IFNs and other extracellular signaling proteins. *Science* **264**, 1415-21.
- de Lalla, C., Galli, G., Aldrighetti, L., Romeo, R., Mariani, M., Monno, A., Nuti, S., Colombo, M., Callea, F., Porcelli, S. A. et al.** (2004). Production of profibrotic cytokines by invariant NKT cells characterizes cirrhosis progression in chronic viral hepatitis. *J Immunol* **173**, 1417-25.

- de Souza, A. P., Tang, B., Tanowitz, H. B., Factor, S. M., Shtutin, V., Shirani, J., Taylor, G. A., Weiss, L. M. and Jelicks, L. A.** (2003). Absence of interferon-gamma-inducible gene IGTP does not significantly alter the development of chagasic cardiomyopathy in mice infected with *Trypanosoma cruzi* (Brazil strain). *J Parasitol* **89**, 1237-9.
- Decker, T., Lew, D. J., Mirkovitch, J. and Darnell, J. E., Jr.** (1991). Cytoplasmic activation of GAF, an IFN-gamma-regulated DNA-binding factor. *Embo J* **10**, 927-32.
- Durbin, J. E., Hackenmiller, R., Simon, M. C. and Levy, D. E.** (1996). Targeted disruption of the mouse Stat1 gene results in compromised innate immunity to viral disease. *Cell* **84**, 443-50.
- Eberl, G. and MacDonald, H. R.** (2000). Selective induction of NK cell proliferation and cytotoxicity by activated NKT cells. *Eur J Immunol* **30**, 985-92.
- Esteban, L. M., Tsoutsman, T., Jordan, M. A., Roach, D., Poulton, L. D., Brooks, A., Naidenko, O. V., Sidobre, S., Godfrey, D. I. and Baxter, A. G.** (2003). Genetic control of NKT cell numbers maps to major diabetes and lupus loci. *J Immunol* **171**, 2873-8.
- Exley, M., Garcia, J., Balk, S. P. and Porcelli, S.** (1997). Requirements for CD1d recognition by human invariant Valpha24+ CD4-CD8- T cells. *J Exp Med* **186**, 109-20.
- Feng, C. G., Collazo-Custodio, C. M., Eckhaus, M., Hieny, S., Belkaid, Y., Elkins, K., Jankovic, D., Taylor, G. A. and Sher, A.** (2004). Mice deficient in LRG-47 display increased susceptibility to mycobacterial infection associated with the induction of lymphopenia. *J Immunol* **172**, 1163-8.
- Fischer, H. G., Stachelhaus, S., Sahm, M., Meyer, H. E. and Reichmann, G.** (1998). GRA7, an excretory 29 kDa *Toxoplasma gondii* dense granule antigen released by infected host cells. *Mol Biochem Parasitol* **91**, 251-62.
- Fitzgerald-Bocarsly, P., Feldman, M., Mendelsohn, M., Curl, S. and Lopez, C.** (1988). Human mononuclear cells which produce interferon-alpha during NK(HSV-FS) assays are HLA-DR positive cells distinct from cytolytic natural killer effectors. *J Leukoc Biol* **43**, 323-34.

- Fitzgerald, K. A., Palsson-McDermott, E. M., Bowie, A. G., Jefferies, C. A., Mansell, A. S., Brady, G., Brint, E., Dunne, A., Gray, P., Harte, M. T. et al. (2001).** Mal (MyD88-adaptor-like) is required for Toll-like receptor-4 signal transduction. *Nature* **413**, 78-83.
- Forestier, C., Molano, A., Im, J. S., Dutronc, Y., Diamond, B., Davidson, A., Illarionov, P. A., Besra, G. S. and Porcelli, S. A. (2005).** Expansion and hyperactivity of CD1d-restricted NKT cells during the progression of systemic lupus erythematosus in (New Zealand Black x New Zealand White)F1 mice. *J Immunol* **175**, 763-70.
- Fujii, S., Liu, K., Smith, C., Bonito, A. J. and Steinman, R. M. (2004).** The linkage of innate to adaptive immunity via maturing dendritic cells in vivo requires CD40 ligation in addition to antigen presentation and CD80/86 costimulation. *J Exp Med* **199**, 1607-18.
- Fujii, S., Shimizu, K., Smith, C., Bonifaz, L. and Steinman, R. M. (2003).** Activation of natural killer T cells by alpha-galactosylceramide rapidly induces the full maturation of dendritic cells in vivo and thereby acts as an adjuvant for combined CD4 and CD8 T cell immunity to a coadministered protein. *J Exp Med* **198**, 267-79.
- Gadola, S. D., Silk, J. D., Jeans, A., Illarionov, P. A., Salio, M., Besra, G. S., Dwek, R., Butters, T. D., Platt, F. M. and Cerundolo, V. (2006).** Impaired selection of invariant natural killer T cells in diverse mouse models of glycosphingolipid lysosomal storage diseases. *J Exp Med* **203**, 2293-303.
- Gapin, L., Matsuda, J. L., Surh, C. D. and Kronenberg, M. (2001).** NKT cells derive from double-positive thymocytes that are positively selected by CD1d. *Nat Immunol* **2**, 971-8.
- Gavrilescu, L. C., Butcher, B. A., Del Rio, L., Taylor, G. A. and Denkers, E. Y. (2004).** STAT1 is essential for antimicrobial effector function but dispensable for gamma interferon production during *Toxoplasma gondii* infection. *Infect Immun* **72**, 1257-64.
- Geissmann, F., Cameron, T. O., Sidobre, S., Manlongat, N., Kronenberg, M., Briskin, M. J., Dustin, M. L. and Littman, D. R. (2005).** Intravascular immune

- surveillance by CXCR6+ NKT cells patrolling liver sinusoids. *PLoS Biol* **3**, e113.
- George, C. X., Wagner, M. V. and Samuel, C. E.** (2005). Expression of interferon-inducible RNA adenosine deaminase ADAR1 during pathogen infection and mouse embryo development involves tissue-selective promoter utilization and alternative splicing. *J Biol Chem* **280**, 15020-8.
- Ghosh, A., Praefcke, G. J., Renault, L., Wittinghofer, A. and Herrmann, C.** (2006). How guanylate-binding proteins achieve assembly-stimulated processive cleavage of GTP to GMP. *Nature* **440**, 101-4.
- Ghosh, A., Uthaiyah, R., Howard, J., Herrmann, C. and Wolf, E.** (2004). Crystal structure of IIGP1: a paradigm for interferon-inducible p47 resistance GTPases. *Mol Cell* **15**, 727-39.
- Gilly, M. and Wall, R.** (1992). The IRG-47 gene is IFN-gamma induced in B cells and encodes a protein with GTP-binding motifs. *J Immunol* **148**, 3275-81.
- Godfrey, D. I., Pellicci, D. G. and Smyth, M. J.** (2004). Immunology. The elusive NKT cell antigen--is the search over? *Science* **306**, 1687-9.
- Goetschy, J. F., Zeller, H., Content, J. and Horisberger, M. A.** (1989). Regulation of the interferon-inducible IFI-78K gene, the human equivalent of the murine Mx gene, by interferons, double-stranded RNA, certain cytokines, and viruses. *J Virol* **63**, 2616-22.
- Gombert, J. M., Herbelin, A., Tancrede-Bohin, E., Dy, M., Carnaud, C. and Bach, J. F.** (1996). Early quantitative and functional deficiency of NK1+-like thymocytes in the NOD mouse. *Eur J Immunol* **26**, 2989-98.
- Gonzalez-Aseguinolaza, G., Van Kaer, L., Bergmann, C. C., Wilson, J. M., Schmiege, J., Kronenberg, M., Nakayama, T., Taniguchi, M., Koezuka, Y. and Tsuji, M.** (2002). Natural killer T cell ligand alpha-galactosylceramide enhances protective immunity induced by malaria vaccines. *J Exp Med* **195**, 617-24.
- Gorbacheva, V. Y., Lindner, D., Sen, G. C. and Vestal, D. J.** (2002). The interferon (IFN)-induced GTPase, mGBP-2. Role in IFN-gamma-induced murine fibroblast proliferation. *J Biol Chem* **277**, 6080-7.
- Govoni, G., Vidal, S., Cellier, M., Lepage, P., Malo, D. and Gros, P.** (1995).

Genomic structure, promoter sequence, and induction of expression of the mouse Nramp1 gene in macrophages. *Genomics* **27**, 9-19.

**Green, V. J., Kokkotou, E. and Ladias, J. A.** (1998). Critical structural elements and multitarget protein interactions of the transcriptional activator AF-1 of hepatocyte nuclear factor 4. *J Biol Chem* **273**, 29950-7.

**Grone, H. J.** (2007). Normal development and function of invariant natural killer T cells in mice with isoglobotrihexosylceramide (iGb3) deficiency. *Proc Natl Acad Sci USA* **104**, 5977-82.

**Guenzi, E., Topolt, K., Cornali, E., Lubeseder-Martellato, C., Jorg, A., Matzen, K., Zietz, C., Kremmer, E., Nappi, F., Schwemmle, M. et al.** (2001). The helical domain of GBP-1 mediates the inhibition of endothelial cell proliferation by inflammatory cytokines. *Embo J* **20**, 5568-77.

**Guenzi, E., Topolt, K., Lubeseder-Martellato, C., Jorg, A., Naschberger, E., Benelli, R., Albin, A. and Sturzl, M.** (2003). The guanylate binding protein-1 GTPase controls the invasive and angiogenic capability of endothelial cells through inhibition of MMP-1 expression. *Embo J* **22**, 3772-82.

**Gutierrez, M. G., Master, S. S., Singh, S. B., Taylor, G. A., Colombo, M. I. and Deretic, V.** (2004). Autophagy is a defense mechanism inhibiting BCG and Mycobacterium tuberculosis survival in infected macrophages. *Cell* **119**, 753-66.

**Halonen, S. K., Taylor, G. A. and Weiss, L. M.** (2001). Gamma interferon-induced inhibition of Toxoplasma gondii in astrocytes is mediated by IGTP. *Infect Immun* **69**, 5573-6.

**Haque, S. J. and Williams, B. R.** (1994). Identification and characterization of an interferon (IFN)-stimulated response element-IFN-stimulated gene factor 3-independent signaling pathway for IFN-alpha. *J Biol Chem* **269**, 19523-9.

**Hardy, K. J. and Sawada, T.** (1989). Human gamma interferon strongly upregulates its own gene expression in peripheral blood lymphocytes. *J Exp Med* **170**, 1021-6.

**Hefti, H. P., Frese, M., Landis, H., Di Paolo, C., Aguzzi, A., Haller, O. and Pavlovic, J.** (1999). Human MxA protein protects mice lacking a functional alpha/beta interferon system against La crosse virus and other lethal viral infections. *J*

*Virology* **73**, 6984-91.

**Hemmi, H., Kaisho, T., Takeuchi, O., Sato, S., Sanjo, H., Hoshino, K., Horiuchi, T., Tomizawa, H., Takeda, K. and Akira, S.** (2002). Small anti-viral compounds activate immune cells via the TLR7 MyD88-dependent signaling pathway. *Nat Immunol* **3**, 196-200.

**Honey, K., Benlagha, K., Beers, C., Forbush, K., Teyton, L., Kleijmeer, M. J., Rudensky, A. Y. and Bendelac, A.** (2002). Thymocyte expression of cathepsin L is essential for NKT cell development. *Nat Immunol* **3**, 1069-74.

**Huber, S., Sartini, D. and Exley, M.** (2003). Role of CD1d in coxsackievirus B3-induced myocarditis. *J Immunol* **170**, 3147-53.

**Ihle, J. N. and Kerr, I. M.** (1995). Jaks and Stats in signaling by the cytokine receptor superfamily. *Trends Genet* **11**, 69-74.

**Ikeda, H., Old, L. J. and Schreiber, R. D.** (2002). The roles of IFN gamma in protection against tumor development and cancer immunoediting. *Cytokine Growth Factor Rev* **13**, 95-109.

**Ilyinskii, P. O., Wang, R., Balk, S. P. and Exley, M. A.** (2006). CD1d mediates T-cell-dependent resistance to secondary infection with encephalomyocarditis virus (EMCV) in vitro and immune response to EMCV infection in vivo. *J Virol* **80**, 7146-58.

**Isaacs, A. and Lindenmann, J.** (1957). Virus interference. I. The interferon. *Proc R Soc Lond B Biol Sci* **147**, 258-67.

**Jarrossay, D., Napolitani, G., Colonna, M., Sallusto, F. and Lanzavecchia, A.** (2001). Specialization and complementarity in microbial molecule recognition by human myeloid and plasmacytoid dendritic cells. *Eur J Immunol* **31**, 3388-93.

**Jayawardena-Wolf, J., Benlagha, K., Chiu, Y. H., Mehr, R. and Bendelac, A.** (2001). CD1d endosomal trafficking is independently regulated by an intrinsic CD1d-encoded tyrosine motif and by the invariant chain. *Immunity* **15**, 897-908.

**Jiang, G. and Sladek, F. M.** (1997). The DNA binding domain of hepatocyte nuclear factor 4 mediates cooperative, specific binding to DNA and heterodimerization with the retinoid X receptor alpha. *J Biol Chem* **272**, 1218-25.

- Joyce, S., Woods, A. S., Yewdell, J. W., Bennink, J. R., De Silva, A. D., Boesteanu, A., Balk, S. P., Cotter, R. J. and Bratkiewicz, R. R. (1998). Natural ligand of mouse CD1d1: cellular glycosylphosphatidylinositol. *Science* **279**, 1541-4.
- Kaiser, F., Kaufmann, S. H. and Zerrahn, J. (2004). IIGP, a member of the IFN inducible and microbial defense mediating 47 kDa GTPase family, interacts with the microtubule binding protein hook3. *J Cell Sci* **117**, 1747-56.
- Kang, S. J. and Cresswell, P. (2002). Calnexin, calreticulin, and ERp57 cooperate in disulfide bond formation in human CD1d heavy chain. *J Biol Chem* **277**, 44838-44.
- Kang, S. J. and Cresswell, P. (2002). Regulation of intracellular trafficking of human CD1d by association with MHC class II molecules. *Embo J* **21**, 1650-60.
- Kang, S. J. and Cresswell, P. (2004). Saposins facilitate CD1d-restricted presentation of an exogenous lipid antigen to T cells. *Nat Immunol* **5**, 175-81.
- Kawagishi, A., Kubosaki, A., Takeyama, N., Sakudo, A., Saeki, K., Matsumoto, Y., Hayashi, T. and Onodera, T. (2003). Analysis of T-cell receptor Vbeta gene from infiltrating T cells in insulinitis and myocarditis in encephalomyocarditis virus-infected BALB/C mice. *Biochem Biophys Res Commun* **310**, 791-5.
- Kawahara, K., Moll, H., Knirel, Y. A., Seydel, U. and Zahringer, U. (2000). Structural analysis of two glycosphingolipids from the lipopolysaccharide-lacking bacterium *Sphingomonas capsulata*. *Eur J Biochem* **267**, 1837-46.
- Kawano, T., Cui, J., Koezuka, Y., Toura, I., Kaneko, Y., Motoki, K., Ueno, H., Nakagawa, R., Sato, H., Kondo, E. et al. (1997). CD1d-restricted and TCR-mediated activation of valpha14 NKT cells by glycosylceramides. *Science* **278**, 1626-9.
- Kawasaki, S., Moriguchi, R., Sekiya, K., Nakai, T., Ono, E., Kume, K. and Kawahara, K. (1994). The cell envelope structure of the lipopolysaccharide-lacking gram-negative bacterium *Sphingomonas paucimobilis*. *J Bacteriol* **176**, 284-90.
- King, M. C., Raposo, G., Lemmon, M. A. (2004). Inhibition of nuclear import and cell-cycle progression by mutated forms of the dynamin-like GTPase MxB. *Proc Natl Acad Sci U S A* **101**, 8957-62.
- Kinjo, Y., Wu, D., Kim, G., Xing, G. W., Poles, M. A., Ho, D. D., Tsuji, M.,

- Kawahara, K., Wong, C. H. and Kronenberg, M.** (2005). Recognition of bacterial glycosphingolipids by natural killer T cells. *Nature* **434**, 520-5.
- Kitamura, H., Iwakabe, K., Yahata, T., Nishimura, S., Ohta, A., Ohmi, Y., Sato, M., Takeda, K., Okumura, K., Van Kaer, L. et al.** (1999). The natural killer T (NKT) cell ligand alpha-galactosylceramide demonstrates its immunopotentiating effect by inducing interleukin (IL)-12 production by dendritic cells and IL-12 receptor expression on NKT cells. *J Exp Med* **189**, 1121-8.
- Klaunig, J. E., Goldblatt, P. J., Hinton, D. E., Lipsky, M. M., Chacko, J. and Trump, B. F.** (1981). Mouse liver cell culture. I. Hepatocyte isolation. *In Vitro* **17**, 913-25.
- Kobayashi, E., Motoki, K., Uchida, T., Fukushima, H. and Koezuka, Y.** (1995). KRN7000, a novel immunomodulator, and its antitumor activities. *Oncol Res* **7**, 529-34.
- Kochs, G., Haener, M., Aebi, U. and Haller, O.** (2002). Self-assembly of human MxA GTPase into highly ordered dynamin-like oligomers. *J Biol Chem* **277**, 14172-6.
- Kochs, G. and Haller, O.** (1999). Interferon-induced human MxA GTPase blocks nuclear import of Thogoto virus nucleocapsids. *Proc Natl Acad Sci U S A* **96**, 2082-6.
- Koga, R., Hamano, S., Kuwata, H., Atarashi, K., Ogawa, M., Hisaeda, H., Yamamoto, M., Akira, S., Himeno, K., Matsumoto, M. et al.** (2006). TLR-dependent induction of IFN-beta mediates host defense against *Trypanosoma cruzi*. *J Immunol* **177**, 7059-66.
- Kotenko, S. V., Gallagher, G., Baurin, V. V., Lewis-Antes, A., Shen, M., Shah, N. K., Langer, J. A., Sheikh, F., Dickensheets, H. and Donnelly, R. P.** (2003). IFN-lambdas mediate antiviral protection through a distinct class II cytokine receptor complex. *Nat Immunol* **4**, 69-77.
- Kronenberg, M. and Locksley, R. M.** (2003). Constitutive cytokine mRNAs mark natural killer (NK) and NK T cells poised for rapid effector function. *J Exp Med* **198**, 1069-76.
- Krug, A., Towarowski, A., Britsch, S., Rothenfusser, S., Hornung, V., Bals, R., Giese, T., Engelmann, H., Endres, S., Krieg, A. M. et al.** (2001). Toll-like receptor

expression reveals CpG DNA as a unique microbial stimulus for plasmacytoid dendritic cells which synergizes with CD40 ligand to induce high amounts of IL-12. *Eur J Immunol* **31**, 3026-37.

**LaFleur, D. W., Nardelli, B., Tsareva, T., Mather, D., Feng, P., Semenuk, M., Taylor, K., Buergin, M., Chinchilla, D., Roshke, V. et al.** (2001). Interferon-kappa, a novel type I interferon expressed in human keratinocytes. *J Biol Chem* **276**, 39765-71.

**Langer, J. A., Cutrone, E. C. and Kotenko, S.** (2004). The Class II cytokine receptor (CRF2) family: overview and patterns of receptor-ligand interactions. *Cytokine Growth Factor Rev* **15**, 33-48.

**Lantz, O. and Bendelac, A.** (1994). An invariant T cell receptor alpha chain is used by a unique subset of major histocompatibility complex class I-specific CD4+ and CD4-8- T cells in mice and humans. *J Exp Med* **180**, 1097-106.

**Lapaque, N., Takeuchi, O., Corrales, F., Akira, S., Moriyon, I., Howard, J. C. and Gorvel, J. P.** (2006). Differential inductions of TNF-alpha and IGTP, IIGP by structurally diverse classic and non-classic lipopolysaccharides. *Cell Microbiol* **8**, 401-13.

**Lehn, M., Weiser, W. Y., Engelhorn, S., Gillis, S. and Remold, H. G.** (1989). IL-4 inhibits H2O2 production and antileishmanial capacity of human cultured monocytes mediated by IFN-gamma. *J Immunol* **143**, 3020-4.

**Lemaigre, F. P., Durviaux, S. M., Truong, O., Lannoy, V. J., Hsuan, J. J. and Rousseau, G. G.** (1996). Hepatocyte nuclear factor 6, a transcription factor that contains a novel type of homeodomain and a single cut domain. *Proc Natl Acad Sci U S A* **93**, 9460-4.

**Lew, D. J., Decker, T., Strehlow, I. and Darnell, J. E.** (1991). Overlapping elements in the guanylate-binding protein gene promoter mediate transcriptional induction by alpha and gamma interferons. *Mol Cell Biol* **11**, 182-91.

**Lisbonne, M., Diem, S., de Castro Keller, A., Lefort, J., Araujo, L. M., Hachem, P., Fourneau, J. M., Sidobre, S., Kronenberg, M., Taniguchi, M. et al.** (2003). Cutting edge: invariant V alpha 14 NKT cells are required for allergen-induced airway

inflammation and hyperreactivity in an experimental asthma model. *J Immunol* **171**, 1637-41.

**Ma, X., Chow, J. M., Gri, G., Carra, G., Gerosa, F., Wolf, S. F., Dzialo, R. and Trinchieri, G.** (1996). The interleukin 12 p40 gene promoter is primed by interferon gamma in monocytic cells. *J Exp Med* **183**, 147-57.

**MacMicking, J. D.** (2004). IFN-inducible GTPases and immunity to intracellular pathogens. *Trends Immunol* **25**, 601-9.

**MacMicking, J. D.** (2005). Immune control of phagosomal bacteria by p47 GTPases. *Curr Opin Microbiol* **8**, 74-82.

**MacMicking, J. D., Taylor, G. A. and McKinney, J. D.** (2003). Immune control of tuberculosis by IFN-gamma-inducible LRG-47. *Science* **302**, 654-9.

**Mallevaey, T., Zanetta, J. P., Faveeuw, C., Fontaine, J., Maes, E., Platt, F., Capron, M., de-Moraes, M. L. and Trottein, F.** (2006). Activation of invariant NKT cells by the helminth parasite schistosoma mansoni. *J Immunol* **176**, 2476-85.

**Martens, S. and Howard, J.** (2006). The interferon-inducible GTPases. *Annu Rev Cell Dev Biol* **22**, 559-89.

**Martens, S., Parvanova, I., Zerrahn, J., Griffiths, G., Schell, G., Reichmann, G. and Howard, J. C.** (2005). Disruption of Toxoplasma gondii parasitophorous vacuoles by the mouse p47-resistance GTPases. *PLoS Pathog* **1**, e24.

**Martens, S., Sabel, K., Lange, R., Uthaiyah, R., Wolf, E. and Howard, J. C.** (2004). Mechanisms regulating the positioning of mouse p47 resistance GTPases LRG-47 and IIGP1 on cellular membranes: retargeting to plasma membrane induced by phagocytosis. *J Immunol* **173**, 2594-606.

**Matsuda, J. L., Gapin, L., Sidobre, S., Kieper, W. C., Tan, J. T., Ceredig, R., Surh, C. D. and Kronenberg, M.** (2002). Homeostasis of V alpha 14i NKT cells. *Nat Immunol* **3**, 966-74.

**Matsuda, J. L., Naidenko, O. V., Gapin, L., Nakayama, T., Taniguchi, M., Wang, C. R., Koezuka, Y. and Kronenberg, M.** (2000). Tracking the response of natural killer T cells to a glycolipid antigen using CD1d tetramers. *J Exp Med* **192**, 741-54.

**Matsuura, A., Kinebuchi, M., Chen, H. Z., Katabami, S., Shimizu, T., Hashimoto,**

- Y., Kikuchi, K. and Sato, N.** (2000). NKT cells in the rat: organ-specific distribution of NK T cells expressing distinct V alpha 14 chains. *J Immunol* **164**, 3140-8.
- Mattner, J., Debord, K. L., Ismail, N., Goff, R. D., Cantu, C., 3rd, Zhou, D., Saint-Mezard, P., Wang, V., Gao, Y., Yin, N. et al.** (2005). Exogenous and endogenous glycolipid antigens activate NKT cells during microbial infections. *Nature* **434**, 525-9.
- McNab, F. W., Berzins, S. P., Pellicci, D. G., Kyparissoudis, K., Field, K., Smyth, M. J. and Godfrey, D. I.** (2005). The influence of CD1d in postselection NKT cell maturation and homeostasis. *J Immunol* **175**, 3762-8.
- Meier, E., Fah, J., Grob, M. S., End, R., Staeheli, P. and Haller, O.** (1988). A family of interferon-induced Mx-related mRNAs encodes cytoplasmic and nuclear proteins in rat cells. *J Virol* **62**, 2386-93.
- Meier, E., Kunz, G., Haller, O. and Arnheiter, H.** (1990). Activity of rat Mx proteins against a rhabdovirus. *J Virol* **64**, 6263-9.
- Melen, K. and Julkunen, I.** (1997). Nuclear cotransport mechanism of cytoplasmic human MxB protein. *J Biol Chem* **272**, 32353-9.
- Melen, K., Ronni, T., Broni, B., Krug, R. M., von Bonsdorff, C. H. and Julkunen, I.** (1992). Interferon-induced Mx proteins form oligomers and contain a putative leucine zipper. *J Biol Chem* **267**, 25898-907.
- Meraz, M. A., White, J. M., Sheehan, K. C., Bach, E. A., Rodig, S. J., Dighe, A. S., Kaplan, D. H., Riley, J. K., Greenlund, A. C., Campbell, D. et al.** (1996). Targeted disruption of the Stat1 gene in mice reveals unexpected physiologic specificity in the JAK-STAT signaling pathway. *Cell* **84**, 431-42.
- Miura, T. A., Carlson, J. O., Beaty, B. J., Bowen, R. A. and Olson, K. E.** (2001). Expression of human MxA protein in mosquito cells interferes with LaCrosse virus replication. *J Virol* **75**, 3001-3.
- Molano, A., Park, S. H., Chiu, Y. H., Nosseir, S., Bendelac, A. and Tsuji, M.** (2000). Cutting edge: the IgG response to the circumsporozoite protein is MHC class II-dependent and CD1d-independent: exploring the role of GPIs in NK T cell activation and antimalarial responses. *J Immunol* **164**, 5005-9.

- Mombaerts, P., Iacomini, J., Johnson, R. S., Herrup, K., Tonegawa, S. and Papaioannou, V. E.** (1992). RAG-1-deficient mice have no mature B and T lymphocytes. *Cell* **68**, 869-77.
- Mosmann, T. R. and Coffman, R. L.** (1989). TH1 and TH2 cells: different patterns of lymphokine secretion lead to different functional properties. *Annu Rev Immunol* **7**, 145-73.
- Muhlethaler-Mottet, A., Otten, L. A., Steimle, V. and Mach, B.** (1997). Expression of MHC class II molecules in different cellular and functional compartments is controlled by differential usage of multiple promoters of the transactivator CIITA. *Embo J* **16**, 2851-60.
- Nakayama, M., Yazaki, K., Kusano, A., Nagata, K., Hanai, N. and Ishihama, A.** (1993). Structure of mouse Mx1 protein. Molecular assembly and GTP-dependent conformational change. *J Biol Chem* **268**, 15033-8.
- Nelson, D. E., Virok, D. P., Wood, H., Roshick, C., Johnson, R. M., Whitmire, W. M., Crane, D. D., Steele-Mortimer, O., Kari, L., McClarty, G. et al.** (2005). Chlamydial IFN-gamma immune evasion is linked to host infection tropism. *Proc Natl Acad Sci U S A* **102**, 10658-63.
- Novick, D., Cohen, B. and Rubinstein, M.** (1994). The human interferon alpha/beta receptor: characterization and molecular cloning. *Cell* **77**, 391-400.
- Olszewski, M. A., Gray, J. and Vestal, D. J.** (2006). In silico genomic analysis of the human and murine guanylate-binding protein (GBP) gene clusters. *J Interferon Cytokine Res* **26**, 328-52.
- Paget, C., Mallevaey, T., Speak, A. O., Torres, D., Fontaine, J., Sheehan, K. C., Capron, M., Ryffel, B., Faveeuw, C., Leite de Moraes, M. et al.** (2007). Activation of Invariant NKT Cells by Toll-like Receptor 9-Stimulated Dendritic Cells Requires Type I Interferon and Charged Glycosphingolipids. *Immunity* **27**, 597-609.
- Park, S. H., Benlagha, K., Lee, D., Balish, E. and Bendelac, A.** (2000). Unaltered phenotype, tissue distribution and function of Valpha14(+) NKT cells in germ-free mice. *Eur J Immunol* **30**, 620-5.
- Park, S. H., Roark, J. H. and Bendelac, A.** (1998). Tissue-specific recognition of

- mouse CD1 molecules. *J Immunol* **160**, 3128-34.
- Park, S. H., Weiss, A., Benlagha, K., Kyin, T., Teyton, L. and Bendelac, A.** (2001). The mouse CD1d-restricted repertoire is dominated by a few autoreactive T cell receptor families. *J Exp Med* **193**, 893-904.
- Parvanova, I.** (2005). Analysis of the role of the p47 GTPase IIGP1 in Resistance against Intracellular Pathogens. Ph.D Thesis.
- Patterson, J. B., Thomis, D. C., Hans, S. L. and Samuel, C. E.** (1995). Mechanism of interferon action: double-stranded RNA-specific adenosine deaminase from human cells is inducible by alpha and gamma interferons. *Virology* **210**, 508-11.
- Pavlovic, J., Haller, O. and Staeheli, P.** (1992). Human and mouse Mx proteins inhibit different steps of the influenza virus multiplication cycle. *J Virol* **66**, 2564-9.
- Pavlovic, J., Zurcher, T., Haller, O. and Staeheli, P.** (1990). Resistance to influenza virus and vesicular stomatitis virus conferred by expression of human MxA protein. *J Virol* **64**, 3370-5.
- Pellicci, D. G., Hammond, K. J., Uldrich, A. P., Baxter, A. G., Smyth, M. J. and Godfrey, D. I.** (2002). A natural killer T (NKT) cell developmental pathway involving a thymus-dependent NK1.1(-)CD4(+) CD1d-dependent precursor stage. *J Exp Med* **195**, 835-44.
- Perussia, B.** (1991). Lymphokine-activated killer cells, natural killer cells and cytokines. *Curr Opin Immunol* **3**, 49-55.
- Pestka, S., Krause, C. D. and Walter, M. R.** (2004). Interferons, interferon-like cytokines, and their receptors. *Immunol Rev* **202**, 8-32.
- Pfefferkorn, E. R. and Pfefferkorn, L. C.** (1977). Specific labeling of intracellular *Toxoplasma gondii* with uracil. *J Protozool* **24**, 449-53.
- Pichyangkul, S., Yongvanitchit, K., Kum-arb, U., Hemmi, H., Akira, S., Krieg, A. M., Heppner, D. G., Stewart, V. A., Hasegawa, H., Looareesuwan, S. et al.** (2004). Malaria blood stage parasites activate human plasmacytoid dendritic cells and murine dendritic cells through a Toll-like receptor 9-dependent pathway. *J Immunol* **172**, 4926-33.
- Porubsky, S., Speak, A. O., Luckow, B., Cerundolo, V., Platt, F. M. and Praefcke,**

- G. J., Kloep, S., Benschaid, U., Lilie, H., Prakash, B. and Herrmann, C.** (2004). Identification of residues in the human guanylate-binding protein 1 critical for nucleotide binding and cooperative GTP hydrolysis. *J Mol Biol* **344**, 257-69.
- Praefcke, G. J. and McMahon, H. T.** (2004). The dynamin superfamily: universal membrane tubulation and fission molecules? *Nat Rev Mol Cell Biol* **5**, 133-47.
- Prakash, B., Praefcke, G. J., Renault, L., Wittinghofer, A. and Herrmann, C.** (2000). Structure of human guanylate-binding protein 1 representing a unique class of GTP-binding proteins. *Nature* **403**, 567-71.
- Prakash, B., Renault, L., Praefcke, G. J., Herrmann, C. and Wittinghofer, A.** (2000). Triphosphate structure of guanylate-binding protein 1 and implications for nucleotide binding and GTPase mechanism. *Embo J* **19**, 4555-64.
- Pyz, E., Naidenko, O., Miyake, S., Yamamura, T., Berberich, I., Cardell, S., Kronenberg, M. and Herrmann, T.** (2006). The complementarity determining region 2 of BV8S2 (V beta 8.2) contributes to antigen recognition by rat invariant NKT cell TCR. *J Immunol* **176**, 7447-55.
- Qian, X., Samadani, U., Porcella, A. and Costa, R. H.** (1995). Decreased expression of hepatocyte nuclear factor 3 alpha during the acute-phase response influences transthyretin gene transcription. *Mol Cell Biol* **15**, 1364-76.
- Rich, K. A., Burkett, C. and Webster, P.** (2003). Cytoplasmic bacteria can be targets for autophagy. *Cell Microbiol* **5**, 455-68.
- Riley, R. L.** (1998). Neonatal immune response. In: Encyclopedia of Immunology. 2nd ed. New York:Academic Press **Vol 3** (Delves PJ, Roitt IM, eds), 1818-1821.
- Roark, J. H., Park, S. H., Jayawardena, J., Kavita, U., Shannon, M. and Bendelac, A.** (1998). CD1.1 expression by mouse antigen-presenting cells and marginal zone B cells. *J Immunol* **160**, 3121-7.
- Roberts, R. M., Liu, L., Guo, Q., Leaman, D. and Bixby, J.** (1998). The evolution of the type I interferons. *J Interferon Cytokine Res* **18**, 805-16.
- Roberts, T. J., Sriram, V., Spence, P. M., Gui, M., Hayakawa, K., Bacik, I., Bennink, J. R., Yewdell, J. W. and Brutkiewicz, R. R.** (2002). Recycling CD1d1 molecules present endogenous antigens processed in an endocytic compartment to

NKT cells. *J Immunol* **168**, 5409-14.

**Rocha-Campos, A. C., Melki, R., Zhu, R., Deruytter, N., Damotte, D., Dy, M., Herbelin, A. and Garchon, H. J.** (2006). Genetic and functional analysis of the Nkt1 locus using congenic NOD mice: improved Valpha14-NKT cell performance but failure to protect against type 1 diabetes. *Diabetes* **55**, 1163-70.

**Romero, J. F., Eberl, G., MacDonald, H. R. and Corradin, G.** (2001). CD1d-restricted NK T cells are dispensable for specific antibody responses and protective immunity against liver stage malaria infection in mice. *Parasite Immunol* **23**, 267-9.

**Rousset, F., Malefijt, R. W., Slierendregt, B., Aubry, J. P., Bonnefoy, J. Y., Defrance, T., Banchereau, J. and de Vries, J. E.** (1988). Regulation of Fc receptor for IgE (CD23) and class II MHC antigen expression on Burkitt's lymphoma cell lines by human IL-4 and IFN-gamma. *J Immunol* **140**, 2625-32.

**Sad, S., Marcotte, R. and Mosmann, T. R.** (1995). Cytokine-induced differentiation of precursor mouse CD8<sup>+</sup> T cells into cytotoxic CD8<sup>+</sup> T cells secreting Th1 or Th2 cytokines. *Immunity* **2**, 271-9.

**Sagiv, Y., Hudspeth, K., Mattner, J., Schrantz, N., Stern, R. K., Zhou, D., Savage, P. B., Teyton, L. and Bendelac, A.** (2006). Cutting edge: impaired glycosphingolipid trafficking and NKT cell development in mice lacking Niemann-Pick type C1 protein. *J Immunol* **177**, 26-30.

**Samadani, U. and Costa, R. H.** (1996). The transcriptional activator hepatocyte nuclear factor 6 regulates liver gene expression. *Mol Cell Biol* **16**, 6273-84.

**Samadani, U., Qian, X. and Costa, R. H.** (1996). Identification of a transthyretin enhancer site that selectively binds the hepatocyte nuclear factor-3 beta isoform. *Gene Expr* **6**, 23-33.

**Sandelin, A., Alkema, W., Engstrom, P., Wasserman, W. W. and Lenhard, B.** (2004). JASPAR: an open-access database for eukaryotic transcription factor binding profiles. *Nucleic Acids Res* **32**, D91-4.

**Santiago, H. C., Feng, C. G., Bafica, A., Roffe, E., Arantes, R. M., Cheever, A., Taylor, G., Vieira, L. Q., Aliberti, J., Gazzinelli, R. T. et al.** (2005). Mice deficient

in LRG-47 display enhanced susceptibility to *Trypanosoma cruzi* infection associated with defective hemopoiesis and intracellular control of parasite growth. *J Immunol* **175**, 8165-72.

**Schibler, U. and Sierra, F.** (1987). Alternative promoters in developmental gene expression. *Annu Rev Genet* **21**, 237-57.

**Schindler, C. and Darnell, J. E., Jr.** (1995). Transcriptional responses to polypeptide ligands: the JAK-STAT pathway. *Annu Rev Biochem* **64**, 621-51.

**Schrem, H., Klempnauer, J. and Borlak, J.** (2002). Liver-enriched transcription factors in liver function and development. Part I: the hepatocyte nuclear factor network and liver-specific gene expression. *Pharmacol Rev* **54**, 129-58.

**Schwemmler, M., Weining, K. C., Richter, M. F., Schumacher, B. and Staeheli, P.** (1995). Vesicular stomatitis virus transcription inhibited by purified MxA protein. *Virology* **206**, 545-54.

**Seder, R. A. and Paul, W. E.** (1994). Acquisition of lymphokine-producing phenotype by CD4<sup>+</sup> T cells. *Annu Rev Immunol* **12**, 635-73.

**Sheppard, P., Kindsvogel, W., Xu, W., Henderson, K., Schlutsmeyer, S., Whitmore, T. E., Kuestner, R., Garrigues, U., Birks, C., Roraback, J. et al.** (2003). IL-28, IL-29 and their class II cytokine receptor IL-28R. *Nat Immunol* **4**, 63-8.

**Simon, A., Fah, J., Haller, O. and Staeheli, P.** (1991). Interferon-regulated Mx genes are not responsive to interleukin-1, tumor necrosis factor, and other cytokines. *J Virol* **65**, 968-71.

**Sivakumar, V., Hammond, K. J., Howells, N., Pfeffer, K. and Weih, F.** (2003). Differential requirement for Rel/nuclear factor kappa B family members in natural killer T cell development. *J Exp Med* **197**, 1613-21.

**Skold, M., Xiong, X., Illarionov, P. A., Besra, G. S. and Behar, S. M.** (2005). Interplay of cytokines and microbial signals in regulation of CD1d expression and NKT cell activation. *J Immunol* **175**, 3584-93.

**Sladek, F. M., Zhong, W. M., Lai, E. and Darnell, J. E., Jr.** (1990). Liver-enriched transcription factor HNF-4 is a novel member of the steroid hormone receptor superfamily. *Genes Dev* **4**, 2353-65.

- Sorace, J. M., Johnson, R. J., Howard, D. L. and Drysdale, B. E.** (1995). Identification of an endotoxin and IFN-inducible cDNA: possible identification of a novel protein family. *J Leukoc Biol* **58**, 477-84.
- Staheli, P. and Haller, O.** (1985). Interferon-induced human protein with homology to protein Mx of influenza virus-resistant mice. *Mol Cell Biol* **5**, 2150-3.
- Stark, G. R., Kerr, I. M., Williams, B. R., Silverman, R. H. and Schreiber, R. D.** (1998). How cells respond to interferons. *Annu Rev Biochem* **67**, 227-64.
- Stetson, D. B., Mohrs, M., Reinhardt, R. L., Baron, J. L., Wang, Z. E., Gapin, L., Takaoka, A., Mitani, Y., Suemori, H., Sato, M., Yokochi, T., Noguchi, S., Tanaka, N. and Taniguchi, T.** (2000). Cross talk between interferon-gamma and -alpha/beta signaling components in caveolar membrane domains. *Science* **288**, 2357-60.
- Svensson, H., Cederblad, B., Lindahl, M. and Alm, G.** (1996). Stimulation of natural interferon-alpha/beta-producing cells by *Staphylococcus aureus*. *J Interferon Cytokine Res* **16**, 7-16.
- Tabeta, K., Georgel, P., Janssen, E., Du, X., Hoebe, K., Crozat, K., Mudd, S., Shamel, L., Sovath, S., Goode, J. et al.** (2004). Toll-like receptors 9 and 3 as essential components of innate immune defense against mouse cytomegalovirus infection. *Proc Natl Acad Sci U S A* **101**, 3516-21.
- Taylor, G. A., Collazo, C. M., Yap, G. S., Nguyen, K., Gregorio, T. A., Taylor, L. S., Eagleson, B., Secret, L., Southon, E. A., Reid, S. W. et al.** (2000). Pathogen-specific loss of host resistance in mice lacking the IFN-gamma-inducible gene IGTP. *Proc Natl Acad Sci U S A* **97**, 751-5.
- Taylor, G. A., Feng, C. G. and Sher, A.** (2004). p47 GTPases: regulators of immunity to intracellular pathogens. *Nat Rev Immunol* **4**, 100-9.
- Taylor, G. A., Jeffers, M., Largaespada, D. A., Jenkins, N. A., Copeland, N. G. and Woude, G. F.** (1996). Identification of a novel GTPase, the inducibly expressed GTPase, that accumulates in response to interferon gamma. *J Biol Chem* **271**, 20399-405.
- Taylor, G. A., Stauber, R., Rulong, S., Hudson, E., Pei, V., Pavlakis, G. N., Resau, J. H. and Woude, G. F.** (1997). The inducibly expressed GTPase localizes to

- the endoplasmic reticulum, independently of GTP binding. *J Biol Chem* **272**, 10639-45.
- Terskikh, A. V., Easterday, M. C., Li, L., Hood, L., Kornblum, H. I., Geschwind, D. H. and Weissman, I. L.** (2001). From hematopoiesis to neuropoiesis: evidence of overlapping genetic programs. *Proc Natl Acad Sci U S A* **98**, 7934-9.
- Theofilopoulos, A. N., Baccala, R., Beutler, B. and Kono, D. H.** (2005). Type I interferons (alpha/beta) in immunity and autoimmunity. *Annu Rev Immunol* **23**, 307-36.
- Thomas, S. Y., Lilly, C. M. and Luster, A. D.** (2006). Invariant natural killer T cells in bronchial asthma. *N Engl J Med* **354**, 2613-6; author reply 2613-6.
- Tomura, M., Yu, W. G., Ahn, H. J., Yamashita, M., Yang, Y. F., Ono, S., Hamaoka, T., Kawano, T., Taniguchi, M., Koezuka, Y. et al.** (1999). A novel function of Valpha14+CD4+NKT cells: stimulation of IL-12 production by antigen-presenting cells in the innate immune system. *J Immunol* **163**, 93-101.
- Trinchieri, G.** (1995). Interleukin-12: a proinflammatory cytokine with immunoregulatory functions that bridge innate resistance and antigen-specific adaptive immunity. *Annu Rev Immunol* **13**, 251-76.
- Ullman, K. S., Northrop, J. P., Verweij, C. L. and Crabtree, G. R.** (1990). Transmission of signals from the T lymphocyte antigen receptor to the genes responsible for cell proliferation and immune function: the missing link. *Annu Rev Immunol* **8**, 421-52.
- Uthaiyah, R. C., Praefcke, G. J., Howard, J. C. and Herrmann, C.** (2003). IIGP1, an interferon-gamma-inducible 47-kDa GTPase of the mouse, showing cooperative enzymatic activity and GTP-dependent multimerization. *J Biol Chem* **278**, 29336-43.
- Uze, G., Lutfalla, G. and Gresser, I.** (1990). Genetic transfer of a functional human interferon alpha receptor into mouse cells: cloning and expression of its cDNA. *Cell* **60**, 225-34.
- van der Poll, T., Keogh, C. V., Guirao, X., Buurman, W. A., Kopf, M. and Lowry, S. F.** (1997). Interleukin-6 gene-deficient mice show impaired defense against pneumococcal pneumonia. *J Infect Dis* **176**, 439-44.

- Van Rhijn, I., Koets, A. P., Im, J. S., Piebes, D., Reddington, F., Besra, G. S., Porcelli, S. A., van Eden, W. and Rutten, V. P.** (2006). The bovine CD1 family contains group 1 CD1 proteins, but no functional CD1d. *J Immunol* **176**, 4888-93.
- Venezia, T. A., Merchant, A. A., Ramos, C. A., Whitehouse, N. L., Young, A. S., Shaw, C. A. and Goodell, M. A.** (2004). Molecular signatures of proliferation and quiescence in hematopoietic stem cells. *PLoS Biol* **2**, e301.
- Vilcek, J.** (2003). Novel interferons. *Nat Immunol* **4**, 8-9.
- Wagner, R. R., Snyder, R. M., Hook, E. W. and Luttrell, C. N.** (1959). Effect of bacterial endotoxin on resistance of mice to viral encephalitides; including comparative studies of the interference phenomenon. *J Immunol* **83**, 87-98.
- Wei, D. G., Lee, H., Park, S. H., Beaudoin, L., Teyton, L., Lehuen, A. and Bendelac, A.** (2005). Expansion and long-range differentiation of the NKT cell lineage in mice expressing CD1d exclusively on cortical thymocytes. *J Exp Med* **202**, 239-48.
- Wheelock, E. F.** (1965). Interferon-like virus-inhibitor induced in human leukocytes by phytohemagglutinin. *Science* **149**, 310-1.
- Wu, D., Xing, G. W., Poles, M. A., Horowitz, A., Kinjo, Y., Sullivan, B., Bodmer-Narkevitch, V., Plettenburg, O., Kronenberg, M., Tsuji, M. et al.** (2005). Bacterial glycolipids and analogs as antigens for CD1d-restricted NKT cells. *Proc Natl Acad Sci U S A* **102**, 1351-6.
- Wynn, T. A., Nicolet, C. M. and Paulnock, D. M.** (1991). Identification and characterization of a new gene family induced during macrophage activation. *J Immunol* **147**, 4384-92.
- Yoshida, K., Taga, T., Saito, M., Suematsu, S., Kumanogoh, A., Tanaka, T., Fujiwara, H., Hirata, M., Yamagami, T., Nakahata, T. et al.** (1996). Targeted disruption of gp130, a common signal transducer for the interleukin 6 family of cytokines, leads to myocardial and hematological disorders. *Proc Natl Acad Sci U S A* **93**, 407-11.
- Yoshida, M., Takeuchi, M. and Streilein, J. W.** (2000a). Participation of pigment epithelium of iris and ciliary body in ocular immune privilege. 1. Inhibition of T-cell

- activation in vitro by direct cell-to-cell contact. *Invest Ophthalmol Vis Sci* **41**, 811-21.
- Yoshida, R., Yoshioka, T., Yamane, S., Matsutani, T., Toyosaki-Maeda, T., Tsuruta, Y. and Suzuki, R.** (2000b). A new method for quantitative analysis of the mouse T-cell receptor V region repertoires: comparison of repertoires among strains. *Immunogenetics* **52**, 35-45.
- Yoshimoto, T., Bendelac, A., Hu-Li, J. and Paul, W. E.** (1995). Defective IgE production by SJL mice is linked to the absence of CD4+, NK1.1+ T cells that promptly produce interleukin 4. *Proc Natl Acad Sci U S A* **92**, 11931-4.
- Yoshimoto, T. and Paul, W. E.** (1994). CD4pos, NK1.1pos T cells promptly produce interleukin 4 in response to in vivo challenge with anti-CD3. *J Exp Med* **179**, 1285-95.
- Zerrahn, J., Schaible, U. E., Brinkmann, V., Guhlich, U. and Kaufmann, S. H.** (2002). The IFN-inducible Golgi- and endoplasmic reticulum- associated 47-kDa GTPase IIGP is transiently expressed during listeriosis. *J Immunol* **168**, 3428-36.
- Zhang, H. M., Yuan, J., Cheung, P., Luo, H., Yanagawa, B., Chau, D., Stephan-Tozy, N., Wong, B. W., Zhang, J., Wilson, J. E. et al.** (2003). Overexpression of interferon-gamma-inducible GTPase inhibits coxsackievirus B3-induced apoptosis through the activation of the phosphatidylinositol 3-kinase/Akt pathway and inhibition of viral replication. *J Biol Chem* **278**, 33011-9.
- Zhou, D., Cantu, C., 3rd, Sagiv, Y., Schrantz, N., Kulkarni, A. B., Qi, X., Mahuran, D. J., Morales, C. R., Grabowski, G. A., Benlagha, K. et al.** (2004). Editing of CD1d-bound lipid antigens by endosomal lipid transfer proteins. *Science* **303**, 523-7.
- Zhou, D., Mattner, J., Cantu, C., 3rd, Schrantz, N., Yin, N., Gao, Y., Sagiv, Y., Hudspeth, K., Wu, Y. P., Yamashita, T. et al.** (2004). Lysosomal glycosphingolipid recognition by NKT cells. *Science* **306**, 1786-9.

## *Acknowledgement*

*First, I would like to express my heartiest gratitude to Professor **Jonathan Howard** for giving me an opportunity to work under his supervision. His positive attitude, constant encouragement and sustained interest in my project proved essential for my successful PhD work.*

*I convey my sincere heartfelt gratitude to Matthias Cramer for all the helps with my visa, contract and all the administrative affairs.*

*I would also like to thank Dr. Sascha Martens, for providing valuable guidance in the beginning of my work and Thorsten Klamp for helping me with Northern blot technique. Thanks to Christoph Rohde for helping me all the time and being my excellent German teacher. Thanks to Cemali and Revathy, who helped me through esp. for the first year when I just arrived in Germany.*

*Special thanks to Rita Lange who helped me a lot in the beginning with the laboratory techniques. I would forward my thanks to her for being so nice. Thanks to Gaby Vopper and Claudia Poschner for being really friendly and cooperative.*

*I also owe my thanks to all my dear colleges in the lab. Thanks to Stephie, Natasa, Sasha Khaminets, Julia, Iana, Yang and Tao for their valuable friendship and making my stay in the lab extremely wonderful. Thanks to Stephan for the help in preparation of the final version of the thesis.*

*I would like to thank Iana Parvanova, who kindly provided her Irga6 KO mice for me to analyze. Thanks to Elisabeth and Dr. Margarete Odenthal who provided us the opportunity to use their Laser Microdissection facilities. Thanks to Dr. Olaf Utermöhlen for helping me with the infection of mice with *Listeria monocytogenes*. Thanks also to Dr. Gaby Reichmann for helping with the *T.gondii* experiments.*

*I would also like to thank Dr. Daniel D. Pinschewer in Zürich and Prof. Dr. Marina Freudenberg in Freiberg for providing warmhearted accommodation and helping with mice obtaining. I owe my thanks to Dr. Oberdan LEO in BELGIUM, Dr. Thomas Kolbe in Vienna, Dr. Heike Weighardt in Munich, Prof. Dr. Ari Waisman in Mainz, Mr. Rudolf Jörg in Zürich, Dr. Jocelyne Demengeo in Portugal, Prof. Dr. Jens Brüning in Köln for providing all the genetic modified mice and germ-free mice.*

*I would like to thank all the people who directly or indirectly helped me in the completion of my PhD project.*

*Finally, I owe my acknowledgement to the **Graduate School in Genetics and Functional Genomics, University of Köln** for offering me the fellowship for my PhD studies.*

## Erklärung

Ich versichere, dass ich die von mir vorgelegte Dissertation selbständig angefertigt, die benutzten Quellen und Hilfsmittel vollständig angegeben und die Stellen der Arbeit einschließlich Tabellen und Abbildungen-, die anderen Werke im Wortlaut oder dem Sinn nach entnommen sind, in jedem Einzelfall als Entlehnung kenntlich gemacht habe; dass diese Dissertation noch keiner anderen Fakultät oder Universität zur Prüfung vorgelegen hat; dass sie- abgesehen von unten angegebenen beantragten Teilpublikationen- noch nicht veröffentlicht ist, sowie, dass ich eine Veröffentlichung vor Abschluss des Promotionsverfahrens nicht vornehmen werde. Die Bestimmungen dieser Promotionsordnung sind mir bekannt. Die von mir vorgelegte Dissertation ist von Prof. Dr. Jonathan Howard betreut worden.

Köln, Nov 2007

Jia Zeng

Teilpublikation:

**Zeng, J.** (2003) Induced and Constitutive Expression of the P47 Resistance GTPases in the Mouse. Master Thesis, Northeast Normal University, Jilin P.R.China

# Curriculum Vitae

**Name:** Jia Zeng  
**Address:** Escher Str. 125,  
50739, Köln, Deutschland  
**E-mail:** [jia.zeng@uni-koeln.de](mailto:jia.zeng@uni-koeln.de)  
**Date of Birth:** 20.11.1976  
**Place of Birth:** Nei Mongol, P. R. China  
**Nationality:** P. R. China

## School studies

1992-1995: Yantai No.1 Middle School,  
Shandong, P. R. China

## University studies

1995-1999: Bachelor of Science (Biology),  
Northeast Normal University, Chang Chun, P.R. China

2000-2003: Master of Science (Cell Biology),  
Northeast Normal University, Chang Chun, P.R. China

## Doctoral studies

04.2004- 11.2007: Faculty of Mathematics and Natural Science  
University of Cologne  
Supervisor: Prof. Dr. Jonathan Howard  
Institute for Genetics  
University of Cologne, Cologne, Germany

## Lebenslauf

**Name:** Jia Zeng

**Adresse:** Escher Str, 125,  
50739, Köln, Deutschland.

**E-mail:** [jia.zeng@uni-koeln.de](mailto:jia.zeng@uni-koeln.de)

**Geburtsdatum:** 20.11.1976

**Geburtsort:** Nei Mongol, V. R. China

**Nationalität:** V. R. China

### Schulausbildung

1992-1995: Yantai No.1 Middle School,  
Shandong, P.R. China

### Universität Studium

1995-1999: Bachelor of Science (Biology),  
Northeast Normal University, Chang Chun, V.R. China

2000-2003: Master of Science (Cell Biology),  
Northeast Normal University, Chang Chun, V.R. China

### Promotions Studium

04.2004- 11.2007: Mathematisch-Naturwissenschaftliche Fakultät  
Universität zu Köln  
Betreuerin: Prof. Dr. Dr. Jonathan Howard  
Institut Für Genetik  
Universität zu Köln, Köln, Deutschland